A SPATIAL AND TEMPORAL 3D SLAB-BASED METHODOLOGY FOR OPTIMIZED CONCRETE PAVEMENT ASSET MANAGEMENT

A Dissertation
Presented to
The Academic Faculty

by

Georgene Malone Geary

In Partial Fulfillment
of the Requirements for the Degree
Doctor of Philosophy in the
School of Civil and Environmental Engineering

Georgia Institute of Technology
December 2019

A SPATIAL AND TEMPORAL 3D SLAB-BASED METHODOLOGY FOR OPTIMIZED CONCRETE PAVEMENT ASSET MANAGEMENT

Approved by:

Dr. Yi-Chang (James) Tsai Advisor
School of Civil and Environmental Engineering
Georgia Institute of Technology

Dr. Kimberly Kurtis
School of Civil and Environmental Engineering
Georgia Institute of Technology

Dr. James Lai, Emeritus
School of Civil and Environmental Engineering
Georgia Institute of Technology

Dr. Steven French
Dean, College of Design,
School of City and Regional Planning
Georgia Institute of Technology

Dr. Adjo Amekudzi-Kennedy
School of Civil and Environmental Engineering
Georgia Institute of Technology

Dr. Michael Darter
Department of Civil and Environmental Engineering, Emeritus Professor
University of Illinois, Urbana-Champaign

Date Approved: November 4, 2019

In dedication to my parents, George and LaVerne, who raised nine children and two grandchildren on a milkman's salary. They taught me that anything was possible.

ACKNOWLEDGEMENTS

I would like to thank my advisor, Dr. Tsai, for taking a chance on me as one of his team and encouraging me to take on this enlightening endeavor as a non-traditional student.

I also want to specifically thank Vince Cartillier for teaching me what 3D data is and how to use it, Nora Belmiloudi-Michel and Vidhyalakshmi Sundara Raman (Vidya) for patiently working with me on the faulting application and Anirban Chatterjee for all his work on Slabviewer2 and responding to my endless questions. I would like to recognize current students April Gadsby, Cibi Pranav Pasupathipalayam Sivashanmugam, and Nicholas Six and previous graduate students Lauren Gardner, Jeff (Bo) Price and Chieh (Ross) Wang for always making me feel like a fellow graduate student. As you all go off into the world and do great things do not forget "Data torta satis nihil admittes". I also need to thank my significant other, Bill Phillips, for putting up with my idea of retirement.

This material is based upon work supported by the National Science Foundation Graduate Research Fellowship under Grant No. DGE-1650044. Any opinions, findings, and conclusions or recommendations expressed in this material are those of the author(s) and do not necessarily reflect the views of the National Science Foundation.

TABLE OF CONTENTS

LIST OF TABLES

LIST OF FIGURES

LIST OF SYMBOLS AND ABBREVIATIONS

3DSBM	3D Slab Based Methodology
AASHTO	American Association of State Highway and Transportation Agencies
CPR	Concrete Pavement Restoration
FDR	Full Depth Slab Replacement
GFM	Georgia Faultmeter
GTSV	Georgia Tech Sensing Van
HPMS	Highway Performance Monitoring System
IQR	Interquartile Range
IRI	International Roughness Index
JPC or JPCP	Jointed Plain Concrete Pavement
KDAve	Average value from the Kernel smoothed curve
KDDelta curve	Difference between two different years Kernel smoothed curves
LTPP	Long Term Pavement Performance
ADS	Automatic Distress Survey
MDS	Manual Distress Survey
MTTF	Mean Time to Failure
MRD	Materials Related Distress
NCHRP	National Cooperative Highway Research Program
OS_Hazard rate	Original slab condition hazard rate
PMED	AASHTO Pavement Mechanistic-Empirical Design software
RSL	Remaining Service Life
RSL_yrs	Remaining Service life in years
RSLOS	Remaining Service Life of the Original Slabs
SbS	Slab States
NC	Not Cracked
L1	Slab with longitudinal crack longer than 1 ft, starting at a transverse joint
T1	Slab with transverse crack longer than 1 ft, starting at a longitudinal joint
L2	Slab with longitudinal crack longer than 75% of the length of the slab
T2	Slab with transverse crack (T1) longer than 6 ft
CC	Slab with crack that touches two adjacent joints at a corner
SS	Slab cracked into three pieces
R or RNC	Slab that has been repaired
Slab State condition	
CS	Current slabs state
OS	Original slabs state
SV2	Slabviewer2 software

SUMMARY

Management of cracking in jointed plain concrete (JPC) pavement assets is currently monitored at the Federal level using a value of percent transverse cracked slabs per 0.1 mile. While this may provide additional data than percent cracked per mile, this indicator still does not provide sufficient information related to the asset to make informed decisions on the remaining life and subsequent investment needed to maintain JPC pavements. With over 20 State DOTs now collecting 3D pavement data using 3D laser technology, the opportunity exists to develop a more robust method to manage and evaluate JPC pavements using this relatively new technology.

This dissertation presents a novel 3D Slab-Based Methodology, using 3D pavement data for improved management of JPC pavements. The proposed methodology consists of four modules: 1) slab states module with high granularity and finer severity classification that enables us to make more accurate and reliable Maintenance, Rehabilitation and Reconstruction (MR&R) decisions that could not be achieved previously, 2) a fundamental spatial-temporal analysis module which incorporates the importance of cracking orientation, 3) Kernel Density (KD) smoothing-based crack patterns to visualize and spatially analyze crack severity patterns in multiple scales (e.g. 0.1 mile or 1 miles), and 4) Remaining Service Life (RSL)-based cracking behavior to predict the remaining pavement life more reliably.

In Module 1, the individual pavement slabs are characterized into “slab severity states” based on the orientation, type and extent of cracking in the JPC pavement using the 3D pavement data. From this granular data different patterns and failure modes based on

cracking are identified. Module 2 includes a) spatial pattern analysis using individual slab severity states isolated by cracking orientation and b) longitudinal-transverse crack pattern analysis both spatially and temporally. Module 3 considers spatial pattern analysis using Kernel Density (KD) to explore the situations with clustered cracked slabs or randomly distributed fatigue failure driven cracked slabs (one requires localized treatment and the other requires considerations of replacing the entire lane). These slab-based spatial-temporal crack patterns also enable people to visualize and quantitatively evaluate the severity change over time so this information can be used to categorize and prioritize the pavements for MR&R. It also provides a continuous representation of the pavement that can be analyzed and correlated with other continuous type measurements in the future, such as IRI and Traffic Speed Deflectometers. Module 4 takes the approach of defining an original slab location reference to define Remaining Service life (RSL)-based cracking. The remaining life and deterioration rate are combined to provide an end-of-life definition and data to be used in future Life Cycle Cost Analysis for making optimal decisions on lane reconstruction.

The methodology is validated using case studies of three different categories of Georgia JPC pavements. The validation shows that the methodology provides a valuable means to study the insight of crack deterioration behavior for making informed MR&R decisions by leveraging the 3D pavement data that has become widely available. The 3D Slab-Based Methodology is a more robust condition assessment tool that provides an immense amount of information as compared to the existing evaluation method.

CHAPTER 1. INTRODUCTION

Jointed plain concrete pavements are a long lasting, low maintenance option for highway infrastructure. Additional knowledge relating to the actual life and condition of JPC will serve the highway industry for years to come.

1.1. Background

There are over four million miles of roads in the United States roadway network, almost 3 million of these roads are paved. This network supported over 3.2 trillion miles of vehicle trips in 2017 alone. With the ongoing challenge of the management of this immense and significant asset, it is shocking that asset management of our nation's infrastructure has only just recently become a national issue with the passage of the Moving Ahead for Progress in the 21st Century (MAP-21) transportation bill in 2012. MAP-21 required all State Departments of Transportation to develop Transportation Asset Management plans that identify how they will monitor and manage the condition of their infrastructure. These asset management plans require knowing what assets the States have, the condition of the asset, and, how they plan to effectively manage that asset. The Fixing America's Surface Transportation (FAST) ACT, passed in 2015 continues the focus on asset management and performance measures for proactive management of the nation's transportation system.

Pavements are a major part of our roadway infrastructure assets. The sustainable and cost effective management of pavements requires adequate design, reliable pavement distress forecasting, and long-term maintenance and rehabilitation planning. Sustainable

maintenance and rehabilitation strategies require accurate pavement condition and deterioration behavior. Currently, we lack the ability to efficiently collect information and use this information on the condition of the roadway system to properly manage the condition and serviceability of these pavements. To do this we need to be able to make quick predictions of the maintenance and rehabilitation needs, along with projecting the life cycle of these assets. Technologies are now being implemented that can reliably support the intelligent management of these infrastructure systems. One such technology is 2D imagery and 3D laser technology mounted on vehicles and operated at highway speeds to capture and analyze large amounts of video data of the condition of our pavements.

Currently all States collect information on their roadway network for planning purposes. More States are moving away from the historically used manual surveys into more automated methods. Manual surveys typically only take a sample of the entire network and are used to estimate the condition of the complete network. Automated surveys can cover the entire network and are getting more sophisticated, but typical 2D images cannot always provide reproducible data due to false negatives and lighting, among other issues. The advancement of 3D laser technology provides an innovative opportunity to collect and use 3D pavement surface data along with 2D images to automatically collect detailed crack data in the field. Several recent advancements in automated evaluation of 2D and 3D data for pavements at Georgia Tech, developed from the competitively selected U.S. DOT and National Academies, National Cooperative Highway Research Projects, Innovations Deserving Exploratory Analysis (NCHRP IDEA) projects, make this new research area possible. For example, cracks had been previously identified simply due to

lighting contrast from 2D images, but now with the combination of 2D and 3D technologies the location and width of cracking can accurately be determined. Recent improvements in detection algorithms developed at Georgia Tech have made the data easier to access and manipulate. The newly developed algorithms enable the extraction of detailed crack characteristics with research grade granularity, including location, orientation, length, width, depth and topological patterns, which makes it feasible to study the crack characteristics and deterioration behavior in the real-world environment.

The Georgia Tech Sensing Vehicle (GTSV) is equipped with the following: an integrated 2D imaging system, a 3D laser system (LCMS, manufactured by INO/Pavemetrics), a mobile light detection and ranging (LiDAR), a high-resolution inertia measurement unit (IMU) (manufactured by Applanix), a high-accuracy differential GPS, and a high-frequency distance measuring instrument (DMI) (shown in Figure 1-1).

The GTSV has been intensively utilized by Dr. Tsai's Georgia Tech research team since 2010 on various state and federal level research projects and applications. In two national demonstration projects (Remote Sensing and GIS-enabled Asset Management System, RS-GAMS Phases I and II) sponsored by the USDOT Office of the Assistant Secretary for Research and Technology (USDOT/OST-R) [Tsai & Wang, 2013; Tsai & Wang, 2014] Dr. Tsai's team successfully performed pioneering work by critically validating the use of high-resolution, 2D/3D pavement images for the automatic evaluation of pavement conditions, including cracking, rutting, concrete joint faulting, potholes, etc.

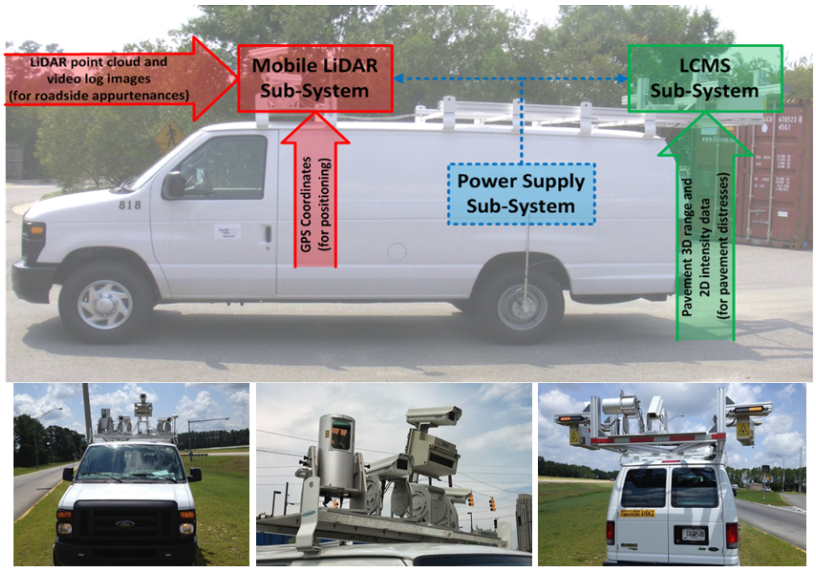

Figure 1-1 Georgia Tech Sensing Vehicle [Tsai & Wang, 2014]

As a continuous effort, the NCHRP Innovations Deserving Exploratory Analysis (IDEA) program sponsored the Georgia Tech to use 2D/3D pavement images for automatic evaluation of pavement raveling (Tsai & Wang, 2015a) in a research project entitled "Development of an Asphalt Pavement Raveling Detection Algorithm Using Emerging 3D Laser Technology and Macrotexture Analysis." The research results have been published in several peer-reviewed journals. The research includes using full-lane-width-coverage 3D pavement surface data to automatically detect and measure cracking (Tsai & Feng 2012; Jiang & Tsai, 2015) and its deterioration (Jiang et. al., 2016), rutting (Tsai & Li, 2013; Tsai, et. al., 2015), concrete joint faulting (Tsai et. al., 2012), project-level micro-milling pavement surface texture construction quality control (Tsai et. al. 2014), automated raveling detection and classification (Tsai & Wang, 2015), and automatic pothole detection (Tsai & Chatterjee, 2017). Figure 1-2 shows a 3D pavement surface image taken from the 3D laser system.

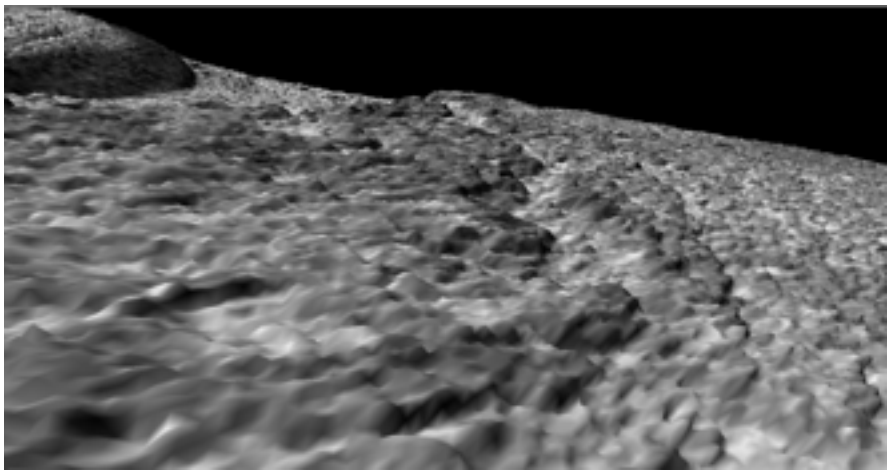

Figure 1-2 3D data showing pavement surface

Georgia Tech is also involved in developing national data standards for managing this vast amount of data. FHWA has been leading a five-year pooled-fund research effort (TPF-5(299)) with over 25 State DOTs to improve the quality and standardize pavement surface distress data collection. This effort is currently being extended to a phase II (TPF-5(399)), with the intent to also start looking into analysis. As part of the original pooled-fund, and due to the efforts of Dr. Tsia's research team, a new .psi standard file format for 3D pavement data has been developed and is currently being vetted nationally. Demand for ways to manage and efficiently use this vast amount of data is increasing and will be necessary for both asphalt and JPC pavements. The State DOTs are interested in using this data, and with 3D pavement surface and automatic crack detection and classification, this detailed level of crack data and severity can be easily obtained in the future for all DOTs. The key research question in this PhD thesis is how to utilize this detailed level of crack information to optimize pavement asset management.

Cracking and faulting are the major slab level distresses that are used to measure Jointed Plain Concrete Pavements (JCPC) performance. Distresses in JPCP, similar to any

real-world in place field installation of construction resources (like buildings or dams), are influenced by a number of issues: foundation support, strength and quality of materials used, original construction quality, environment, age, loading, etc. Along with IRI (international roughness index), cracking and faulting are the three performance measures required by the Federal government as part of the Highway Performance Monitoring System (HPMS) to report the condition of JPCP for asset management purposes. IRI is measured in 0.1 mile increments of the pavement, but cracking and faulting are measured as related to individual slabs. Historically this information has been gathered by sampling or aggregating the data into averages or one mile increments. With the recent Federal requirements to provide the distress information in a finer manner, along with the increase in capabilities of high speed profilers and high speed 3D lasers, high quality individual slab level data that was previously only available in a limited manner is now available. This includes cracking in a spatial and temporal manner for each individual slab and faulting measurements at each joint and crack. As this data is maintained over time, the timing and location of cracking in slabs or faulting at joints or cracks can provide information on the causes of distress and their influencing factors. For example, measuring early cracking in concrete pavements points to a materials or construction related issue or increasing rates of faulting along with certain types of cracking can identify a base/foundation issue for a section or a complete pavement project.

1.2. Research Objective

The aim of this research is to use this new 3D technology and 3D pavement data to understand and model how cracks in concrete pavements grow spatially and temporally through a slab-based multi-scale representation and propagation using large-scale detailed

crack characteristics that were not previously available. This information can be used to improve forecasting of pavement distress, with the ultimate goal of improving the management of our roadway network. The approach is to classify the cracking state of individual slabs and then using statistical techniques and probabilistic methods to model the spatial and temporal changes in the slab, and in the slab system. Unlike homogeneous constructed materials, such as metals, understanding and predicting concrete pavement deterioration behavior still remains a challenge since concrete pavements are non-homogenous, composite, quasi-brittle materials. But, probabilistic methods are successfully being used currently in bridge and pavement deterioration models. These models are typically based on some type of rating and reduction in rating over time. This research is different in that it is using cracking 'states' in slabs to model deterioration in concrete pavements. This research also looks at the basics of slab cracking in concrete pavements, developing a reliability model for cracking failure based on existing data and observations using the concept of Remaining Service Life (RSL) of the original JPC slabs. Kernel density(KD) regression is also used to model the crack characteristics and patterns topologically which can be managed at multiple scales (e.g. 1 slab, 0.1 mile (~25 slabs), 1 mile (~250 slabs) and larger sections (600+ slabs) as part of a project). KD can also be used to compare the fatigue related distress to conditions expected from end-of-life patterns by focusing on transverse cracking. The combination of the statistical models of the pavement section and the appropriate rate of cracking failure can then be used to develop optimum maintenance and rehabilitation strategies for the road infrastructure.

This research provides a means to use continuously collected 3D pavement data of in service concrete pavements to predict future deterioration. The contribution is a 3D Slab-

Based Methodology that includes new statistical indicators to describe JPC pavement performance and includes reliability engineering tools to compare and predict cracking deterioration rates.

1.3. Dissertation Organization

This dissertation is organized as follows: Chapter 2 is a literature review on concrete pavements and existing cracking/faulting models and data, including summary of findings. Chapter 3 presents an outline of the four modules that compose the 3D Slab-Based Methodology and covers the two fundamental modules: slab severity states and spatial temporal considerations. Chapter 4 describes Module 3, analysis of patterns using kernel density smoothing curves and the statistical analysis indicators developed, KDAve and IQR. Chapter 5 presents Module 4, a remaining service life (RSL) prediction technique using the concept of original slabs and reliability-based failure. Chapter 6 covers one particular application: the applications of the 3D data to improve PMED local calibration. Chapter 7 provides conclusions and recommendations for future research. The Appendix includes an in-depth Case Study of 4 different categories of pavement sections utilized in this research.

CHAPTER 2. LITERATURE REVIEW

2.1. Jointed Plain Concrete Pavements

Jointed Plain Concrete (JPC) Pavements are typically constructed from slip form pavers in a relatively continuous manner, and joints are made using a saw after placement and initial set of the concrete to control expected shrinkage cracking. These joints define the limits of a typical "slab" used in this research. Dowel bars may or may not be placed at the joints prior to construction to provide additional load transfer at the joints. Similarly, tie bars may or may not be located between adjacent lanes. Typical JPC pavements used for public roadways are on the order of 6 to 12 inches thick. Foundations for concrete pavements are recommended to be designed to be non-erodible and stable. This literature review focuses on how JPC is measured and treated for deterioration by State DOTs and then looks in more detail on cracking and faulting models and the existing available data on cracking and faulting.

2.1.1. Deterioration Mechanisms

In jointed plain concrete pavements (JPCP) crack initiation occurs shortly after the pavement is placed due to the (expected) shrinkage of the concrete as it hardens. If joints are properly and timely made (sawed) those cracks are initiated at the end of the 'notched' saw cuts and propagate downward through the concrete pavement to the base rather quickly as shown in Figure 2-1.

Pavements are jointed to address this expected shrinkage related to concrete hardening. Preferably, these would be the only cracks in jointed concrete pavements. Instead, due to a number of different possible factors as noted below, cracks are initiated in other areas of

concrete pavements. Crack initiation in concrete is typically considered a result of excessive tensile force on the concrete, since concrete tensile strength is typically ~10 times less than its compressive strength.

Crack initiation in concrete pavements can occur due to:

- shrinkage or other material related stresses,
- thermal expansion/contraction stresses,
- loading stresses,
- stress in the slab due to loss of support, or,
- any combination of these.

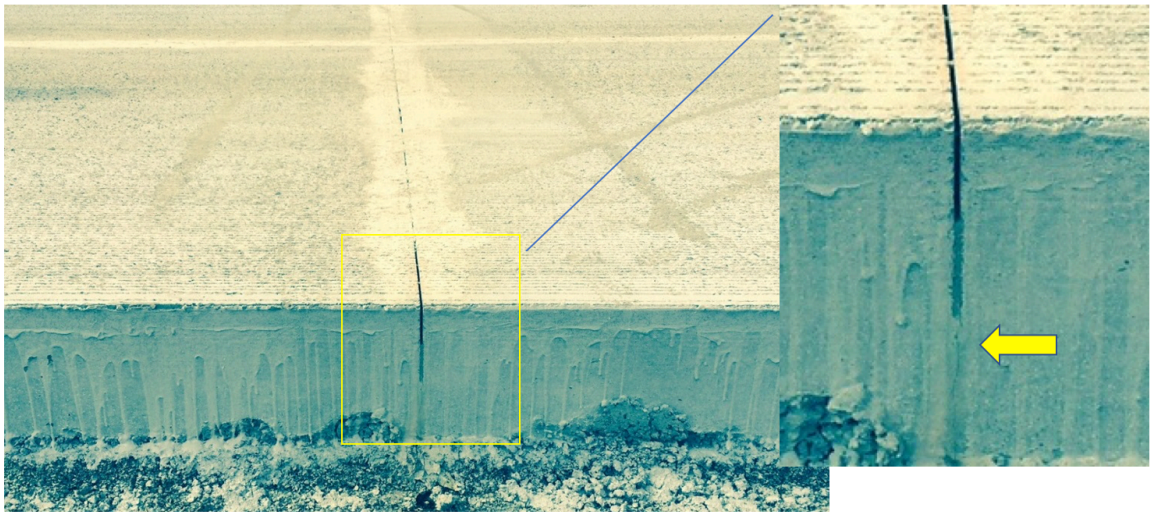

Figure 2-1 Cracking below a notched joint in JPC Pavement (taken at Illinois Tollway, 2015)

Shrinkage was noted previously and is controlled by jointing the pavement. Materials related stresses including D-cracking, alkali-silica reaction and others can contribute to or cause cracking and/or spalling, but these types of distresses are outside the purview of this effort, which is intended to focus on fatigue related cracking. Environmental, loading and support conditions have the most effect on fatigue related cracking.

Curling and warping of concrete pavements is a known source of environmental stress in pavement slabs. Curling and warping are due to the top and bottom of the slab experiencing different temperature or moisture conditions, respectively. This can occur for temperature when the surface is exposed to a hot sunny day, while the bottom is in contact with a cooler subgrade. In this case, the slab would contract more on the top and cause the slab to curl up, with the center above the edges, as shown in Figure 2-2a). Warping can affect the slab similarly, when the dryer side of the slab is in contact with the subgrade and the surface is wetter as shown in Figure 2-2b). Curling and warping work independently but can have additive effects or offset each other. Cool, dry nights with wet, warm subgrade conditions are the most typical additive condition and so can be the most detrimental, where the stresses are compounded like shown in Figure 2-2c) [Taylor, 2006].

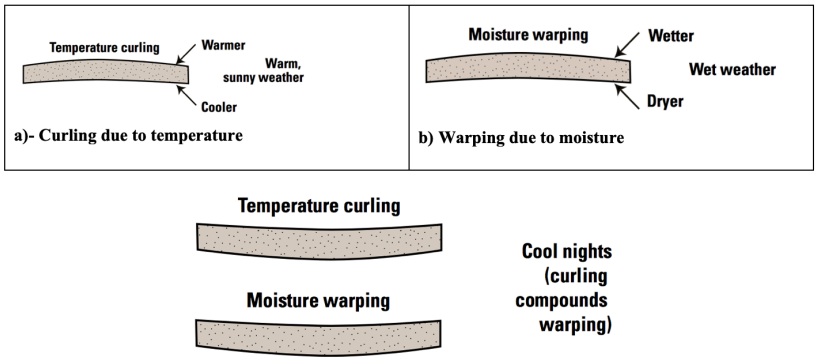

Figure 2-2 Curling and Warping in JPC pavements

Different levels of curl and warp can be built into a pavement depending upon the condition at time of construction. Some efforts to measure built-in curl and warp of pavements have been made but they are not standardized and they typically involve making measurements at different temperatures and environmental conditions [Chang etal., 2008 and Ceylan etal.,

2007]. Built in curl and warp have been identified as having an effect on performance of jointed plain concrete pavements, especially in the reproducibility of smoothness (IRI) measurements [Yu etal., 1998]. Built-in curl and warp has also been linked to increased longitudinal cracking [Signore etal., 2012].

2.1.2. Distress Forecasting Models

As noted in the Introduction, IRI, faulting and cracking are now required to be collected and submitted to the FHWA by every State DOT for JPC pavements. IRI is relatively standardized and measured in accordance with AASHTO R 43 [AASHTO, 2017b]. Faulting is described in more detail in the following section, Section 2.1.3. Cracking is defined by FHWA for Highway Performance Monitoring (HPMS) purposes as a slab cracked transversely at least half the width of the slab, but does not include longitudinal cracks or corner breaks [FHWA, 2016]. State DOTs have been collecting pavement distress data on concrete pavements since at least the 1970s for their own purposes and they have recognized that all types of cracking need to be considered. Therefore, although the specific terminology can be different, longitudinal, transverse, and corner cracking are all common cracking types collected for JPC by many state DOTs as noted in Table 2-1. There are also a variety of other different distresses measured by the State DOTs for concrete pavement, such as shoulder drop-off, patching, pumping, but this research focuses on cracking.

Table 2-1 Cracking Distresses Collected by Selected State DOTs

	OR	NC	CA	IN	FL	IL	GA
Corner Break/Crack	X	X	X	X	X	X	X
Shattered Slab	X	X Divided Slab(VA)	X 3rd Stage Cracking	O	X	O	X
Transverse Cracking	X	X	X	X	X	X	X
Longitudinal Cracking	X	X	X	X	X	X	X

X=Identified as being collected, O= Not Identified as being collected
*[references: Oregon DOT(2010), North Carolina DOT (2011), CalTrans (2015), Indiana DOT (2010), Florida DOT (2015), Illinois DOT(2010), Georgia DOT (2016)]

Many States use the Long-Term Pavement Performance (LTPP) Distress Identification Manual [Miller and Ballenger, 2004] definitions of cracking, or variations of those general definitions, but some have their own criteria for measuring pavement distress. Many states also use divided/shattered slab to denote a slab with multiple types of different intersecting cracks, this definition is not in the LTPP distress manual. This level of distress in a slab has a higher urgency for slab replacement because multiple cracking in a single slab can lead to a variety of worsening distresses such as spalling, differential settlement or popouts. States typically do not differentiate wheel-path and non-wheel path cracking in JPC, even if the State differentiates the wheel-path cracking for asphalt pavements. Most states define severity levels based on crack width; some combine with spalling and faulting. States typically do not have a minimum width to define a crack, anything visible can be considered low severity, but they may have a minimum length. Almost all States collect the highest severity cracking level in a slab and report only that measure. Some states measure a sample of the roadway, typically 0.1 mile of each mile [Janisch, 2015], but some states measure the complete mile. Almost all report cracking distress by a number of slabs

per length or a percentage of slabs basis, Oregon is an exception in that they record the length of longitudinal cracks and the number of transverse cracks. Oregon also uses a sampling approach that rates just the first 0.1 mile of every mile.

Condition ratings used by different State DOTs can use these three types of data: (1) distresses (such as cracking and faulting), (2) surface related measures (such as IRI or friction) and, less frequently, (3) structural (such as pavement thickness or falling weight deflectometer data). Pavement condition ratings provided to the public typically use one overall rating to provide clarity to customers, but often that rating is a composite of different factors or different individual ratings. Some of the ways a composite rating is developed is by identifying a distress related index and a separate IRI related index, or by weighting the individual distress and IRI values and subtracting them from a base value [AASHTO, 2012]. Georgia DOT uses this latter method in their JPCPACEs rating by deducting individual weighted points from 100 based on the type and amount of distress in a one-mile section, along with an included deduct value based on IRI. Illinois DOT 's CRS value similarly deducts points from a base level, but they start at 9.0 and use a statistically developed regression formula based on distress history and IRI to calculate the deductions. Figure 2-3 is the classical pavement condition curve that is typically used to describe pavement deterioration and maintenance, where the x-axis is time and the pavement condition (y-axis) is related to the rating system used (i.e. 0 to 100 for Georgia or 0 to 9 for Illinois). Note that the S curve starts out relatively flat, then undergoes an area of changing conditions, becoming relatively linear for a period of time before it flattens out towards the end.

Research for Washington State DOT proposed they use separate individual indices for IRI, faulting and cracking [Jackson, 2009]. A recent FHWA publication recommended a type of dual pavement condition rating, separating distresses and surface related measures. The

prime surface related measure is IRI, but others like friction can be considered. The distresses used for JPC were cracking and faulting. It was also recommended to include rate of change into the analysis for more accurate asset management decisions [Jiang, 2016 and Baladi etal., 2017].

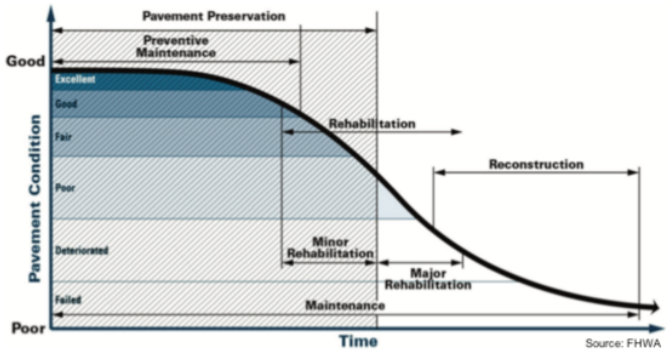

Figure 2-3 Pavement Condition and Maintenance Curve (Van Dam et al., 2019)

Many studies have found inconsistent trends in concrete pavement deterioration, or the models developed did not fit the concrete pavements as well as the models used for asphalt surfaced pavements. Lack of data was often cited as one of the concerns with the concrete models. Inconsistencies with using the same model as the asphalt pavements was also noted. Pennsylvania DOT attempted concrete models using 5 years data and either found they did not have enough data or the data was so inconsistent it was unusable [Wolters, 2010]. Illinois DOT previously used a two slope regression model for both asphalt and concrete, but recently changed the concrete model to a survival-type model due to poor lack of fit in the previous concrete models. Since they did not have data on the age of the pavements, they used previous rating values instead of pavement age for the older pavements, but plan to use age of pavement for newer pavements [Ozer, 2018]. Other States that use some type of survival-type model for cracking in concrete pavement include California [Lea, 2014].

2.1.3. Faulting

Faulting is caused by a change in elevation of a concrete slab near a joint. It is reported as the difference in elevation of an approach slab as compared to the elevation of a leave slab at a joint or crack. Based on the amount of movement and type of joint, it also involves loss of aggregate interlock and/or movement or distress of dowels in the case of doweled pavements. In colloquial terms faulting is the 'thumpity-thump' you sometimes hear and feel on concrete pavements as you cross over the joints. Beyond noise, increases in faulting have been correlated to increases in IRI in previous studies [Selezneva et al., 2000]. Faulting can be a major problem in undoweled pavements on erodible bases.

Manual faulting measurements have long been performed using a Georgia Faultmeter (GFM) which was first built by the Georgia DOT in 1987 [Stone, 1991]. Figure 2-4 shows how a faulting measurement is taken with the GFM. The legs are placed on the leave slab and the probe measures the faulting from the approach slab. The GFM reads out in positive or negative integer readings (i.e. -2, -1, 0, 1, 2) that are equivalent to 1/32" (0.03 inch or 0.8 mm) measurements. It can measure positive and negative faulting. Positive faulting is a drop in elevation along the direction of travel and negative faulting is a rise in elevation in the direction of travel, as shown in the figure. Positive faulting is considered the expected change due to traffic effects. Negative faulting, while still possible, has also been linked to data errors such as measuring faulting at cracked or repaired areas, excessive joint

sealant, placing the GFM in the wrong direction or just due to the accuracy of the

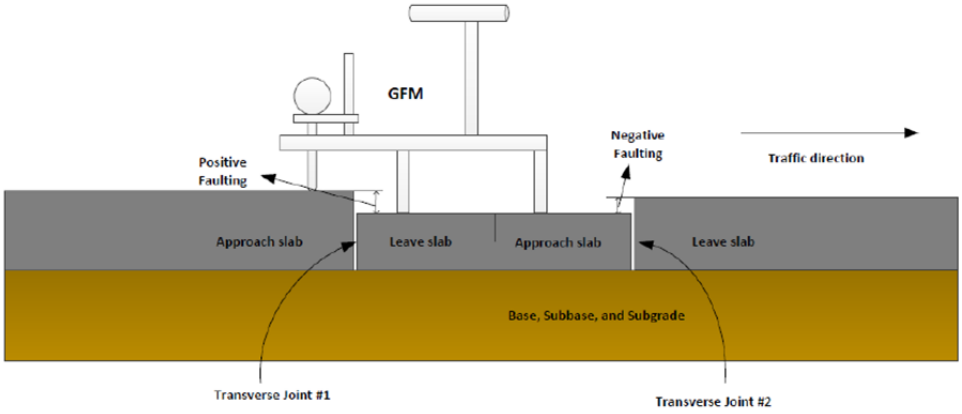

Figure 2-4 Georgia Faultmeter Operation [Agurla and Lin, 2015]

measurement itself when the actual elevation difference is near 0 [Selezneva et al., 2000].

AASHTO R 36, Evaluating Faulting of Concrete Pavements, is the current standard for faulting measurements [AASHTO, 2017a]. R 36-17 currently provides three methods to measure the faulting value: manual, automatic Method A and automatic Method B. The current Automatic methods both use one longitudinal profile from a High Speed Inertial Profiler (HSIP) to compute faulting. A proposed Method C using 3D pavement data has been submitted to AASHTO for consideration.

Faulting values can be reported by joint, as an average value per length or an index value. Some states use severity levels for faulting but most use the average faulting, although there are different ways State DOTs use to compute average faulting (e.g., some including the negative faulting as an absolute value and some do not include negative faulting values).

3D analysis of faulting data has the benefit of being able to identify joints and also provides a 3 dimensional view of the edge of the pavement that can be used to smooth out irregularities, like spalling, while also being able to measure as close to the joint as possible to remove curl, warp and longitudinal profile aspects. Preliminary studies of faulting measurements using 3D pavement data performed by Tsai [Geary et al., 2018, Tsai et al., 2012 and Tsai et al., 2011] and others [Wang et al., 2014] have shown potential improved results over HSIP methods.

2.1.4. Treatment Methods and Timing

Treatment methods used by the States for concrete pavement preservation and maintenance are very straightforward and consistent and are shown in Table 2-2. FHWA has sponsored training in concrete pavement maintenance and there is online web-based National Highway Institute (NHI) training for Concrete Pavement Preservation. Partial depth repairs (PDR) are typically used for repairing spalling and localized deterioration such as scaling. Full depth repair (FDR) is used for all types of cracking [Smith et al., 2014].

Concrete continuously moves (expands and contracts) due to environmental conditions so cracks can also open and close. Therefore, crack sealing is also used to seal incompressible materials out of stable (non-working) cracks.

Table 2-2 Treatments Used by States and Expected Performance

Maintenance Treatment	Use	Treatment Life, Years
Partial Depth Repair (PDR)	Used for spalling or corner breaks that do not go all the way through the slab (~$\frac{1}{3}$ to $\frac{1}{2}$ slab thickness)	5 to 15
Full Depth Repair (FDR)	Can repair cracked slabs, can reduce faulting due to cracked slabs	5 to 15
Dowel Bar Retrofit (DBR)	To repair faulted cracks, or, for undoweled pavements in good condition, used to prevent/repair faulting	10 to 15
Joint Reseal/Crack Seal	Protects pavement from water intrusion that can cause faulting or cracking	2 to 8
Diamond Grind	Restores ride (IRI) and friction, need to repair any cracking or faulting first	8 to 15
Slab Stabilization/ Slab Jacking	Used to fill voids below slabs that can cause cracking or result in faulting.	N/A

(Portions compiled from the CPTECH Guide [Smith etal., 2014])

2.1.5. Summary

Cracking and faulting are the major distresses for fatigue of concrete pavements. Environmental and loading conditions, concrete material properties and thickness, concrete slab size (length and width), presences of dowels and foundation stability are the major considerations of cracking and faulting in concrete pavements. Materials related distress (MRD) and built-in stresses (built-in curl and warp) can also have a large effect but are mainly outside the scope of this research. However, it is recognized in this research that attention should be placed on measuring transverse and longitudinal cracking separately to provide some indication of curl and warp effects, which has been recognized as being a factor in longitudinal cracking. Concrete pavement forecasting models have typically relied on combinations of cracking, faulting and other distresses and age. More recent recommendations have included separating ride (IRI) and distress conditions, while also

considering the rate of deterioration in the structural index to provide a more accurate prediction of future behavior. It is also noted that:

- Cracking at an individual slab level and location has mainly been used in an aggregated (i.e. cracked slabs per mile) manner.

- Cracking as a performance indicator nationally focuses mainly on transverse cracking. Longitudinal and corner cracking should be addressed for effective pavement management.

- Combining actual deterioration rates (i.e. increase in cracking per mile) with identified distresses has been identified as an important component in pavement management.

- Investigation of cracking at the slab level has the potential to drive new methods to predict deterioration and provide new procedures to maintain and mitigate distress in concrete pavements.

The 3D slab-based methodology proposed in this research looks at concrete pavements at a slab level, while also recognizing all the major types of cracking (transverse, longitudinal and corner) and including a rate of deterioration component (also called hazard rate), as described later in Section 4.

Concrete pavement rehabilitation (CPR) is relatively straightforward. Slabs that exhibit cracking can be repaired (PDR) or replaced (FDR), faulting can be arrested by retrofitting joints (DBR) and faulting (and therefore IRI) can be improved by diamond grinding. Concrete pavement engineers have a similar conundrum as asphalt engineers who have

often wondered, “how many times can I do a thin mill and resurface on the same pavement before I should perform full rehabilitation?”. The concrete pavement engineers question is “how many times can I do full depth slab repair and diamond grind this pavement section before major rehabilitation is necessary?” The true need in the concrete pavement rehabilitation area is identifying the fatigue life of the pavement such that the life cycle cost of replacement or overlay (concrete or asphalt) is lower than the life cycle cost of rehabilitation. Percent cracking alone does not indicate if the pavement life can be extended by CPR or if the pavement is at the end of life. It would be a waste of asset life to only use 15% of the ultimate capacity of a JPC pavement. Similarly, if you repair 15% cracked slabs one year and have 15% slabs cracked again the next year that would be a waste of resources and detrimental to the traveling public. Somewhere between these cases lies the optimum cracking pavement life for JPC pavements. This relates to the (1) severity level and (2) deterioration rate of cracking and faulting, both which can be measured using 3D pavement data over time.

As noted earlier, cracking in concrete pavements is related to a combination of factors:

1) Construction conditions can affect warping and curling of the slabs which can affect where and when cracking develops. Construction and materials variability can also affect the variability of the cracking.

2) Environmental conditions, like changes in temperature and moisture, can also have a positive or negative effect depending upon the timing and inherent condition of the concrete slabs.

3) Loading conditions (traffic)

4) Foundation Support

Most of these factors (construction conditions, environment, material properties, loading) should be reasonably the same for pavements constructed using the same typical sections in the same location, placed by the same contractor. Therefore, it is reasonable to consider changes in pavement conditions would be similar for these type pavements. One other condition that does affect cracking, foundation support of the concrete slab, may be expected to be a major contributor to differences in how pavements that meet the other criteria behave. Examination of variability in cracking for pavement sections that perform differently but were constructed and operate under similar conditions should provide information on the variability of the foundation and therefore the propensity of the pavement to continue to deteriorate at an increasing rate due to foundation or support issues.

2.2. Cracking and Faulting Models/Data

2.2.1. Fundamental Cracking Models

Concrete used in jointed plain concrete pavements is typically portland cement concrete, which at its most basic is composed of Portland cement, water and aggregates (fine and coarse). The cement and the water chemically react to create the binder that holds the aggregates together. For the purposes of this discussion on cracking, the chemistry involved will not be discussed since information on it can be found in any Concrete textbook. What is important is that different reactions occur at different times and at different levels and due to that, and the composites that make up concrete, it is not a homogeneous material at the macro or micro level. Recent advances in scanning electron

microscopy (SEM) have provided additional information on the structure of concrete at a nanoscale but much is still unknown [Birgisson et al., 2012]. As shown in Figure 2-5 it is non-homogeneous even at a nanoscale.

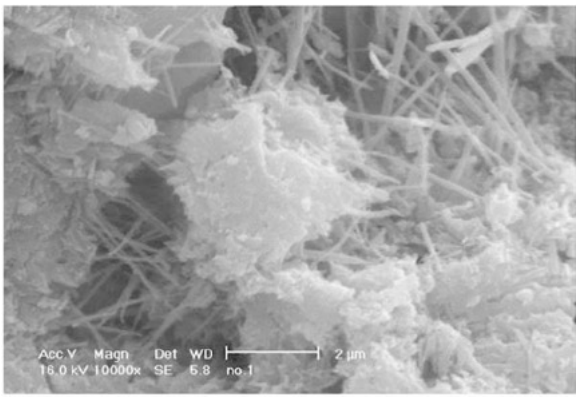

Figure 2-5 SEM picture of concrete structure at nanoscale [Li and Liang, 2011]

Fracture mechanics is the study of how materials fracture or break. It recognizes that materials do not always exhibit their theoretical strength levels due to inherent flaws in the material. Primarily used in metals and glass, it has recently (starting in the 1980s) been expanded to concrete materials. The challenges for using fracture mechanics in concrete is the non-homogeneity of concrete that was discussed earlier. No material is purely homogeneous, but steels and glass are much more so than concrete.

The basics of fracture mechanics is that cracking requires energy both to initiate and to propagate. Larger structures have more energy available to feed the propagation of a crack and, based on Weibull Theory, the larger the volume associated with a material/structure the higher probability of weak areas/flaws/microcracks. Isenberg noted in a 1968 American Concrete Institute (ACI) document on 'Cracking in Concrete' that "strength and stiffness" of concrete "are not permanent properties, but change as microcracking

develops" [Isenberg, 1968]. These considerations are why failure or fracture of a structure cannot be based solely on the theoretical strength (i.e. tensile strength, f'_t) of a material. In addition, these materials have inherent cracks/flaws that also affect the energy and propagation of the crack. Each crack has a crack tip which is under stress (stress intensity factor, K_I) and a zone in front of the crack tip (fracture process zone, FPZ). K_I is proportional to the load applied and is related to the crack length and the geometry of the specimen, so it changes with movement of the crack and different size specimens. The material resists cracking based on its fracture toughness, K_{Ic}, which is the critical value of K_I. Propagation of the crack relies on the fracture energy, G where the critical crack energy is termed G_f. The crack propagates only if G reaches G_f. G and K_{Ic} are basic material properties. The fracture toughness and the critical crack energy are related by Youngs Modulus, E, and the Poisson ratio, ν, of the material as shown in Equation 2-1.

$$K_{Ic} = G_f E' \qquad \text{where} \qquad E' = \frac{E}{1-\nu^2} \qquad \text{Eq. 2-1}$$

Fracture Mechanics looks at three Modes of loading as shown in Figure 2-6. Since Mode I is related to tensile loading, and concrete has a low tensile strength, this is the Mode most considered in concrete [Bazant, 1999].

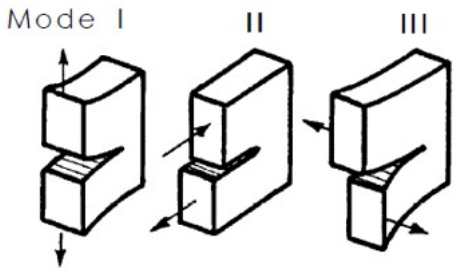

Figure 2-6 Elementary Cracking Modes [Bazant, 1999]

Flaws cause failure (act as stress concentrators since load cannot be carried over cracks) and larger samples have more flaws, therefore size matters in crack propagation. It has also been shown through round robin testing by RILEM that the same concrete mix tested with different sample sizes will provide different values of G_f. The research reported this was related to changes in micocracking due to differences in curing based on the size of the specimen [Karihaloo and Nallathambi, 1991].

S-N curves are empirical measures of fatigue. For laboratory specimens they are developed using notched samples that are subjected to cyclic loading until failure. The disagreement between the S-N relationship between laboratory beams and full scale concrete pavements in the field due to the specimen size effect is well known [Ioannides, 1997]. The definition of failure also contributes to the differences. In a laboratory beam, failure is the partially supported beam breaking in two. In the field different values have been used to define failure. As shown in Figure 2-7, and noted in the referenced TRB paper, the S-N relationship differences shown in the figure were also due to differences in the experiments definition of failure [Roesler and Barenberg, 1999]. The Corp of Engineers data (identified as Field Slabs-Darter) was based on 50% of slabs exhibiting cracking while the AASHO

Road Test (Field Slabs-Vesic and Saxena) used present serviceability index (PSI), a ride comfort based criteria.

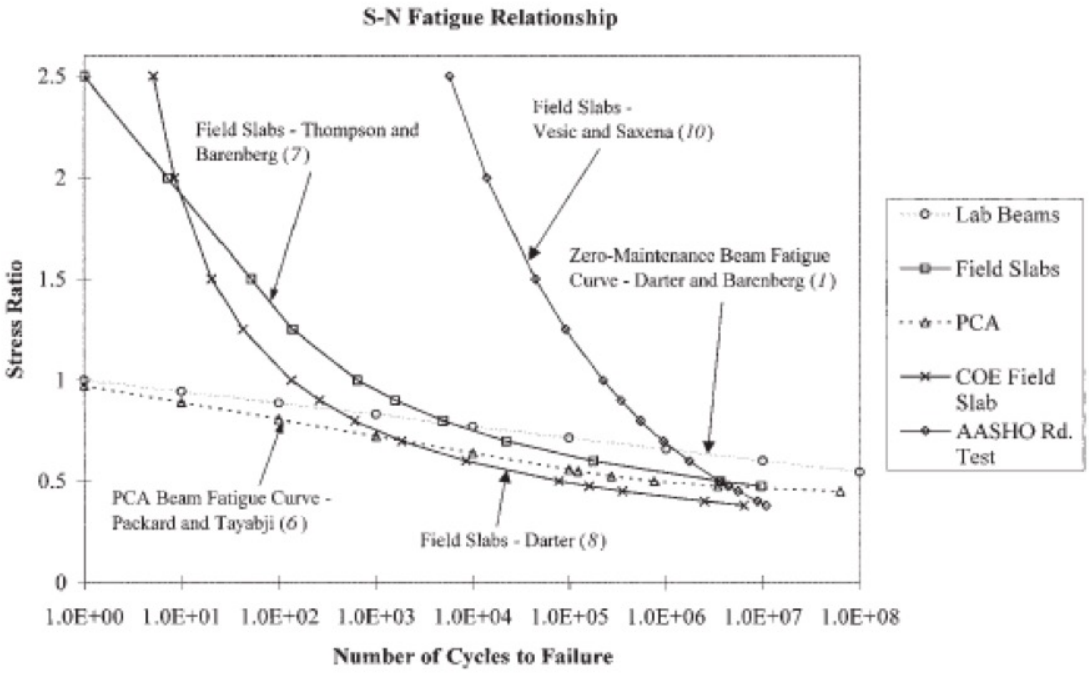

Figure 2-7 Fatigue relationship based on failure definition [Roesler and Barenberg, 1999]

Recent research performed at the University of Illinois advanced the correlation between small-scale properties and flexural capacity and crack propagation of full-scale pavements, but they also recognized that to apply this tool to pavement practitioners "other important effects, such as load transfer between slabs, base type, and slab temperature or moisture curling must be addressed" [Gaedicke and Roesler, 2009].

2.2.2. Cracking and Faulting Models in AASHTO Pavement ME

The most universally used mechanistic based model for concrete pavements in the US is that used by the AASHTO PavementME Design (PMED) procedure, formerly known as

MEPDG (mechanistic –empirical pavement design guide). The procedure uses a mechanistic-empirical approach to identify transverse cracking in concrete slabs. The process considers both loading and thermal (warp and curl) stresses in the pavement at the bottom and the top of the slab. The critical location is considered to be the same midpoint edge location of the slab, with the critical location for bottom-up cracking at the bottom of the slab and the critical location for top-down cracking at the top of the slab as shown in Figure 2-8. The location of the critical loading is different for top-down and bottom-up stresses, with the major tensile load at the bottom of the slab when the truck tires are mid-slab, and the major tensile load at the top of the slab when the truck tires are loading opposite ends of the slab. The PMED does not currently predict longitudinal cracking, but the original research effort recognized "that future additions to this design procedure should fully consider" longitudinal cracking [Yu etal., 2003].

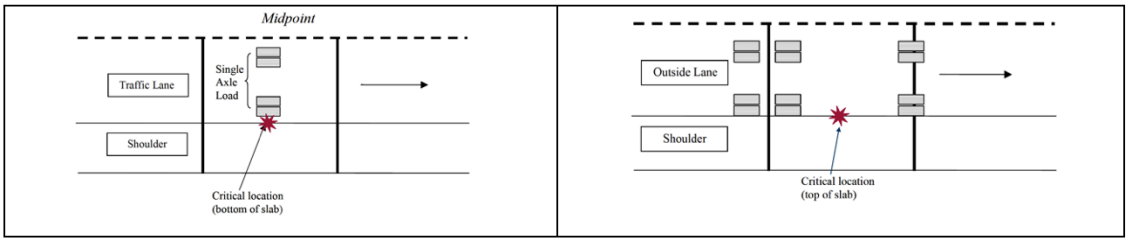

Figure 2-8 PMED critical stress locations [Yu etal., 2003]

AASHTO PavementME damage is based on Miners Theory of accumulated damage, long exemplified by a professor twisting a paper clip back and forth in front of the class a number of times until it breaks. Miners Equation (Equation 2-2) shows the relationship between the number of times the paperclip is stressed (n), and the number of cycles to failure (N). When n=N and C (damage fraction) = 1 the paperclip fails. This model is based

on accumulated affects which are summed together. It does not directly consider any uncertainty or variability in those affects.

$$C = \sum_{i=1}^{k} \frac{n_i}{N_i} \qquad \text{Eq. 2-2}$$

The Mechanistic–Empirical approach that is the foundation of the AASHTO Pavement-ME (PMED) design software uses % transverse slabs cracked per mile to define pavement life for cracking. Slabs are identified to crack when the ultimate tensile stress in the slab is exceeded through accumulated incremental tensile stresses based on Miners Theory. Tensile stresses from environmental and loading effects are both computed and combined. Finite element analysis and neural networks were both used to provide the necessary stresses and related deflections in a computationally efficient manner [ARA, Inc., 2004]. The maximum stress theory method utilized by PMED concentrates on strength criteria such that cracking failure is identified based on the tensile and thermal properties of the concrete, with consideration of the geometry and support of the slab and the friction on the base of the slab. Properties of the concrete are based on test methods of small samples, and strength gain over time is included. This works for pavement design since ultimate conditions (cracked slabs) and not intermediate conditions (crack propagation) are being modeled. In addition, the results are empirically calibrated to full-size slabs which should moderate size effects in the design.

Faulting in PMED is computed using an incremental approach. The incremental damage is a function of the type and erodibility of the base/subbase, rainfall, loading and slab curling. Slab curling based on environmental effects is considered as it is expected that maximum faulting would develop when the temperature differential is such that the joints are open

and the slab is curled upward [ARA Inc., 2003]. But, built-in slab curl or warp is not part of the analysis for either cracking or faulting as measures to define built-in curl and warp are still being developed as noted in Section 2.1.1. Faulting is measured as the mean faulting of all joints in inches (mm). Faulting was also calibrated with full scale testing. Faulting is used with cracking to model IRI changes over time in PMED.

2.2.3. Cracking and Faulting Data from LTPP sections

While 3D pavement data can provide a wealth of information on a project level, since it is a relatively new capability, there is little historical data available. The Long Term Pavement Performance (LTPP) database is the most comprehensive information on pavement performance in the world. The online database currently includes information on 2,548 total pavement sections, 668 of these with concrete surfaces, and over half of these concrete surfaces being JPCP [LTPP Infopave, 2018]. For the JPCP the data includes slab level information on 500 ft (~0.1 mile) segments of hundreds of pavement sections. This data (around 20-30 slabs per section) is comparable, on a very small scale (typical JPC pavements have 175-350 slabs per mile, depending on joint spacing) to what is now available from 3D high speed vehicles. As part of the LTPP experiments the pavement sections are visited periodically (~every 2 years) and distress and condition information is collected at each site. An example of a portion of a LTPP distress crack map is shown in Figure 2-9 for LTPP Section 13-3017. The value of the LTPP data is that it has been collected since the early 1980's, therefore 30 to 40 years of time series data for a number of pavements and the development of cracking by slab are available for different combination of factors. LTPP data was used in calibration of the cracking and faulting

models in AASHTO PMED as noted in Section 2.2.2. The LTPP data was used in this research to study pavement cracking deterioration for JPCP.

LTPP data includes the history of faulting and cracking of the pavement sections all the way down to a slab level (through the individual distress maps performed on a periodic basis as noted above).

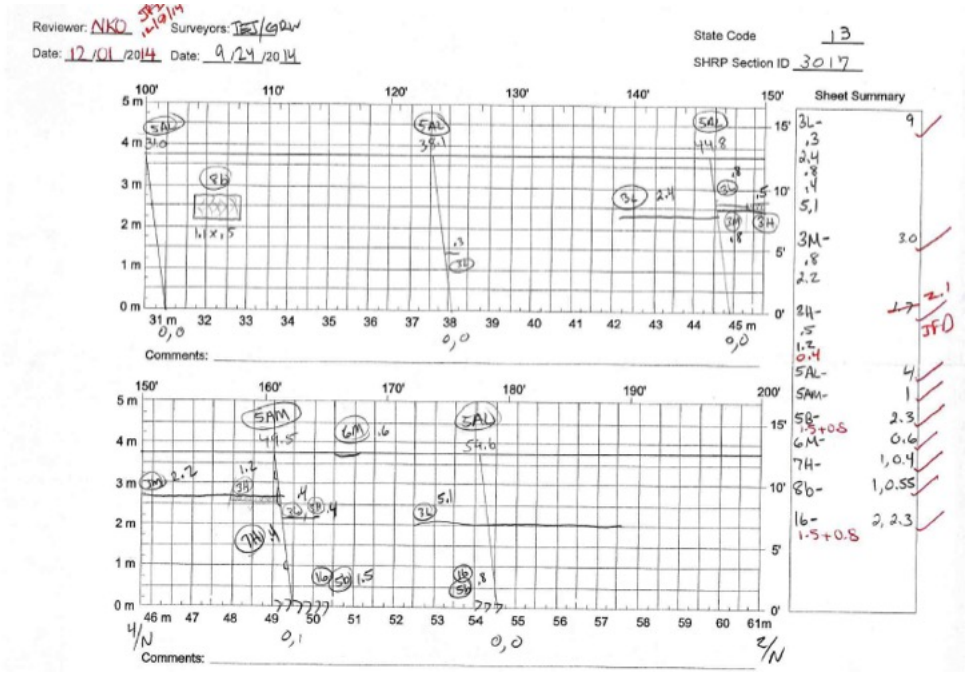

Figure 2-9 LTPP Crack map for a portion of GA Section 133017

A research study performed in 1998 defined good, normal and poor performance of concrete pavements in terms of IRI, faulting and cracking for the LTPP JPC GPS-3 sections. The analysis was performed using the available data from LTPP sections and industry experts opinion. Cracking performance was identified as good if the % transverse cracked slabs were less than the pavements age divided by 4. Poor was considered when the % transverse cracked slabs were greater than the pavements age divided by 2. Normal

performing pavements were identified between these two values. Figure 2-10 shows the different LTPP sections analyzed and where they fell in age and % transverse cracking at the time of the study. In the report it was speculated that some of the very poor performers experienced construction related issues [Khazanovich et al., 1998].

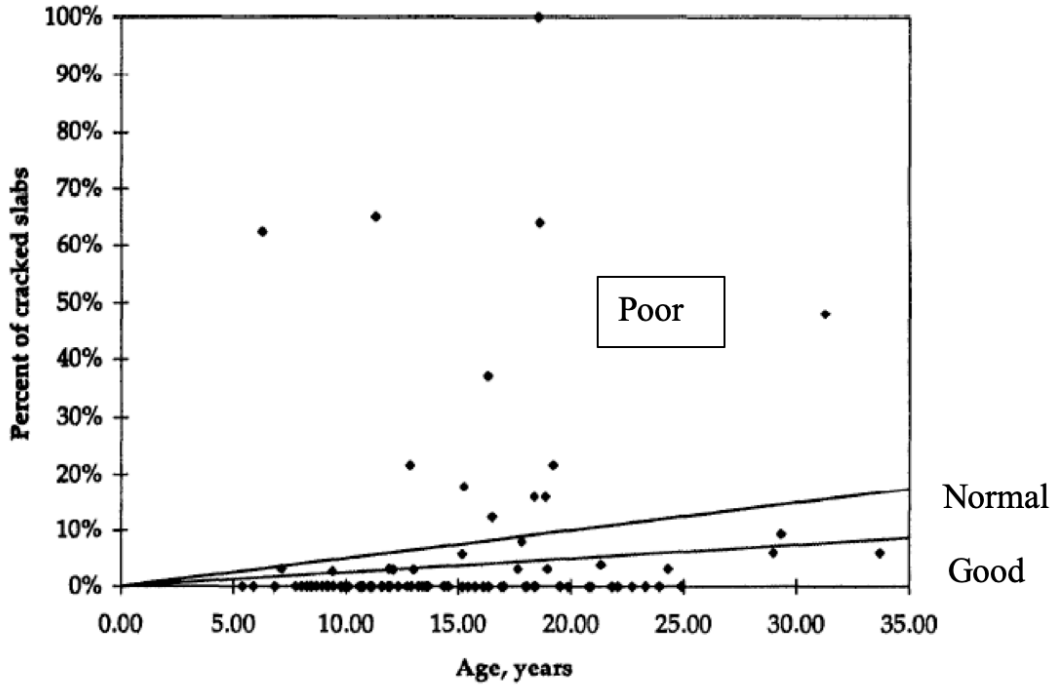

Figure 2-10 Good, Normal and Poor Pavement sections defined by % cracked slabs by age [Khazanovich etal., 1998]

LTPP has been collecting manual faulting measurements since the LTPP program began in 1988. They have also collected faulting with high speed inertial profilers (HSIP), although they did potentially have data issues as the HSIP data did not always detect the joints automatically in the older data [Agurla and Lin, 2014].

2.2.4. Summary

Fracture mechanics in concrete is still evolving since concrete is such a non-homogeneous material. Cracking in concrete pavements is influenced by the invisible microcracking of the pavement structure and the fundamental physics of the need of the cracks tip to follow the easiest route for release of energy, which is also not always visible.

- Concrete material properties, both of the aggregate and of the mix, play a large influence on development and progression of microcracks and cracking. Detailed information on concrete properties are not typically available for the entire highway network.
- Accurately mapping the progression and path of cracks in concrete mathematically is something that will continue to evolve.
    - As such, 3D pavement data at a slab basis can be used to assist in validating fracture mechanics models, but fracture mechanics does not now provide tools to assist in analyzing 3D pavement data.
    - A better understanding of variability in concrete pavements at different scales based on examination of 3D pavement data could benefit fracture mechanics models in the future.
- A clear understanding of failure is necessary to compare results, and different definitions of failure may provide different information. There exists a need to have a common description for failure.

AASHTO Pavement ME Design and the LTPP data are currently the best available sources of distress prediction models and data to analyze concrete pavements.

- 3D pavement data has the capability of working with both of these to improve the modeling and behavior analysis of concrete pavements.
    - 3D pavement data can be used now to compare to the predictions of the PMED and look at the variability in the 3D data as compared to the reliability levels in the PMED for LTPP pavement sections.
    - 3D pavement data can be used to provide future empirical data to develop new and improved PMED models.
    - Combining the LTPP and 3D pavement data provides the historic breadth needed to analyze and make appropriate use of the 3D pavement data capabilities now.
- The LTPP definitions of pavement performance (good, poor, normal) developed using a combination of field data and expert opinion are a consideration in classifying and categorizing pavements using 3D pavement data.

2.3. Detailed Slab Cracking Behavior on Select LTPP Sites and Longitudinal Cracking

2.3.1. LTTP Wet-No-Freeze GPS-3 Sites – Slab Cracking Behavior

The LTPP General Pavement Sections 3 (GPS3) are composed of jointed plain concrete pavements, both doweled and undoweled, that were constructed before being identified as research test sites. The pavements vary in thickness, joint spacing, and base type. For purposes of observing cracking behavior, this research effort was restricted to the LTPP GPS 3 sections in the Wet-No-Freeze (WNF) region of the US. Georgia is located in the

WNF regions, and the 3D pavement data that was also part of this effort all came from Georgia. Cracking was examined based on the pdf version of the individual detailed manual inspection reports (Distress Maps) created as part of the LTPP inspection, based on inspections performed typically every 2 years (See Figure 2-9 in Section 2.2). The inspections were performed manually on site typically with traffic control for close inspection (termed MDS for manual distress survey) or using equipment which collected images and information automatically (noted ADS for automatic distress survey). The inspections included noting the locations and length of cracking on sheets that depicted every slab in the test section. Spalling, other type of cracking (map, D-cracking), patching, and other distress types noted in the LTPP Distress Identification manual were collected and documented by trained inspectors. The length of cracking for each section and other distress values and indicators are included in the InfoPave LTPP database for each section. Fields include length of longitudinal cracking at different distress levels (i.e. LONG_CRACK_L_L for length of longitudinal cracking severity level 1), number and length of transverse cracks (i.e. TRANS_CRACK_NO_L for number of transverse cracks and TRANS_CRACK_L_L for length of transverse cracking severity level 1). The information in the database is summarized by LTPP section and is not separated for each slab. To gather information on a slab level the individual distress maps need to be reviewed individually. Reviewing the individual cracking maps also provided evidence of data inconsistencies in the LTPP data, that will be discussed further later in this section.

Composite Cracking Maps

For each LTPP section the progression of cracking in each slab from each inspection was identified and compiled on to one sheet (front and back) using colors to

depict changes in cracking measured at different years. An example of one side of one of these composite crack maps is shown in Figure 2-11. Each full slab is shown and numbered (note after the first row only the first slab was numbered on the form). The dates of inspections were recorded on the form and noted as NC (not cracked) until the first crack was identified. Dates after cracking were noted in color and also color coded on the slab that was cracked. Cracks that extended in subsequent years show up as different colors to show the progression of cracking in the slab and to identify when a previously cracked slab went from a partial crack to a crack connecting the joints like shown in Slab 8 in Figure 2-11. Slab 8 first experienced longitudinal cracking in 1999 (orange) and one of the cracks extended in 2002 (blue) while the other crack extended all the way across the slab in 2012 (brown). Patching was noted in 2002 (blue) as shown on slab 14 and 15 in the Figure. The other side of the sheet contains the remaining slabs and information on the section (Location, JPC thickness, joint spacing, dowel condition, base/subgrade, AADTT, year constructed and any maintenance noted in the LTPP database).

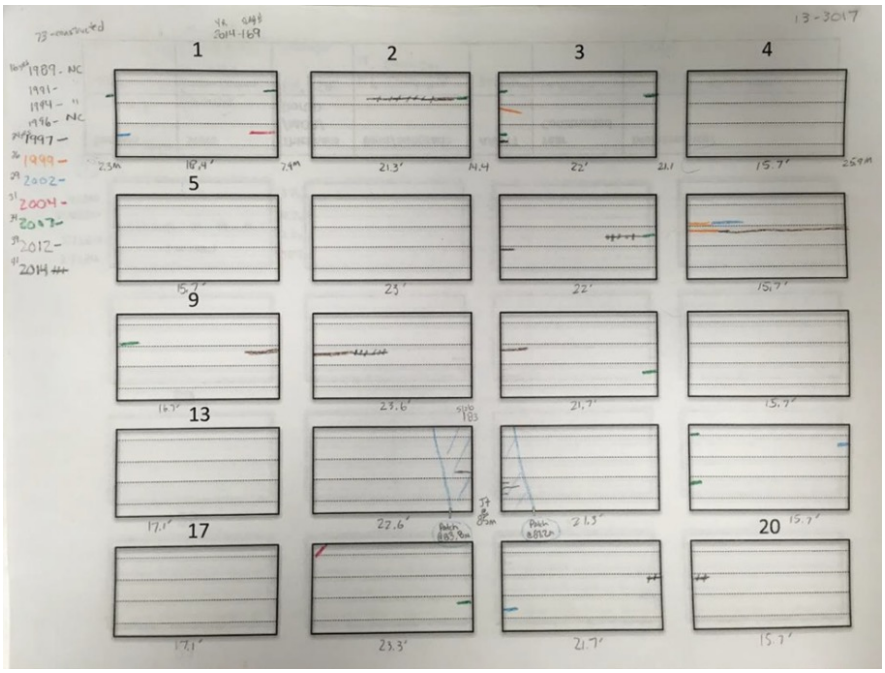

Figure 2-11 Composite Crack Map for LTPP Site 13-3017

From the LTPP database, Section 13-3017 in the Figure was ground in May 2000 and the patching was performed in 2001. Note that the sheet indicates 2002 for the patch at slab 14/15, that is the first inspection date following the patching operation.

GPS-3 WNF

41 sections from 13 different States and Puerto Rico are shown in the Infopave LTPP website (Infopave.fhwa.dot.gov) as part of the GPS 3 experiment in the WNF climatic region. For the purposes of reviewing the cracking behavior on a slab level, only the 33 GPS 3 WNF sections located in or near the southeast were considered. The sections were from 10 States and the number of LTPP sections in each state are: Alabama (1), Arkansas (1), Florida (7), Georgia (8), Kentucky(1), Mississippi(2) Oklahoma(4), North Carolina (5), South Carolina (1) and Texas (3). Two of the seven Florida sites were omitted since they were so cracked at 4 or 5 years or already had removal and placement at first

inspection that it was expected that a construction issue was involved. One of these two sections from Florida was specifically identified as an anomaly in a 1998 LTPP research report on JPC performance of LTPP sites [Khazavonich, 1998]. Another Florida section only had one cracked slab, but it was also the slab where a WIM was placed, and it appeared the crack developed as a direct result of the WIM so it was not considered to be typical cracking behavior. The majority of the sections were 8 to 12 inches thick with joint spacing averaging around 20 ft. Five other sections were omitted since they were anomalies: two of the Florida sites were less than 7.5 inches thick, one Texas section was 12.5 inches and two North Carolina sites had 30 ft joint spacing. The remaining 25 LTPP sites were reviewed for trends in cracking behavior. The range and average of values for several different factors for these sections are shown in Table 2-3.

Table 2-3 Range and Average values for the GPS-3 WNF sections reviewed

25 GPS 3 WNF sections	# slabs in the sections	# cracked slabs *	% cracked slabs *	JPC Thickness (inches)	Construction Date Range
Minimum	20	0	0	7.9	1960
Maximum	33	25	100	11.8	1986
Average	26.7	6.5	26	9.6	1978

*maximum number of slabs with any type of cracking identified at any one inspection

General Cracking Behavior of the LTPP sites

Six of the 25 sections (053011(Arkansas), 133007 and 133011 (Georgia), 283018 (Mississippi), 404157, and 404160(Oklahoma)) have no cracking whatsoever after 30, 33, 41, 26, 29 and 28 years of inspection reports, respectively. Another 7 sections (124000,

133017, 403018, 404162, 483003, 483589) do not have any transverse cracking after 41, 41, 28, and 12 years respectively. Therefore ½ of these LTTP sections are showing no AASHTO PMED distress (main cracking distress modeled in MEPDG and used in the AASHTO PMED software). Of the 6 sections that have no cracking at the last inspection reviewed, 5 of them have cracking identified in the Infopave database as noted below:

- Section 05-3011 in Arkansas shows a transverse crack in the Infopave database in 1992. ADS measurements were used in 1992, but MDS in 1994, 1997, 2003, 2007, 2010 and 2013 showed no cracking, and no maintenance activities were noted.
- Section 13-3007 in Georgia shows a transverse crack in the Infopave database in 2003. ADS measurements were used in 2003, but MDS distress maps from 2004, 2007, 2012 and 2014 show no cracking and no maintenance activities were noted.
- Section 13-3011 in Georgia shows a transverse crack in the Infopave database in 2003. ADS measurements were used in 2003, but MDS distress maps from 2004, 2007, 2009, 2012, 2014 and 2016 show no cracking and no maintenance activities were noted.
- Section 28-3018 in Mississippi shows a transverse crack in the Infopave database in 1993, 1995, 2001 and 2003. ADS measurements were used in those years, but MDS distress maps from 1995, 2003, 2007 and 2010 show no cracking and no maintenance activities were noted.
- Section 40-4160 in Oklahoma shows a transverse crack in the Infopave database in 1993 and 1995. ADS measurements were used in those years, but MDS distress maps from 1994, 1997, 2007, 2009 and 2013 show no cracking and no maintenance activities were noted.

As evidenced by these five sections, some errors were identified in the Infopave database. Based on a close review of the data and the individual LTPP MDS maps, three different scenarios of discrepancies between the database and the LTPP maps were identified.

Scenario 1 – Automated data detection error

The database includes cracking that was identified using early versions of automated detection, which appears to have issues with false positives. At least five sections that were identified as having experienced cracking in the database do not appear to have ever been cracked based on subsequent manual inspections. Visual observation of the results of some of the ADS results show these misidentified cracks are predominately small cracks and they are often found in the center of the slab, not at a joint. This could be due to shading, material related distress issues, map cracking or aggregate popouts. It is possible that other sections are included in the database in a similar situation.

Scenario 2 – Misidentification of cracking type

Based on review of the individual distress maps, crack lengths in the database are in question. It was found in a number of sections (namely sites 133016, 133019, 132020, 213046, 373008, 373807, and 483589) that cracking, especially longitudinal cracking, was later identified as map cracking and not longitudinal cracking. This was predominately cracking that did not extend to a joint or short lengths of longitudinal cracking. Typically, short distances of longitudinal cracking in the center of a slab was identified later as map cracking. Cracks at joints appear to stay where the cracks noted more often, those not going to a joint later were more often noted to be map cracking. One problem identified with longitudinal cracking near a joint was that one year it would be noted as longitudinal

cracking and labeled as spalling the next year. Longitudinal cracking also disappeared without explanation much more often than transverse cracking. This could be to the misidentification as map cracking, or maintenance of the section (diamond grinding).

Scenario 3 – Cracks moving for unknown reasons

Figure 2-12 shows an example of a moving crack. The Figure on the left is Section 13-3020 from 2007 and the Figure on the right is the same portion of the section from the 2009 inspection. Note that the crack in 2007 in Slab #13 either shrinks or it moves closer to the centerline in 2009. Other moving cracks include cracks shown at the corners in in one year and not shown again (403018), and a crack moving from one slab to another in a subsequent inspection (133019). Summary information on the LTPP sites reviewed for this research is included in the Appendix.

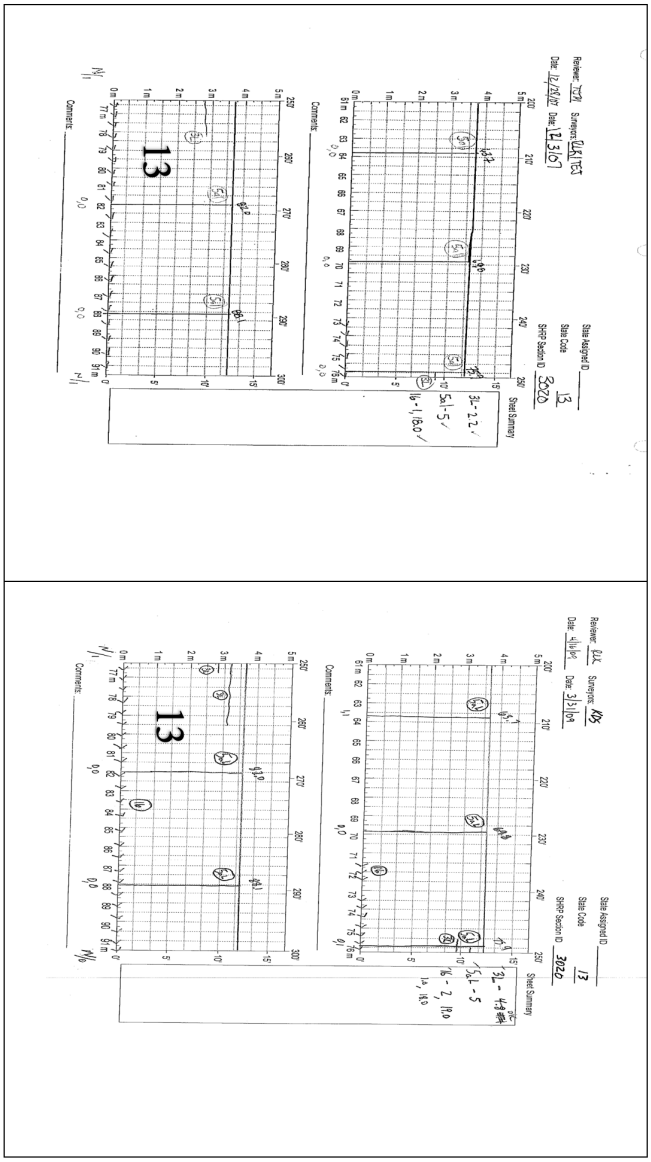

Figure 2-12 a) 2007 inspection and b) 2009 inspection from LTPP 13-3020

The WNF GPS LTPP sections were reviewed to identify typical and unusual patterns of cracking. Based on the 19 projects noted in Appendix Table A- that experienced some type of cracking, 178 slabs were identified as cracked but just 16 of these slabs had both longitudinal and transverse cracking. Half of these slabs contained longitudinal and transverse cracks that did not go from joint to joint, while half had at least one crack touch both sides of the joint (either the transverse or longitudinal joints).

Eleven of the sections noted in Appendix Table A- consist of undoweled pavement, while 14 were doweled. Table 2-4 shows the predominate condition of the cracking as related to the existence of load transfer, as can be seen, the longitudinal only did have a higher number of doweled sections, but when considering a combination of longitudinal and transverse cracking there were a higher number of undoweled sections. It should also be noted that none of the sections contained a 14 ft widened lane.

Table 2-4 Comparison of Cracking Orientation and Dowel Condition

Cracking	D	UD
Only T	2	1
Only L	5	1
Combination T/L	3	6
No cracking	4	3

Specific observations from the LTPP Distress Maps include that of the 33 slabs that cracked completely (joint to joint) transversely,78% (25) completely cracked in one review cycle (typically 2 years). Of the 54 slabs with some type of transverse cracking, 60% (33) cracked completely joint to joint. This shows that for these sections, the majority of the time a transverse crack developed and cracked completely across the slab relatively quickly, instead of slowly cracking over time. This indicates that for transverse cracks the cracks often go all the way through the slab, which is more detrimental than just a surface crack. Transverse cracks that did not crack completely in one inspection cycle typically started cracking at the shoulder joint, but most transverse cracks that could be identified as to where they started also started at the shoulder.

In general, longitudinal cracking predominately was found in the center of the slab or close to the centerline. Longitudinal cracking was observed to both extend out from transverse joint to both adjacent slabs at the same location and to be isolated to one slab. In the LTPP sections reviewed here, as noted previously, longitudinal cracking was more common than transverse. Slabs with transverse cracks were more often found in isolated slabs. In contrast, longitudinal cracking was more often found adjacent to other slabs with longitudinal cracking. Longitudinal cracking that went from joint to joint more often showed up after a number of inspections, while transverse cracking from joint to joint showed up in one inspection more often as noted earlier. An example of this is shown in Figure 2-13. Slab 17 from Section 13-3018 shows longitudinal cracking starting on the left side after 18 years (orange) and then cracking on the right side after 19 years (blue) and then the cracks both extended by year 26 (brown). In year 24 another small crack started below the original crack (green).

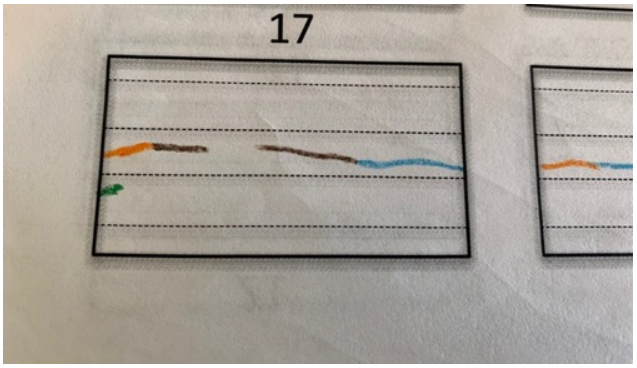

Figure 2-13 Progression of longitudinal cracking over time

Longitudinal cracking was more often found developing in consecutive slabs, while transverse cracking was more often found to skip slabs and fill back in over time. Even for the section that had 21 of 24 slabs transversely cracked (12_3811), the slabs cracked in

alternate years as shown in Figure 2-14. The figure shows that Slab 9 cracked before the first inspection at year 13, the adjacent slab did not crack until 10 years later, and the next slab (slab 11 (brown)) cracked three years later. In this same LTPP section, as shown in the figure, adjacent slabs cracked in consecutive three year time increments. This more uniform spread of cracking is indicative of a normal distribution of material related distress that would be expected with fatigue failure of the concrete, as compared to the clustered longitudinal cracking.

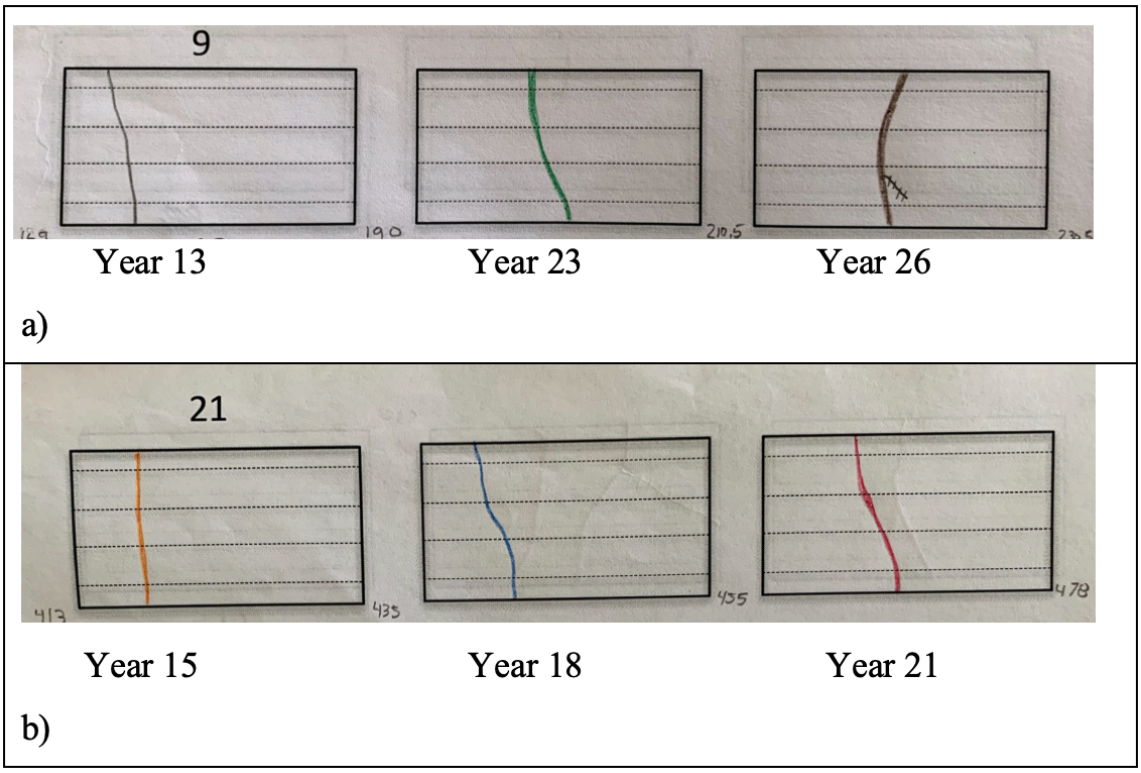

Figure 2-14 a) and b) Transverse cracking over time

2.3.2. Longitudinal Cracking

As noted in Section 2.2.2, AASHTO Pavement ME Design (PMED), does not recognize longitudinal cracking in the estimation of pavement distresses. As noted in the previous

section (2.3.1) and will be discussed later, longitudinal cracking is prevalent in LTPP sections and was identified in Georgia 3D pavement sections. Longitudinal cracking has long been considered an unusual instance in jointed plain concrete pavements resulting from uneven foundation conditions, improperly cut longitudinal joints, dowel or tie bar issues or because of the use of widened lanes. Discussion and research on longitudinal cracking in CRC pavements is much more prevalent than for JPC pavements.

Recently an emphasis on modeling longitudinal cracking, especially as related to patterns identified in the southwest, has been documented. Hiller and Roessler modeled longitudinal cracking in pavements in California related to temperature and moisture gradients [Hiller, 2002]. More recently, Xu and Cebon looked at JPC SPS-2 (specific structural factor experiment) LTPP sites in Arizona and Arkansas and although the amount of cracking in the widened slab sections was higher, they identified longitudinal cracking in both sections with widened slabs and standard slabs. In fact, longitudinal cracking was found in more of the sections than transverse cracking. [Xu, 2017]. Based on an Infopave download of 661 LTPP JPC surfaced pavements, 262 sections had no cracking (40%), 271 identified transverse cracking of some severity level (41%), while 250 identified longitudinal cracking of some severity level (38%). Although some of this cracking may be map cracking as noted earlier, this amount of longitudinal cracking identified appears to be more than would be expected solely based on unusual conditions. As part of this research, pavements in the southeastern states and particularly in Georgia identified longitudinal cracking, and in some cases the sections exhibited longitudinal cracking as the predominate distress.

In terms of identifying cracking distresses, most States identify both transverse cracking and longitudinal cracking. Many also identify corner cracking (or corner break) separately and divided slab (or shattered slab) to identify slabs that have multiple cracks [Wolters, 2010]. Many States treat transverse and longitudinal cracking differently, either by using different severity levels (i.e. OR, CO), measuring them differently (i.e. IA tracks the number of transverse cracks but captures length of longitudinal cracks), or weighting them differently (ie. FL and GA deduct values are twice as high for transverse cracking as longitudinal, where WA uses values of ~1.5 and ~2 for longitudinal and transverse cracking respectively.). Florida specifically notes in their rigid pavement handbook that transverse cracking is more prone to deterioration than longitudinal cracking due to the load transfer effect as a vehicle travels over the transverse crack. The handbook also recognizes that even longitudinal cracks can deteriorate quickly if they are sufficiently open such that water or debris can get into the crack [FDOT, 2015].

A few States identify transverse and longitudinal cracking separately but consider them similarly, recognizing that they represent different mechanisms that can each lead to structural failure. Illinois has the same severity level categories for transverse and longitudinal cracking but notes that transverse cracking "is a normal occurrence and is caused by one or more of the following: heavy vehicular load repetition, thermal and moisture gradient stresses, drying shrinkage stresses, loss of subgrade support, and/or non-functioning contraction joints. " and longitudinal cracking "may be the result of concrete shrinkage, warping stresses, improper sawing, or loss of support." [IDOT, 2010].

2.3.3. Summary

JPC pavement can have a relatively considerable life span, as noted by pavements identified in the LTPP database with no cracking after 30-40 years in service. Therefore, historical data on the actual deterioration of JPC pavements is limited. This increases the importance of 3D pavement data to provide a wide range of information on the mechanisms and patterns of cracking in JPC.

One area in particular that 3D pavement data can assist with is the manifestations of longitudinal cracking. Based on the LTPP data reviewed, longitudinal cracking does occur and it appears to develop differently than transverse cracking, enough so that it potentially may require its own prediction models, separate from transverse cracking.

2.4. Summary of Literature Review and Identified Research Need

JPC Pavements have different mechanisms and manifestations of cracking. State DOTs monitor their JPC pavements in a similar manner, but enough difference exists to prevent the sharing of data. The LTPP data is the most comprehensive database on concrete pavement, but a number of the JPC pavements in service have no cracking, so that limits the amount of cracking data further. The LTPP pavements also only include 25-30 slabs and so miss the variability that can be recognized with a larger data set. Due to the relatively limited number of concrete pavements and their typically long lifespan there is a need to be able to categorize JPC cracking in pavements in a more detailed manner so data can be better utilized.

The current pavement performance measurement of % transverse cracking omits different types of cracking and therefore different failure modes. It is also not very descriptive of

the overall pavement condition. There is a need to characterize JPC cracking considering orientation, spatial patterns and rate of deterioration. Failure models with clear definition of failure are also needed to allow for comparing pavement condition and assessing end-of-life.

CHAPTER 3. 3D SLAB BASED METHODOLOGY: FUNDAMENTALS

This section presents the fundamentals of the spatial and temporal 3D slab-based methodology used to define, analyze, model and apply the information on the distress state of individual slabs and slab systems in a jointed concrete pavement using 3D pavement data. The 3D Slab-Based Methodology consists of 4 Modules, the first two defining and presenting the fundamentals. This section describes Module 1, Slab States and Module 2, Spatial-Temporal Orientation. First a description of the data and data collection method is presented.

3.1. 3D Pavement Data Collection for Concrete Pavements

This section describes how the 3D pavement data was collected and describes 3D pavement data.

The first step is to collect high-resolution 3D pavement data on JPCP, which is necessary for measuring faulting, crack length and crack type. Georgia Tech's sensing vehicle (GTSV), as shown in Figure 3-1, equipped with a 3D line-laser-imaging system (LCMS or laser crack measurement system), global positioning system (GPS), cameras, and a high-resolution distance measurement instrument (DMI), was used to collect the data. With a line scan rate of 5,600 profiles per second, the system used on the sensing van can provide an interval of 0.2 inch (5 mm) in the longitudinal direction (travel direction) driving at up to 62.5 mph (100 km/hr) [Tsai et al., 2015]. On a 30 ft. slab, approximately 7.3 million 3D points can be collected and detailed distress information can be extracted from this set of data. The 3D pavement profile data can achieve a 0.02 inch (0.5 mm) resolution in the z-

direction. In addition to collecting GPS, DMI, and 3D pavement data, GTSV can also collect LiDAR (Light Detection and Ranging) data for inventorying roadway and roadside assets, such as signs [Ai et al., 2015 and Ai et al., 2016], pavement markings, and guardrails.

Figure 3-1 Georgia Tech Sensing Vehicle (GTSV)

GTSV was integrated through the research projects "Remote Sensing and GIS-enabled Asset Management (RS-GAMS) Phase I and II", sponsored by USDOT to develop a cost effective means for asset inventory [Tsai et al., 2013]. After processing the data, XML files containing the raw data and image files for both range and intensity are generated. Georgia Tech post-processes this data into a 'rectified range' that smooths out the overlaps of the two lasers and the transition between each transverse image. New files in XML format are also developed using an automatic crack algorithm developed at Georgia Tech (referred to here as GT XML files) [Jiang, 2015]. Georgia Tech also developed software (Slabviewer2) to further analyze the results from the LCMS. Slabviewer2 (SV2) is a program that was specially developed to assist in analyzing Jointed Plain Concrete Pavements. SV2 is

currently running as a MATLAB program which reads data from the semi-automatically digitized GT XML files. The program uses the rectified range images or 3D images and displays the joints and any cracking in the slabs as shown in Figure 3-2.

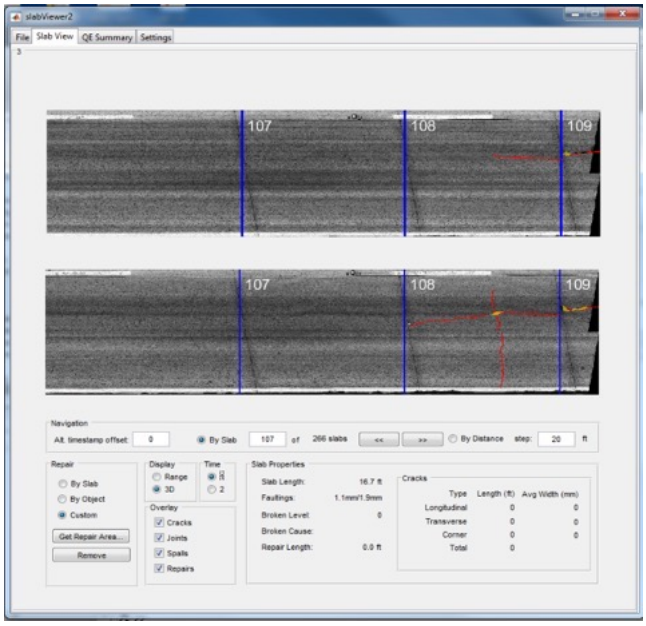

Figure 3-2 Slabviewer 2 (SV2) Application

As well as identifying the slabs by number, the program computes the slab length and identifies any crack length and average crack width previously calculated using the GT algorithm. The results are provided in an Excel output which includes a slab by slab identification of the slab length; average faulting based on the LCMS default method, categorized crack type and severity, and crack length and width. As described later, crack width for sealed cracks was not indicative of the actual crack width and therefore crack length and not crack width was used as a predominate measure in defining slab states. A separate MATLAB program described in a presentation at TRB and in the TRR [Geary et al., 2018] uses the 3D pavement data to compute faulting. At the time of this writing other students under Dr. Tsai are working on incorporating the new faulting algorithm into

Slabviewer2. Faulting was not used in defining slab states, but could be used in the future, especially in relation to determining severity of cracking. As noted earlier, the current standard for faulting (AASHTO R 36) does not have a 3D option for faulting and a procedure was developed using 3D pavement data for an alternative method C, which was provided to AASHTO in 2019 for possible inclusion into the standard.

Although Slabviewer2 provides a length of each slab in the Excel output, that length is not consistent year to year due to a number of factors, including vehicle wander, tire pressure, etc. Discussion of the issues of registering 3D pavement data for pavements has been documented and addressed by others [Wang, 2017] and will not be addressed here beyond describing the methods used to register the sections for this research. With no slab changes in a section over time, JPC pavements can be analyzed by simply consistently identifying the same starting slab each year and using the same number of slabs to represent the same section each year. Unfortunately, slabs also change in length and number due to maintenance efforts, like full depth slab replacement described earlier. Over the six-year time period considered in this research every pavement experienced some type of slab altering rehabilitation. For this reason, it was necessary to rectify the begin and end of each pavement section completely and not rely only on identifying a starting slab and number of slabs. The sections and lab lengths were then normalized by the total mileage. The first year of data, 2013, was used to normalize the mileage in each section.

3.2. 3DSBM Overview

The Methodology as shown in Figure 3-3 consists of four Modules:

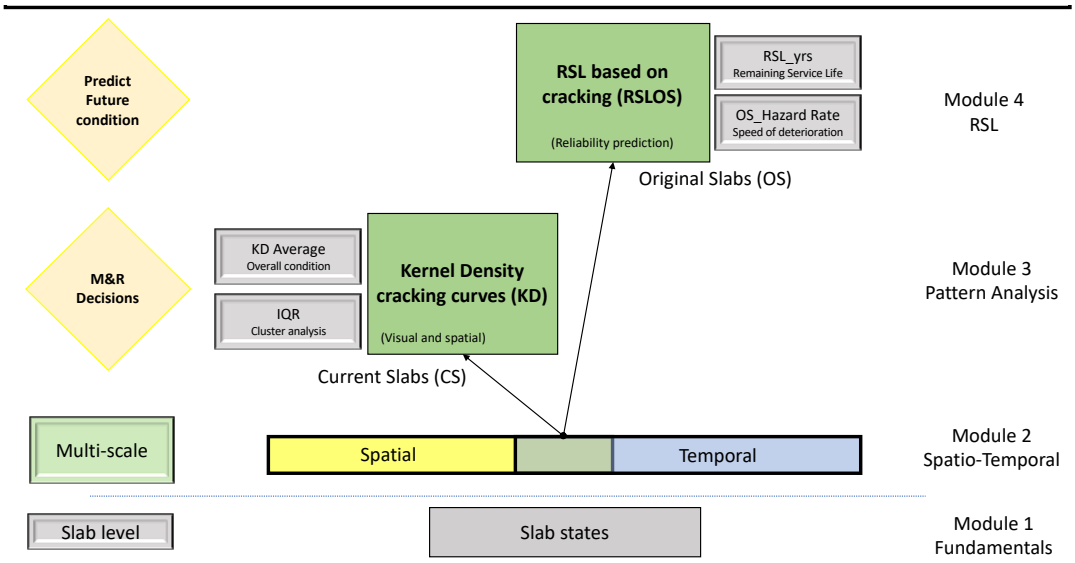

Figure 3-3 3D Slab Based Methodology Modules

1) Slab State Fundamentals:
    a. Identification of individual slabs,
    b. Classification of individual slabs based on cracking orientation, crack length and crack width into slab cracking severity ‘states’,
2) Spatial And Temporal Components:
    a. Aligning/rectifying the slabs in time to measure changes in distress by slab
    b. Analysis of a Pavement Section using Slab State components
3) Classification of the cracking patterns in a section using kernel density (KD) regression smoothing and a numerical transfer function (KDValues) for slab states
    a. Average KD Value (KDAve) and change in KDAve for condition assessment
    b. IQR of the KD values for cluster analysis

4) Prediction of changes in the pavement sections using RSL (remaining service life) concepts and consistent deterioration rates based on original slabs and modeling using Reliability Engineering theory
    a. RSL_yrs indicates the modeled remaining life of the pavement
    b. OS_Hazard rate is the modeled rate of deterioration.

The four 3DSBM Modules provide for the evaluation and prediction of a pavement sections deterioration and maintenance and rehabilitation needs using the aforementioned statistical indicators. The Modules are described in the following sections.

3.3. Module 1: Slab States

The 3DSBM is based on the Slab States and slab classification criteria depicted in Figure 3-4. The slab 'states' are designed to demonstrate a progression of cracking and a predominate orientation of cracking in each individual slab. Categorization is then used to analyze individual pavement sections at multi-scale, using the individual slabs classification.

The three most common distresses used to monitor the condition of JPCP are cracking, faulting and IRI (international roughness index). Of these cracking and faulting can be identified by individual slab, with a slab identified as a section of pavement separated by two transverse joints. Slabs typically are designed to be between 15 and 30 ft in length. IRI is typically reported to the 0.1 mile (~500 ft) or 1 mile level, so it really does not have meaning at a slab level, although the condition of a slab and faulting at a slab level do affect IRI. This research focuses on cracking at the slab level.

Using 3D pavement data, each slab can be categorized and classified, in relation to the predominate type of cracking in the slab, as shown in Figure 3-4. Each crack in the slab is identified as to the length, width and orientation (orientation is defined by the joint that the crack intersects, and the predominate length).

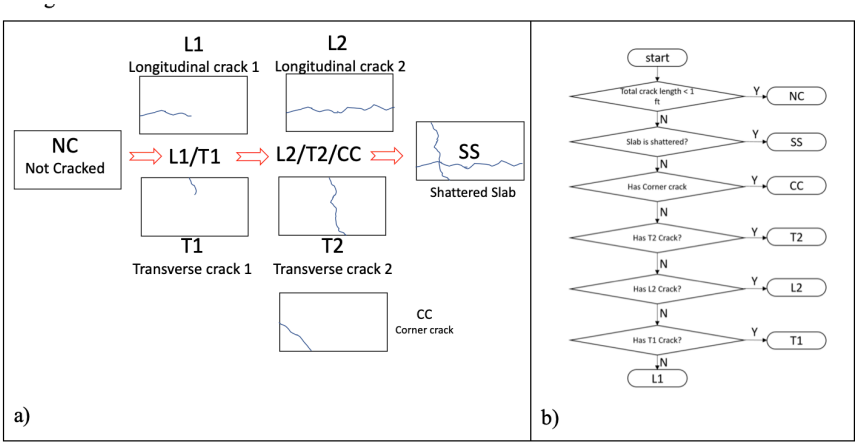

Figure 3-4 a) Slab States and b) Slab Classification Flowchart

Cracking in the slab is identified based on these 'Slab' states. Where:

- NC - Not cracked
- L1- slab with longitudinal crack longer than 1 ft, starting at a transverse joint
- T1 - slab with transverse crack longer than 1 ft, starting at a longitudinal joint
- L2- slab with longitudinal crack (L1) longer than 75% of the length of the slab
- T2- slab with transverse crack (T1) longer than 6 ft
- CC- slab with crack that touches two adjacent joints at a corner
- SS – Slab cracked into three pieces, typically either:
  - [1] Slab which can be classified as L2 and: T1 or T2
  - [2] Slab which can be classified as T2 and: L1 or L2

The orientation differentiates longitudinal cracking from transverse cracking. Corner cracking is identified as cracking that goes from joint to joint but is confined to one quadrant, like shown in Figure 3-5 in the lower left corner. Longitudinal cracking is identified as cracking that occurs in the direction of the longitudinal joint and transverse

cracking is identified as cracking that occurs parallel to the transverse joint, like the crack near the center of the slab in Figure 3-5 (Note that Figure 3-5 would actually be considered a SS since it has two different types of cracking that divide the slab into three pieces).

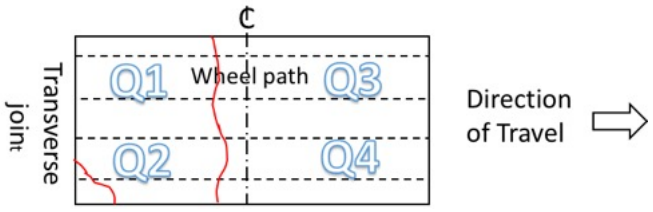

Figure 3-5 Slab level model

The Slab states are aligned with the research level LTPP distress manual cracking types of longitudinal, transverse and corner as shown in Figure 3-6, but note that LTPP does not have a shattered slab (SS) criteria. LTPP instead notes the cracking in each individual slab [Miller and Bellinger, 2014].

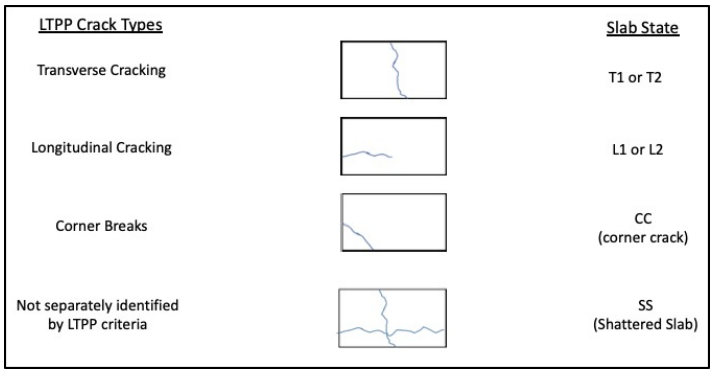

Figure 3-6 LTPP Crack Types and Slab States

Slabs with typical loading, neutral internal stresses and uniform support should suffer fatigue cracking transversely near the center of the slab, as modeled in the AASHTO Pavement ME Design (PMED) software. While longitudinal cracking is not modeled in PMED, it is found in the LTPP sections reviewed, the Georgia 3D pavement sections and

other pavements. As noted previously, some pavements in the LTPP data and in the Georgia 3D pavement data were even identified with primarily longitudinal cracking and therefore it is an important part of cracking that needs to be considered. Longitudinal cracking also needs to be separated from transverse cracking as it tells us something about the internal stresses in the slabs (built-in curl or warp) and/or it tells us the slab is non-uniformly supported. Similarly, corner cracking is typically an indication of loss of support and tells us about non-uniform support in a slab, or if a pattern is identified, in the pavement system itself.

Since concrete is affected by environmental effects (i.e. it contracts and expands under temperature fluctuations), evidence of cracking in concrete slabs can be dependent on the temperature at the time of inspection. LTPP sections are typically monitored every other year, and the 3D pavement data used in this research was collected on a yearly cycle. From inspection of a number of LTPP crack maps it was found that short cracks are especially prone to be identified one inspection time and then later not identified. As noted in Section 2.3, it was found that longitudinal cracks were especially prone to be later identified as map cracking or were truly only surface cracks as they disappeared after diamond grinding. Other transverse cracks were found to also become 'phantom' cracks if they did not start or end at a joint. Cracking that does not extend all the way to a joint indicates that the slab is not actually cracked completely through. This is important, since only a completely cracked slab can settle or move/rock. Cracking itself is detrimental since it allows water into the pavement system, and it is a possible point for spalling to develop. But a slab that is only surface cracked will not allow water ingress, and a crack that is sealed can behave similar to a pavement joint and not develop further distress, if load transfer occurs across

the crack. When a slab is completely cracked there is the potential that the slab acts independently and moves independently, which will lead to further deterioration and is detrimental to vehicular traffic. Therefore, cracking for both longitudinal and transverse cracking was only considered if it started or ended near a joint. Also, although 3D pavement data can provide crack width, it is subject to the same thermal effects as apparent crack length and it can also be masked by a sealed crack, so it was not used solely to define slab 'states', but a comparison of average crack widths for level 1 and level 2 states was found to show statistical differences and can be used to assist in classification of slab states.

It was observed that in a number of LTPP sites short longitudinal cracking at the joints appeared stable over a period of time, this may be due to the dowel bars holding the cracking or the dowel bars being the cause of the initial cracking, instead of fatigue related cracking. This type of multiple cracking was found much less in the transverse direction, and when it was found in the longitudinal direction it tended to be stable over time. For this reason, it was decided to ignore multiple cracks of the same type in a slab. This also simplifies the slab states. Based on these considerations this research uses major changes of two levels to denote a change in slab state instead of number of cracks, lengths of cracks, or crack width. The intent is to model measurable changes in cracks over time as accurately as possible. Even in LTPP research grade manually collected data, as noted previously, cracks were occasionally shown to disappear, or apparently shrink in length or width, over time. In a recent FHWA sponsored research project that used LTPP data from a number of sites, including the two sites shown in Figure 3-7 they found issues with length and classification in cracking in LTPP sites over time and identified these three issues:

pavement temperature, subjectivity of the surveyor, and that use of three severity levels was inherently an issue in variability [Baladi, 2017].

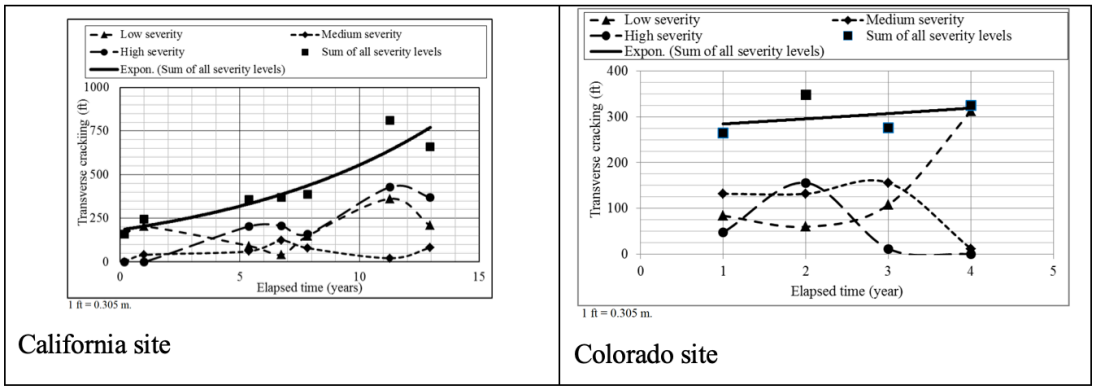

Figure 3-7 Inconsistencies found in LTPP data for cracking and crack severity (from Baladi, 2017)

3D pavement data is therefore classified in this research using the predominate orientation of the cracking and the relative length of the cracking, not according to low, medium or high severity. Slab state T1 or L1 is cracking predominately in the transverse or longitudinal direction, respectively. Cracks that are less than 6 ft long transversely or less than 3/4 the distance of the length of the slab are considered T1 or L1, respectively. The lengths used for the cutoff between level 1 and level 2 were originally based on analysis of available 3D pavement data. The values chosen were shown to provide the most consistent trend in slab state progression based on the available digitized crack mapping of Georgia pavements. (The original proposed differentiation between T1 and T2 was a crack that was 10 feet in length instead of 6 feet.) The intent was to separate partially cracked from fully cracked slabs, as it was considered that a fully cracked slab would not appear to decrease in crack length over time. Because FHWA HPMS requires reporting slabs cracked transversely greater than half the width of the pavement, the definition of T2 was adjusted

from 10 feet to 6 feet to more closely match the HPMS definition, so the 3DSBM could also be used for HPMS reporting. Therefore, slabs with cracking greater than Level 1 (75% of the length for longitudinal and 6 feet for transverse) up to completely cracked from joint to joint are denoted as level 2 (T2 or L2).

Slabs that exhibited cracking in both the longitudinal and transverse direction did exist as noted earlier in Section 2.3. In the case of slabs that included both L1 and T1 cracking but the cracking did not intersect, the T1 designation was deemed to control in deference to the typical cracking type used for design. An example is shown in Figure 3-8. If a slab had a L2 longitudinal crack and a T1 crack that did not intersect, the L2 was deemed to control, since it was a full or close to a fully cracked slab.

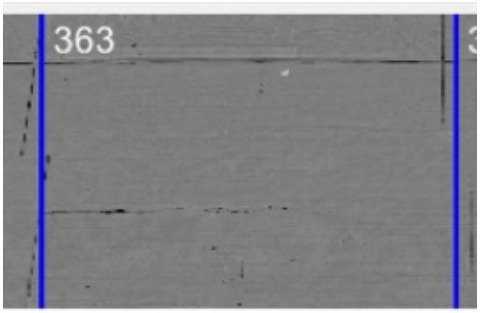

Figure 3-8 Slab with multiple non-intersection cracks

Complete cracks in one quadrant are designated corner cracks (CC). Corner cracks can also start out as L1 or T1 cracks and turn into corner cracks. Slabs with cracking that intersected such that they separated the slab into three or more pieces were considered the worst condition and were designated as shattered slab, SS. The Slabs were also considered in order as shown in Figure 3-4b): L1, T1, L2, T2, CC, SS such that a slab with components

of two different types of cracking would always be considered to be the higher order (i.e. if a slab has a T1 and a L2 crack and it is not considered CC or SS then it would be L2).

Each slab in the LTPP sections of interest and in the 3D pavement data were categorized as to their slab state. The excel files from SV2 provided longitudinal, transverse, corner and total cracking for each slab. The length of the predominate crack was considered in labeling the different levels (1 or 2). Slabs could be defined as L1, L2, T1, T2 or CC based on this information. SS was not able to be confirmed based on the excel data since it did not include points of intersection at the time of this research (Although the SV2 application is being updated to address). Some slabs that were identified as L2 were later identified as L1 due to multiple longitudinal cracks in the slab, not connected but added together by the algorithm. Therefore, slab classification was quality checked visually for each slab using Slabviewer2. It is anticipated that machine learning can be used to perform this slab categorization for future pavement sections, using the existing slabs and slab states to train the algorithm. The development of that is beyond the scope of this project, but it is discussed further in Chapter 7.

3.4. Module 2: Spatial-Temporal Orientation

The slab "states' identified in the previous section are expected to have a typical progression like shown in Figure 3-9. A NC slab would first have cracking extend from a joint predominately in the transverse or longitudinal direction, then the crack would extend to another joint, either fully across the slab or in the case of cracks near a corner, to the adjacent corner. The addition of a different type (L, T or C) of cracking that separates the slab into 3 different pieces leads to a Shattered Slab (SS). Repair or replacement of a slab

leads to a slab that is identified as RNC (repaired, not cracked) or just R, this slab state is described further in Chapter 5.

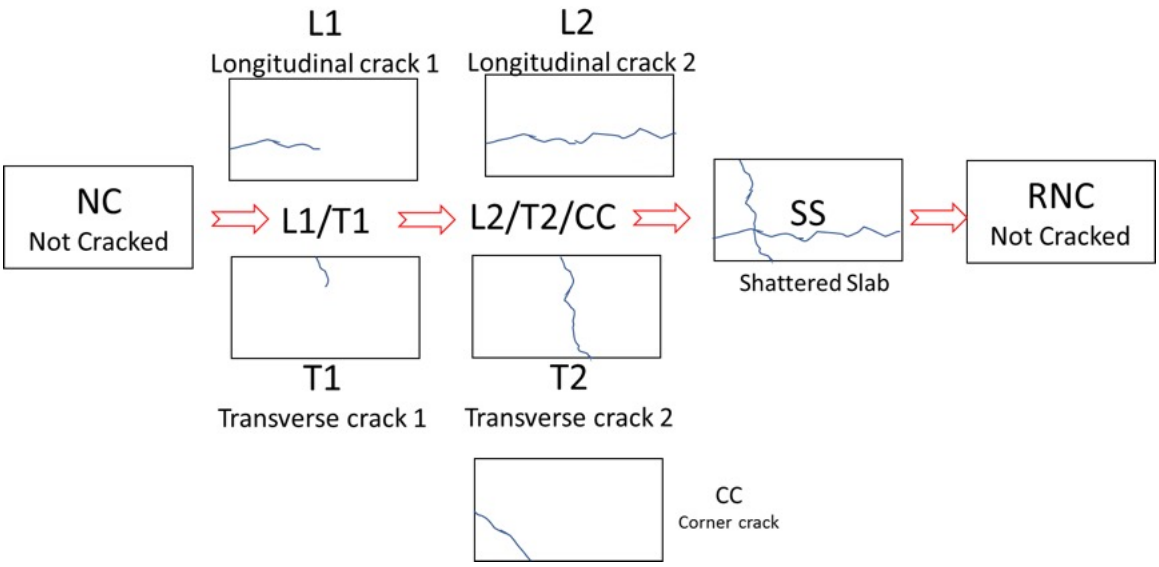

Figure 3-9 Temporal progression of Slab 'States'

Figure 3-10 is an example of the identification of slab states of a pavement section by slab, by year in Excel. It is an excerpt of a complete pavement section that consisted of 200+ slabs. SV2 provides the ability to classify each slab in a section, and with different year's data like shown here, the changes in the individual slabs over time are identified. As an example, Slab 190 and 191 both were L1 in 2013 but identified as SS in 2014 and 2015. In contrast slabs 195 to 197 were not cracked and did not change, and Slab 198 was L1 and stayed in the same state for all three years. (Note a "0" or a blank was used instead of NC in the excel files for ease of visualizing the data.)

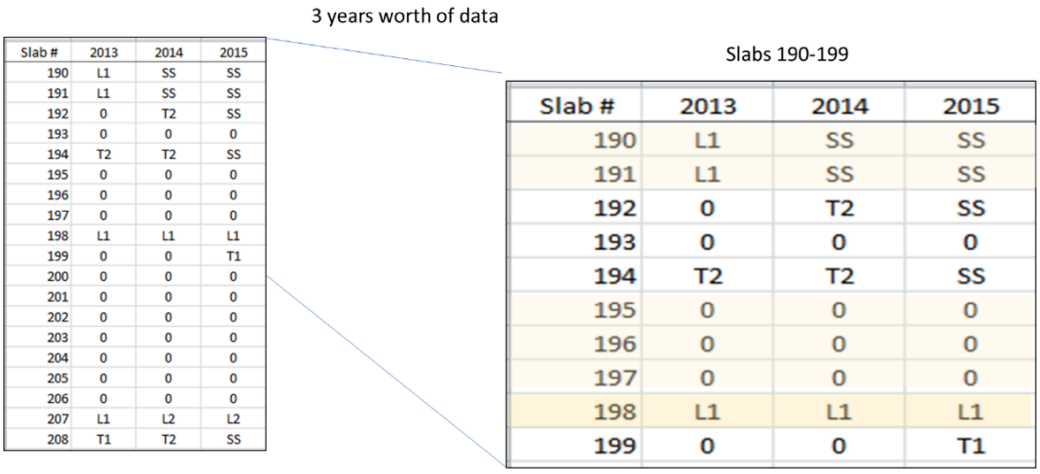

Figure 3-10 Change in Slab States over a three year time frame for a portion of a Georgia roadway [Tsai et al., 2017]

Georeferencing this data allows for overlaying the location of cracked slabs on a roadway map or a topographic map like shown in Figure 3-11, which depicts the location of T2 slabs as black dots along the roadway, and location of T1 slabs as smaller red dots.

Figure 3-11 Georeferenced Slab States on topographic map

The time a slab stays in a level 1 state can also provide information on the nature of the microcracking in the slab. Stable level 1 cracking that does not progress to level 2 indicates that whatever stress caused the initial cracking has been relieved, this type of crack could

potentially be stabilized through sealing the crack instead of replacing the slab. Stable cracking that can be identified completely or almost completely cracked from joint to joint (level 2) may indicate similar final stability. Faulting of the slab or crack would then be used to determine if full depth repair or simply crack sealing is a warranted maintenance treatment. Shattered slabs indicate cracking in more than one direction and can also identify the level of microcracking in the slabs, i.e. a pavement with a high level of slabs going from not cracked (NC) or level 1 (L1 or T1) to SS may indicate a pavement that has already experienced a large amount of microcracking and should be considered for overlay or lane replacement instead of simple full depth repairs. In addition to patterns in spatial and temporal dimensions, patterns in the changes of slab states can be quantified and used to identify the sections that are cracking to a more severe level at a faster rate (i.e. slab states going from NC to T2 or NC to SS). Computer algorithms can be used to automatically extract this information from the 3DSBM slab states.

Spatial and temporal patterns that can be identified by the 3DSBM are best described using actual pavements. Eight different pavement sections (~1mile), were selected for detailed evaluation and the details of each section are provided in the Appendix under Case Studies. The Case study sites are categorized into 3 different major categories (1, 2 and 3) and one minor subcategory (1b), based on the categories identified in previous research by Tsai [Tsai et al., 2012]. The Categories delineate different time periods of designs for Georgia DOT and are described more thoroughly in the Appendix.

Figure 3-12 shows the spatial distribution of different types of cracking in one of these pavement sections at one time (MP 17). The three tiers represent the same pavement in the same year, the x-axis is the distance along the pavement and the lines represent the

actual slabs. The top slabs are the L2 slabs, the middle shows the distribution of T2 slabs and the bottom depicts the SS slabs. The patterns that were identified in LTPP pavements and discussed in Section 2.3 are evident in this section. The L2 slabs are more clustered, without any pattern. The T2 slabs are distributed in a random normal format. The SS slabs appear to be a combination of the L2 and T2 distributions, also as expected, especially since the SS slabs developed almost equally from slabs that were originally longitudinally or transversely cracked (see Appendix for additional details).

Figure 3-12 Spatial Distribution of different types of cracking

MP 17 also provides an example of temporal changes in pavements using 3DSBM. Figure 3-13 shows the condition of the 27 T2 slabs in 2018 and how they grew from 8 T2 slabs in 2013. This pattern also follows the random normal temporal pattern evidenced in the LTPP sections reviewed in Section 2.3.

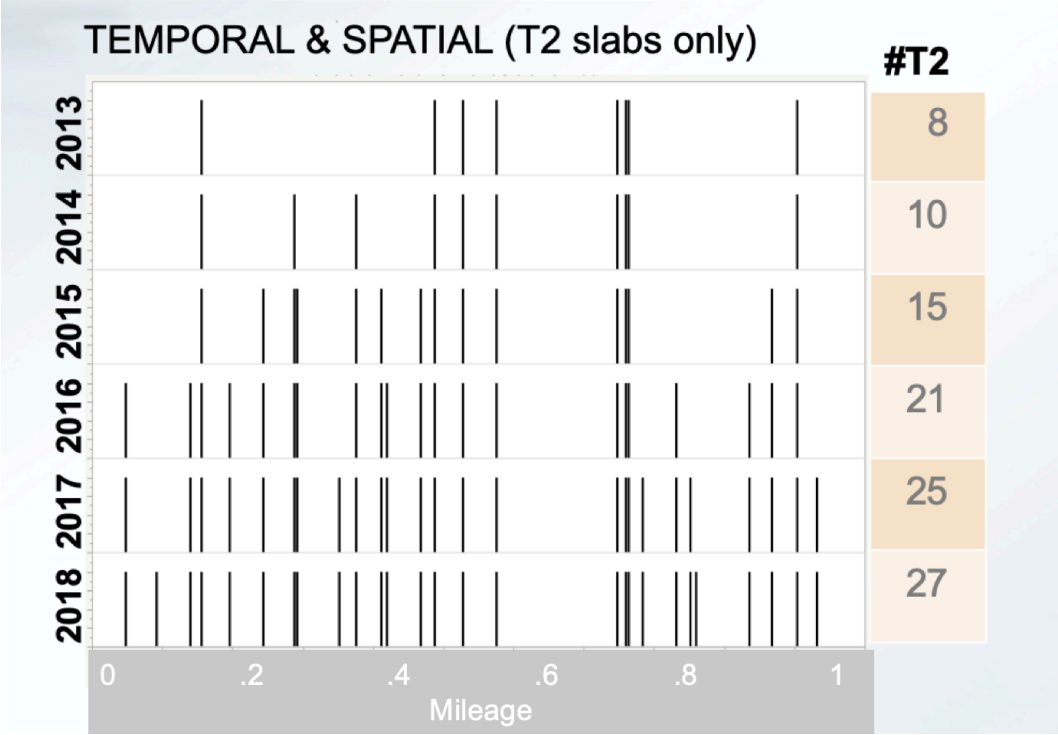

Figure 3-13 Temporal and Spatial distribution of T2 cracking

Another example of a pattern that can be identified due to the granularity of the 3DSBM is shown in Figure 3-14. The graphs on the left shows the location and slab state for slabs that changed state and became shattered slabs (SS) in the following year. In 2013 to 2014 4 L2, 4 L1, 1 CC and 2 T2s deteriorated to SS. In 2014 to 2015 2 L2s, 2 L1 and 10 T2s deteriorated to SS. In one year the predominate slabs that deteriorated to SS were originally longitudinally cracked, but in the next year the predominate slabs that deteriorated to SS were transversely cracked. In the following year (2015 to 2016) only 1 L2 deteriorated to SS (not shown in the figure). The graph on the right shows the growth of SS slabs in this section over time. The total L2, T2 and SS values by year are shown in Table 3-1 and in Figure 3-14.

Table 3-1 Different Slab State Values over time (MP 17, CS)

L2	T2	SS	Year
10	**20**	**17**	2013
8	**21**	**28**	2014
6	**18**	**42**	2015
7	**25**	**43**	2016
8	**26**	**48**	2017
8	**27**	**51**	2018

It is clear that the SS are increasing and that they have developed from both longitudinal cracked slabs and transversely cracked slabs, while the number of L2 and T2 appear relatively flat. If just the transverse cracking or just the longitudinal cracking was considered it appears that the pavement is not changing, while in fact the slabs are deteriorating considerably since they are both turning into SS and developing from not cracked slabs. Since the SS are developing from both longitudinal and transverse cracking it may indicate the amount of microcracking in the pavement segment.

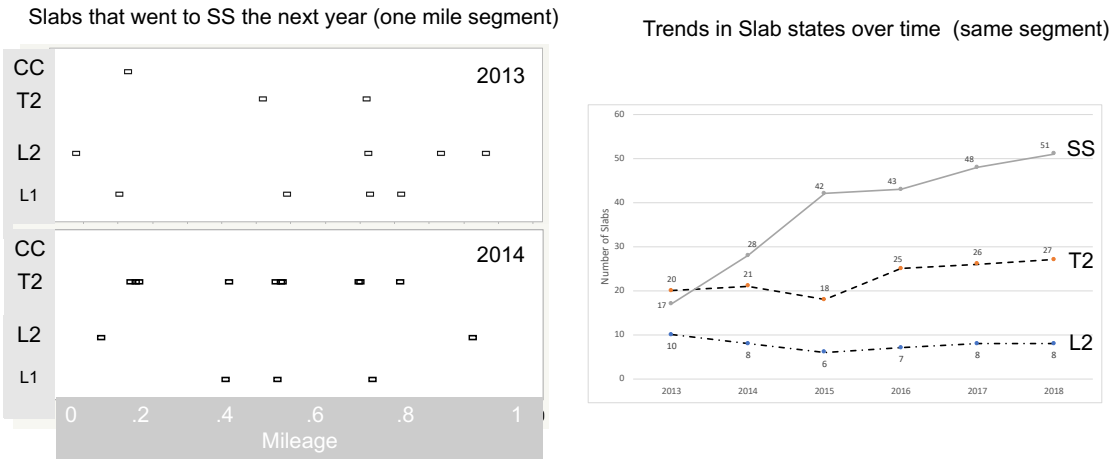

Figure 3-14a) and b) Trends in Cracking Orientation over Time, MP 17

CHAPTER 4. 3DSBM MODULE 3: SPATIAL PATTERN ANALYSIS

Chapter 3 introduced the fundamental Modules 1 and 2 of 3DSBM. This Chapter introduces Module 3 covering spatial pattern analysis.

4.1. Kernel Density

Kernel Density Estimation has been used in a roadway context for analyzing traffic accidents [Hashimoto, 2015], and even the urban dynamics of taxi services [Markou, 2017]. Patterns for hot spots for accident severity for Lincoln, Nebraska was identified using kernel density estimation in a recent TRB paper [Lee, 2019]. In a similar manner, but including the element of time, this analysis uses KD (kernel density) regression. In this context 'hot-spots' are areas of higher distress or clustering of distress. Due to foundation issues, construction issues, or other such factors, cracking in concrete slabs often exhibit clustering.

KD is also used here to quantify and analyze the changes in the slab states over time. Like reading an EKG tells a doctor the condition of a patient's heart and identifies anomalies, KD can be used to assess the condition of the pavement. KD regression uses weights of points and a kernel setting to spread the weight of the distress, creating a smooth curve, instead of just a linear fit. This continuous description of the cracking in the pavement can also be used to correlate to other continuously collected data, like those used to collect smoothness (IRI) or the newer instruments that can measure continuous structural condition (rolling wheel deflectometers/traffic speed deflectometers).

4.1.1. Kernel Density Regression Curve Fitting

Kernel density regression is a non-parametric regression technique that recognizes the condition of adjacent values in creating a smooth regression curve. The values are smoothed using the ksmooth command in R, which produces a smooth curve that is weighted by the individual values (numerical slab states) and the adjacent values based on a certain bandwidth. The function ksmooth uses the Nadaraya-Watson Estimator [Kvam, 2007]. At each point (slab) the slab state value is spread out over a distance by some kernel (K), even if the adjacent slab has no value (i.e. not cracked). Adjacent slabs that have a non-zero slab state will overlap the previous slab by some distance (related to the bandwidth h_n) and the kernel smoothed curve is the summation of each of these values. A simple example is shown in Figure 4-1. The grey columns are the slabs state values after normalizing (see Section 4.2.2). The resulting value for the kernel smoothed curve is the dotted black line.

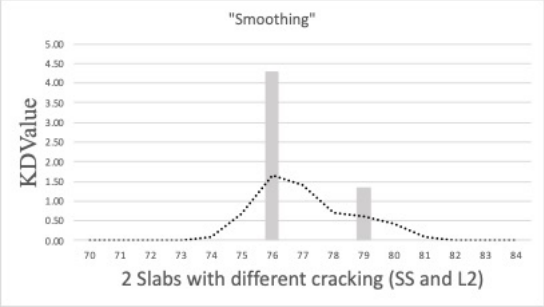

Figure 4-1 Kernel smoothing example

Kernel smoothing is accomplished in this research by transforming the slabs states to numerical data using a transfer function that sets an increasing level of values for the increasing distress of the slab states. The value is termed the KDValue and is shown in the y-axis. The slab states are assigned an x value relating to their location, based on mileage from a starting point. The resulting vector is smoothed by performing a kernel regression

over the section. Using a kernel regression allows the effect of the adjacent slabs to be part of the analysis, as shown in Figure 4-1. The average value of the KD regression y-axis value (KDAve) is used to represent the condition of the pavement. This value can be identified by mile or be scaled into different values, such as 0.1 mile. A non-parametric statistical check for outliers (IQR) is used to identify clustering of cracking. The KD curves for different years of the same pavement can be compared to identify areas of increased distress or identify areas that have been repaired since the last inspection. The following sections describe this process in more detail.

4.2. Average KD (KDAve) and IQR of the pavement sections

The method to compute KDAve and IQR:

1) Assign values to Slab States (0 to 3) based on severity (see Table 4-1)

2) Align Slab state values with mileage from base year

3) Adjust Slab state values based on length (normalize)

4) Perform kernel smoothing for each inspection (year)

5) Use KDcurves to analyze pavement

6) Compare KDcurves from different years to identify areas of deterioration or maintenance

Each step will be addressed in the following section.

1) To evaluate the changes in slab condition over time the slab states were converted to numerical values as noted in Table 4-1. The transfer function values are based on the considered severity of each type of cracking. As noted in Section 2.4, Georgia and Florida consider transverse cracking twice as detrimental in their deduct values than longitudinal cracking, so the L2 value is identified as 1 and the T2 value as 2. A Shattered Slab is a

combination of L2 and T2 and so was given a value of 3. A corner crack is usually considered as detrimental as a T2 or worse due to its propensity to move under traffic, so it was provided a value of 2.5. Due to the concerns of especially L1 cracking later being identified as surface cracking (as noted in Section 2.4) it was considered to not include L1 and T1 in the KD values. After review of a number of sections there appeared to be information lost if they were not included, therefore they were included but provided lesser values as noted in Table 4-1.

Table 4-1 Transfer Function for KD Slab States

	KD Slab State values						
	NC	L1	T1	L2	T2	CC	SS
Numerical value	0	0.25	0.5	1	2	2.5	3

2) Mileage along the pavement is determined by adding the individual slab lengths. The total mileage for 2013 is the baseline mileage. The beginning and ending slabs for each year are identified and the 2013 mileage is used to normalize the subsequent years data. The beginning and ending slabs were identified by a combination of GPS, adjacent slab condition and pavement markings visible in the Range images.

3) The individual slabs are turned into points using the milepoint of the end of the slab. Each point has a value based on the slab states noted in Table 4-1. The value is normalized for the slab length by:

$$KD_{SS} = \text{KD slab State value} * \text{length of the slab in mm} * 0.0002 \qquad \text{(Eq 4-1)}$$

This accounts for replaced slabs with shorter lengths than the original slabs, and normalizes the condition of replaced slabs based on their current length. The normalization is based on a slab length of approximately 16 feet.

4) Kernel smoothing was performed using Statistical packages in R (stats, ModelMetrics and sfsmisc) and the ksmooth function. The results of the regression is a x,y vector with x as the mileage and y as the smoothed distress value.

5) The resulting KD curves (x,y noted above) are plotted and the mean value of the y and the IQR (inter quartile range, 75% value – 25% value of the ys after they are sorted)are computed, also using R.

6) The KD curves from different years can be deducted from the prior years values and the resulting KDdelta curve used to identify changes in slabs (either due to further deterioration or due to maintenance activities).

Figure 4-2 shows the length normalized slab state values for a pavement (KDValue) as a function of distance (Mileage) along a pavement. The values shown as circles are the length normalized slab state values. Curves (noted as KDcurves) for the smoothed regression for this pavement are shown at several different bandwidths. Bandwidths of 0.01(~50 ft) black, 0.05(~250 ft) in blue, 0.1 (~500 ft) in green and 0.2(~1000ft) in red are shown. A bandwidth of 0.01 or ~50 ft provides a balance between following the data and providing a smooth curve. In addition, most of the pavements considered are ~20 ft in length. The AASHTO PMED design method for transverse cracking considers 3 adjacent slabs when considering traffic loading, therefore 50 ft should include approximately 3 slabs

[Yu, 2003]. The bandwidth of 0.01 also provided a clear indication of peaks from clustered slabs, and went to zero in areas of no cracking.

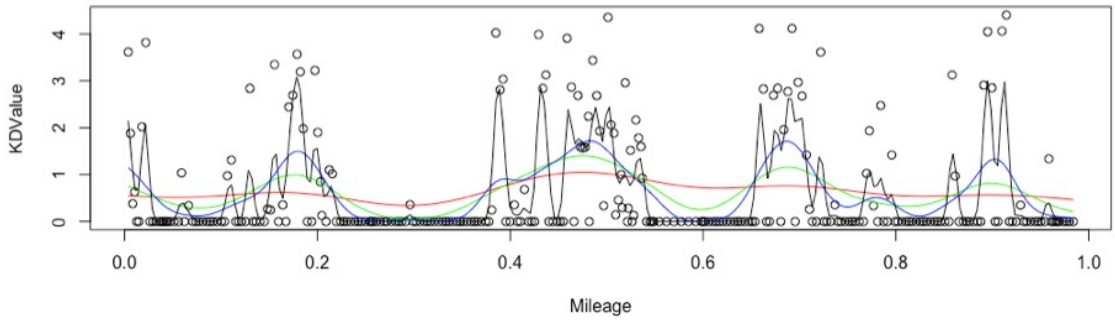

Figure 4-2 KD Values showing curves based on different bandwidths (.01 = black, .05=blue, .1=green, .2=red)

A RMSE comparison of different values of bandwidth was performed to confirm the proposed bandwidth was optimum. Figure 4-10 shows the relationship between the RMSE of the model (actual values compared to smoothed values).

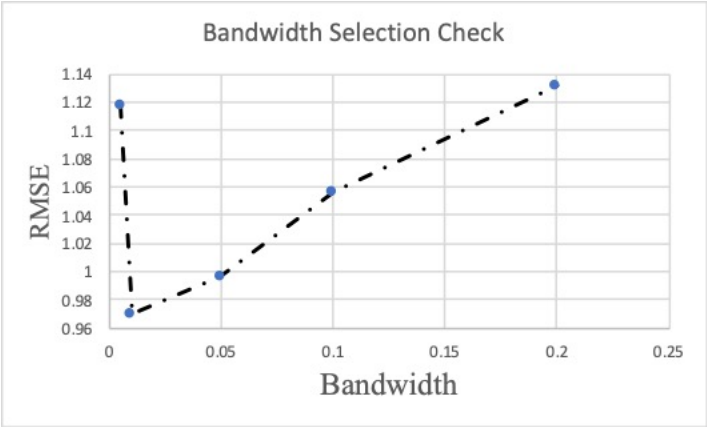

Figure 4-3 RMSE versus bandwidth

A bandwidth of 0.01 also provided the lowest RMSE (Note: Figure 4-10 includes results for bandwidth = 0.005, but that bandwidth is not plotted in Figure 4-9 for clarity.). A gaussian (normal) kernel was used instead of the more common epanechnikov kernel. The

kernel controls the shape, but the bandwidth controls the spread. Fatigue failure that presents as cracking should follow a normal distribution, so a normal kernel aligns with the failure mode, also the kernel itself is not as important as the bandwidth.

Figure 4-11 shows the KDcurve for a pavement as a function of distance along a pavement. It is evident from the figure that there is a cluster of highly distressed slabs concentrated around distance 0.4 to 0.5. The black curve is from 2013 data and the red curve is based on 2018 data, showing an increase in distress in three locations: near 0.3, between ~0.4 and 0.5. and near 1.

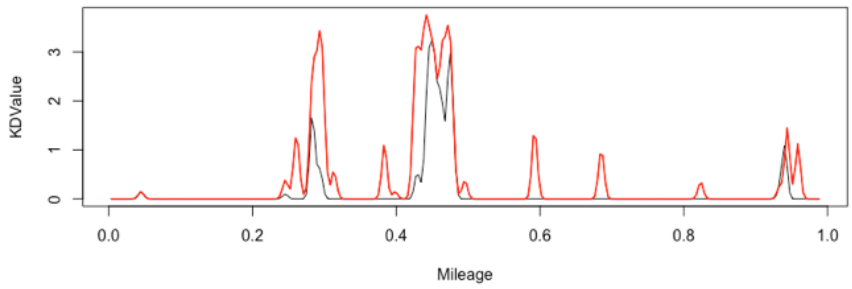

Figure 4-4 KD Curve for a pavement at year 2013 (black) and 2018 (red)

IQR, or interquartile range, is a non-parametric data analysis tool to measure the spread of data. It is used here to quantify clustering of data using the kernel smooth curves. IQR is computed as the difference between the 75th and 25th quartile of the y values. The sorted y values from Figure 4-4 (2013) are shown in Figure 4-5. They have been sorted from the smallest to the largest value. The IQR value is 0. In contrast, a different more uniformly distressed pavement represented by Figure 4-6 has an IQR of 0.99.

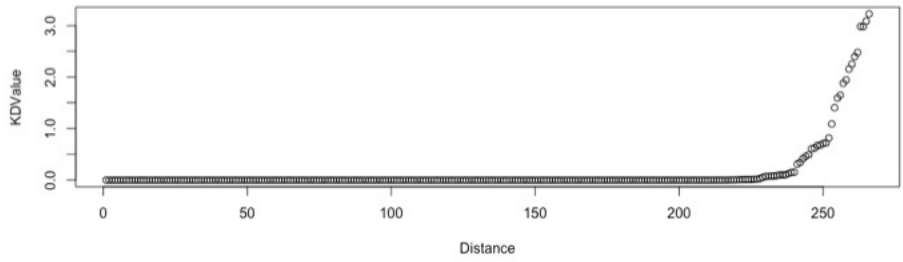

Figure 4-5 Sorted values from KD curve, IQR = 0

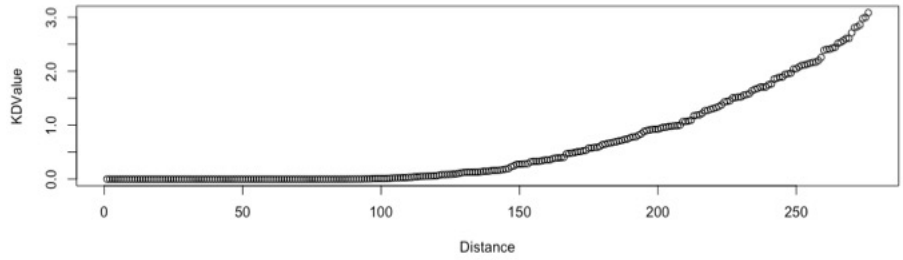

Figure 4-6 Sorted values from KD curve, IQR = 0.99

4.3. IQR of the transverse cracking in the pavement sections

KD curves can also be made from any subset of the Slab States. This section looks at just the transverse (T2) cracking over the length of a pavement. T2 slabs are chosen considering that the typical fatigue behavior is modeled using transverse cracking, and in the LTPP sections it was observed that the transverse cracking typically followed more of a random normal model than a clustered progression of cracking in different slabs. Synthetic data was created using a random normal distribution of cracking of 2%, 4%, 6%, 10%, 20%, etc. as shown in Figure 4-15. KD Ave and IQR values for each section are shown in Table 4-2.

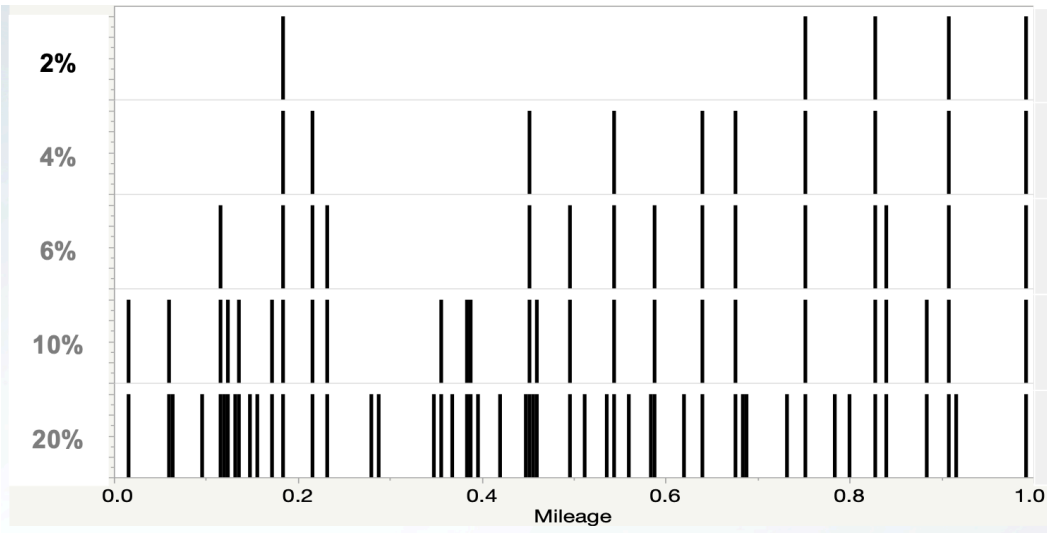

Figure 4-7 Synthetic Data random normal distribution at 2, 4, 6, 10 and 20%

Figure 4-8 on the right hand side shows the sorted KDvalues for a synthetic pavement with 10% cracking which is distributed in a random normal fashion and the values for a synthetic pavement with 10% cracking which has clustered cracking. The IQR values of each of these sections, 0 and 0.48 respectively, is plotted on the left hand side. A number of different random normal distributions were created and analysed to confirm the pattern.

Table 4-2 Synthetic Data TAve and TIQR values

	#slabs cracked/250	TAve	TIQR
RN2%	5	0.04	0
RN4%	10	0.08	0
RN6%	15	0.12	0.08
RN8%	20	0.16	0.09
RN10%	25	0.2	0.48
RN20%	50	0.4	0.57

Since the TIQR for normally distributed cracking changes greatly near 10%, a pavement with 10% cracking and a low TIQR can be identified as clustered, where a pavement with

10% cracking with a TIQR above 0.4 indicates the cracking is more normally distributed. A distributed cracking at 10% would also be indicative of a pavement undergoing fatigue failure. Of course, as has already been discussed, real pavements do not just crack just transversely, therefore the TIQR values are not set at those limits but looking at real pavements can provide an indication of what values are reasonable to use.

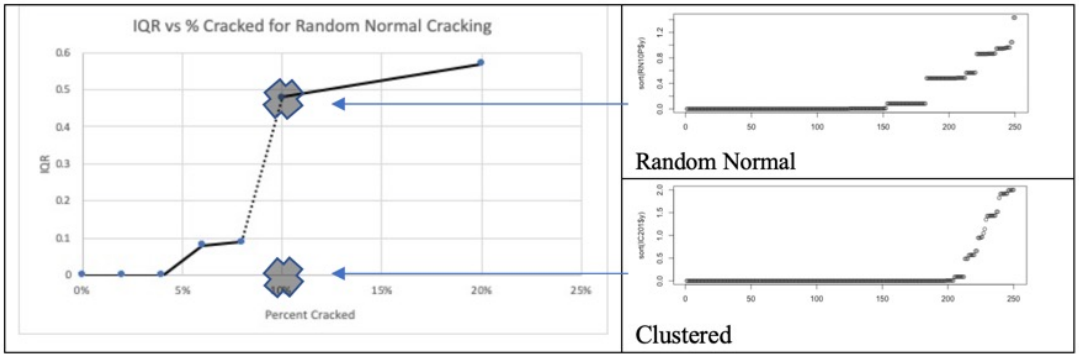

Figure 4-8 Relationship between TIQR and %cracked, random normal distribution

4.4. KDCurves, KDAve and IQR

Colors and bar charts showing pavement condition are commonly used to represent pavements like the examples shown in Figure 4-9 [Iowa State University, 2019 and Tsai et al., 2019]. These provide a visual indication of an overall pavement condition index or the quantity and quality of a certain type of distress. Since this research is focusing on cracking, and there are different types and levels of cracking, the KDcurves provide a new way to view and analyze the data without complicating numerous color schemes. As noted previously, another major benefit of using smoothed curves in comparison to these other

methods is to be able to tie the data to other continuously collected data, like IRI or rolling wheel deflectometers/traffic speed deflectometers.

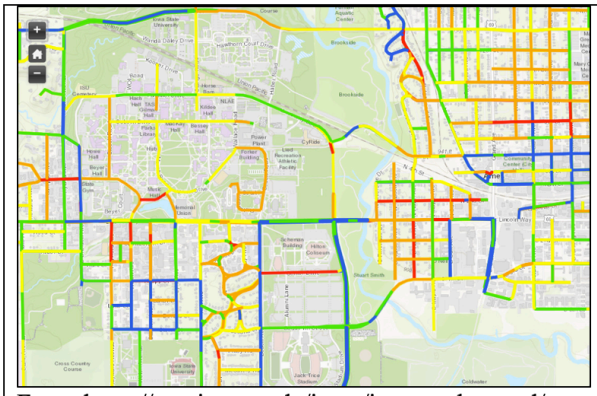

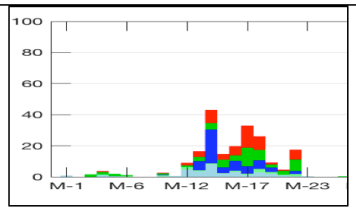

From Tsai 16-01

Figure 4-9 Examples of Pavement Condition Representations

The following sections provides recommendations on potential uses for the KDcurves and the associated statistical values, KDAve and IQR. Although statistical analysis is always limited by the data set, which in this case is focused on Georgia sites in a certain timeframe, it can provide information on potential relationships that can be evaluated later for larger datasets.

4.4.1. KDCurves

Examples of uses of KDCurves for pavement sections reviewed in this research are highlighted here. Curves can be plotted over previous curves to identify changes, like shown in Figure 4-10, or the curves can be numerically subtracted to create KDdelta curves, like Figure 4-11. KDDelta curves could also be beneficial in performing quality assurance checks for the identification of missing maintenance treatments in the pavement

management database, as repaired slabs will show up as negative values, as noted in the circled area of the figure.

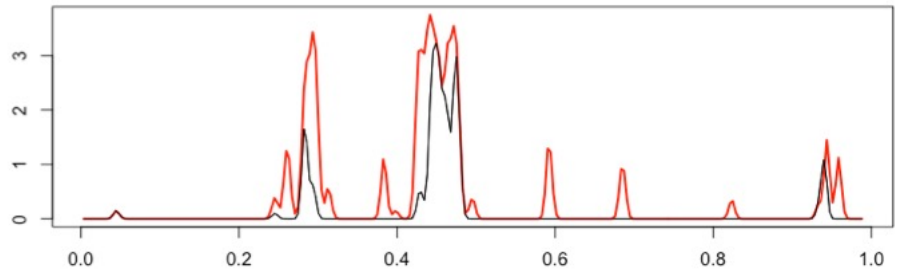

Figure 4-10 KD curve showing changes over time (red= 2018, black = 2013)

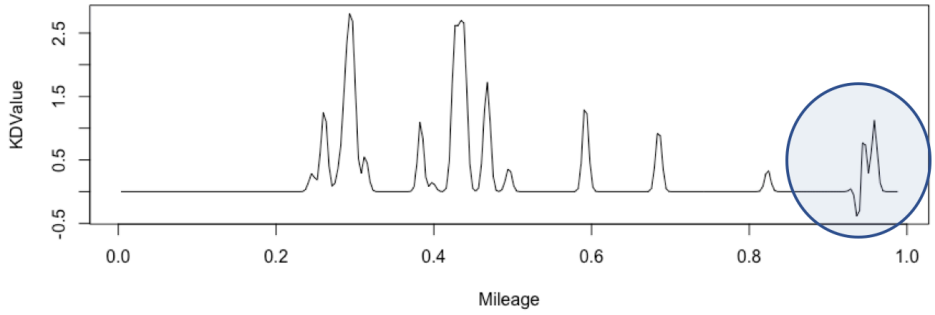

Figure 4-11 KDdelta curve with area of maintenance activity circled

KD curves can be overlaid on topographic maps to identify if any obvious topographic components, such as being over a swamp area or in other low lying areas, may be the cause for any identified clustering.

4.4.2. KDAve

KDAve can be used in the traditional sense as compared to some theoretical perfect condition, where 100% is zero cracking as shown in Figure 4-12. The condition and rate of deterioration of the current slab condition of the section can be monitored in this manner.

Maintenance activities, if substantial, can be identified in the change of KDAve value, as shown in the Figure at year 2015. In the figure MP153 does go all the way back to 100%, as after repairs there was no cracking in a one year time frame. Although the rate of change of KDAve was very similar for these two sections before repairs it is apparent that the rate of cracking after the repairs is much slower for MP 153 than MP 154. This highlights the need to continuously monitor pavements and use pavement specific data to make decisions on pavement maintenance.

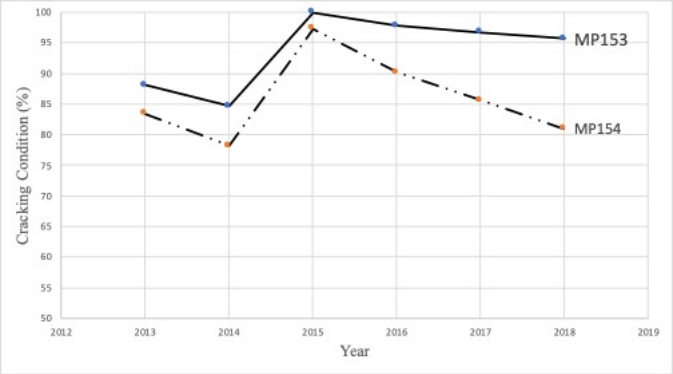

Figure 4-12 MP153 and MP 154, KDAve, 2013 to 2018

4.4.3. KDAve and IQR

TIQR is the IQR value of the pavement only considering the T2 slabs, as noted earlier. The relationship between KDAve and TIQR is shown in Figure 4-13. The points in blue are pavement with predominate transverse cracking. The points in green are predominately longitudinally cracked and the ones in grey are predominately SS. The majority of the sections (33 of the 41 sections) have a TIQR value near or equal to 0. Only sections with a KDAve > 0.4 have a significant non-zero TIQR value. Since the transverse cracking is typically not clustered it will take more cracked slabs to increase the TIQR value. Figure

4-13b shows the same data in a) with synthetic data for hypothetical pavements with only T2 cracking shown as the markers with an (x). The TIQR increased above 0 for the hypothetical pavement at a KDAve of 0.12 (an equivalent T2 percent of 6%). It takes another jump at around KDAve = 0.2 (hypothetical 10% T2 cracking). The hypothetical pavement has a higher TIQR value as it was modeled as a pavement with no repairs, the only cracking is T2, it is distributed in a random normal fashion, and all slabs sizes are the same, 20 ft. In contrast, the real pavements vary in slab size, especially after repairs, and include different combinations of slab states and different levels of clustering. The hypothetical T2 is shown for comparison purposes.

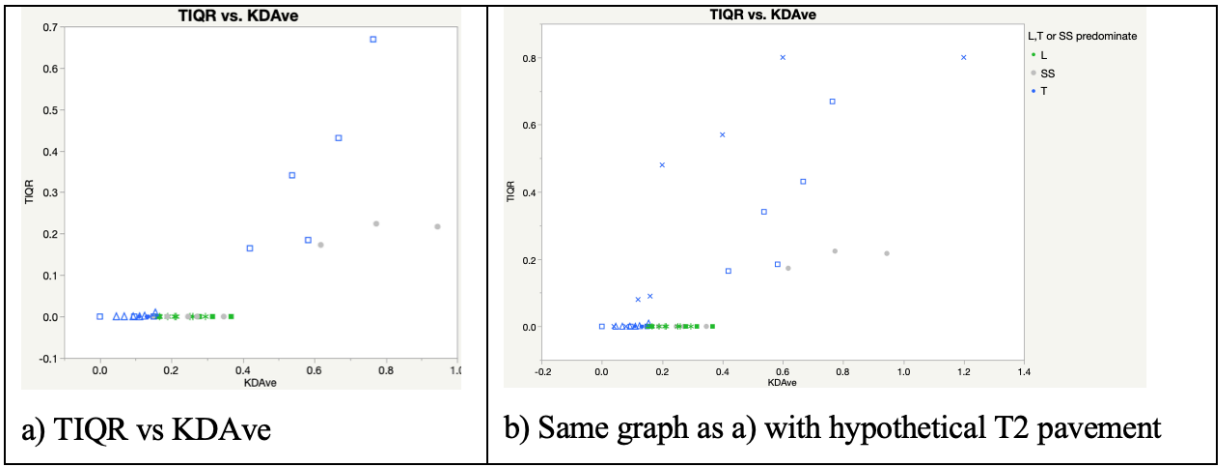

a) TIQR vs KDAve

b) Same graph as a) with hypothetical T2 pavement

Figure 4-13 TIQR vs KDAve relationship

In comparison to TIQR vs KDAve, Figure 4-14 shows the relationship between IQR and KDAve colored as to the predominate cracking in the section. (The points in blue are pavement with predominate transverse cracking. The points in green are predominately longitudinally cracked and the ones in grey are predominately SS.) The points in the small circle to the bottom left of Figure 4-14 (located to the right of KDAve = 0.2 and below IQR

= 0.25) all include sections with HPMS cracking (%T2+SS) greater than 5%. The low IQR and the relatively high cracking indicate clustered cracking, the KDcurves also support the potential for cluster cracking. Based on the available data, the point where the clustering appears to be consistent is when KDAve is greater than 0.2 and the IQR is below 0.25.

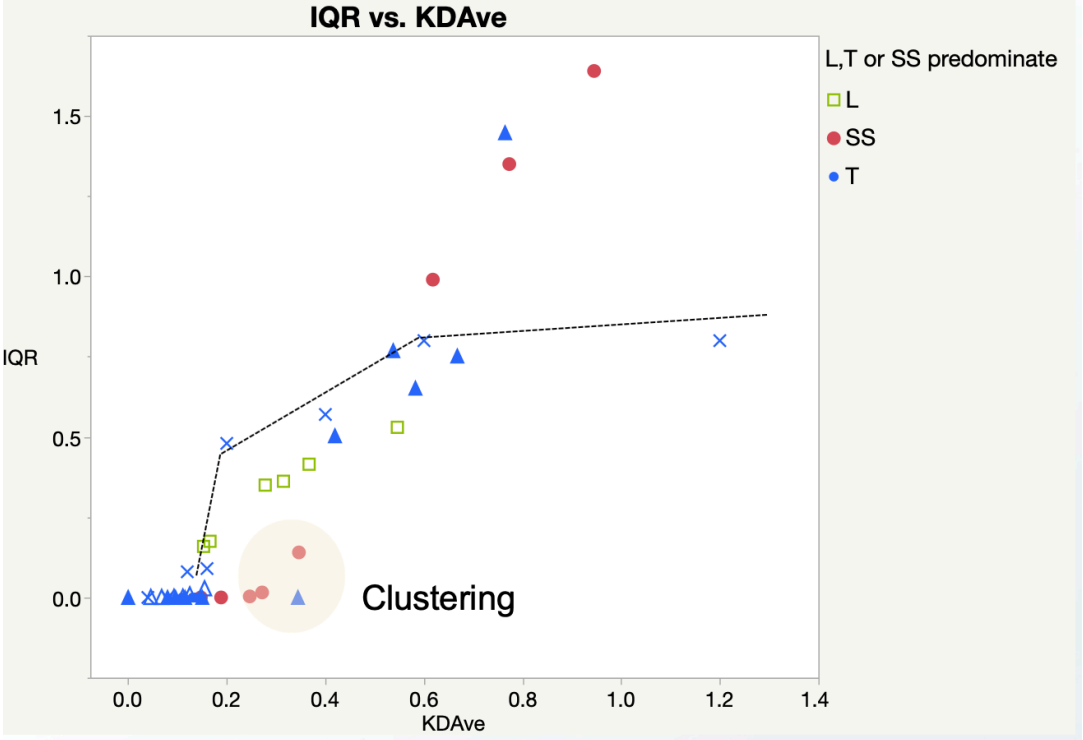

Figure 4-14 IQR vs KDAve relationship compared to random normal

Once again the hypothetical T2 values (x) are shown for comparison. The pavements above the dashed line all have a KDAve greater than 0.5 and an IQR greater than 1. As a comparison the KDCurves for one of the pavements noted in the Clustered area and one of the pavements in the top right of Figure 4-14 are shown in Figure 4-15.

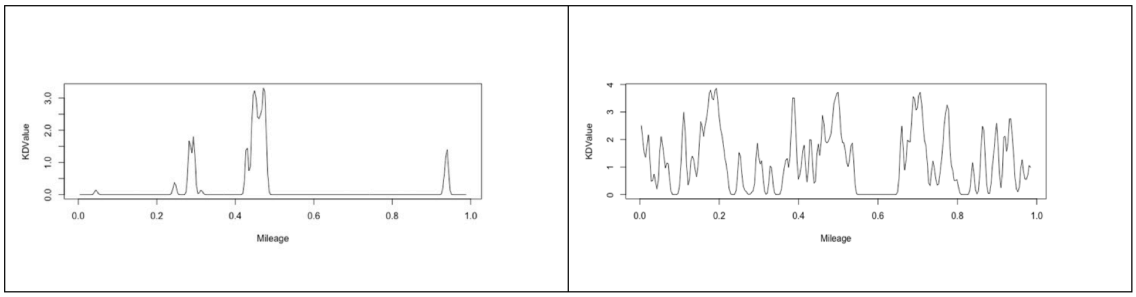

Figure 4-15 a) Clustered and b) not-Clustered KDcurves

Although the limitations of % cracking, and % HPMS cracking in particular have been discussed, since it currently is one of the predominate performance measure for JPC pavements it needs to be considered. Figure 4-16 shows the relationship between % HPMS cracking (defined as T2 + SS cracked slabs) and KDAve. Most of the sections follow somewhat of a linear trend. As expected, the sections with predominate longitudinal cracking do not follow the same trend. The hypothetical T2 only pavement is also shown (denoted by x). The pavements that follow this line closer can be considered the traditional T2 cracking pavements. This provides an opportunity to identify pavements experiencing multiple failure modes, by comparing their %HPMS and KDAve values.

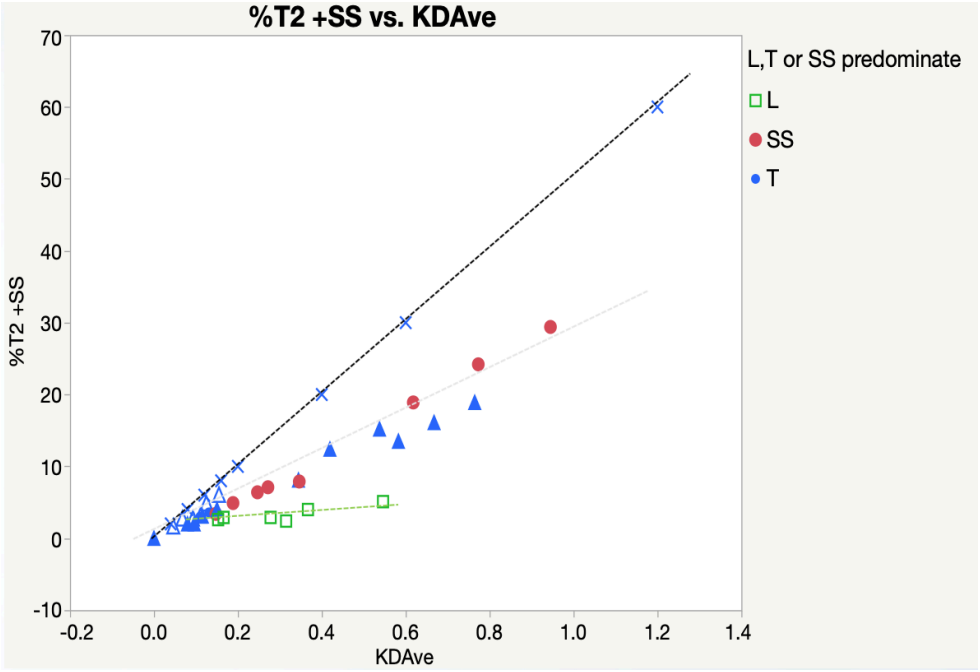

Figure 4-16 HPMS Cracking vs KDAve relationship

Another way to look at this is in Figure 4-17. Sections with predominate longitudinal cracking have a KDAve /HPMS value of greater than 5. This is due to the longitudinal cracking that is accounted for in KDAve but is missing in the HPMS (T2+SS). The points with an x marker are hypothetical pavements with only transverse cracking. The points in blue are pavements with predominate transverse cracking. The points in green are predominately longitudinally cracked.

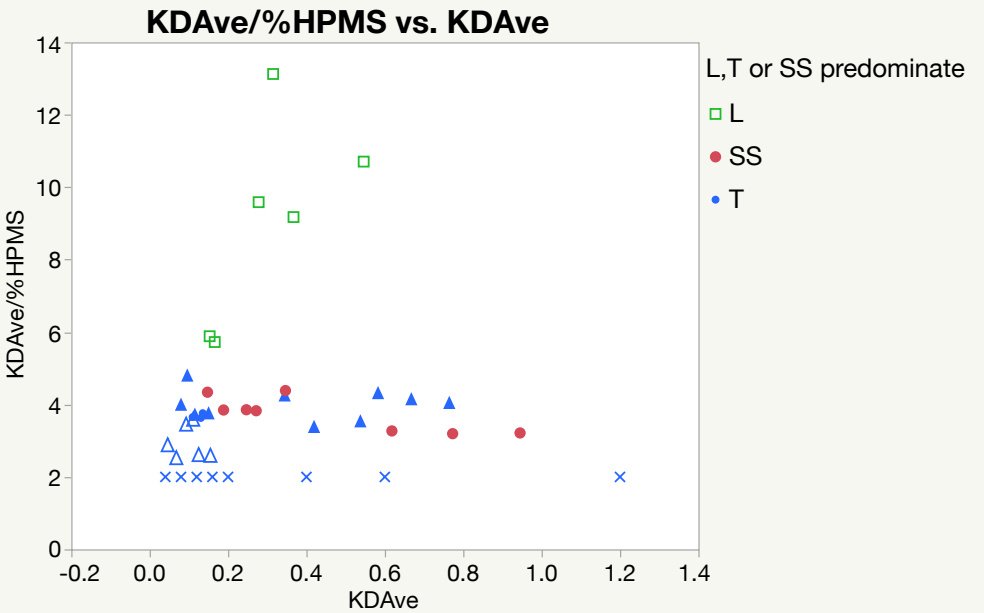

Figure 4-17 Longitudinally Cracked pavements, CS condition

4.5. Multiscale Representation of Pavement Cracking

As noted previously, the KDcurve provides a visual indication of the distress and it can be valuable to look at in multi-scale to see different patterns. Figure 4-18 is the continuous KDcurve for a five mile section of pavement (I-16 WB MP 19-14) for 2013 and 2014. Besides the visual differences in the curves the KDAve and IQR provide a quantitative indication of the increase in cracking in the pavement over time.

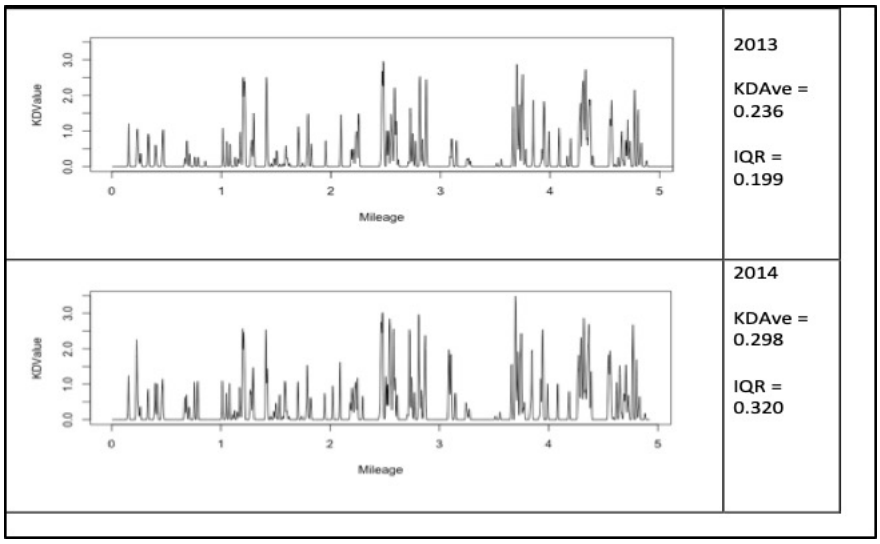

Figure 4-18 MP19-14 KD curves, 2013 and 2014

The histograms in Figure 4-19 and Figure 4-20 are different representations of the section of pavement for 2013, with KD values averaged by 100 slabs and averaged by 50 slabs. The high distress in the area of slab 1250-1300 is masked in the 100 slab representation, but clear in the 50 slab graph.

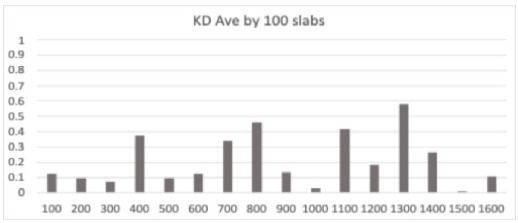

Figure 4-19 MP 19-14, KDAve at 100 slab scale

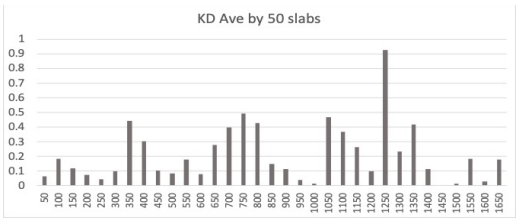

Figure 4-20 MP 19-14, KDAve at 50 slab scale

Although not pursued in this research, algorithms could be developed to look at continuous pavement sections in multi-scale to prioritize areas for repair or to look at how different sections are deteriorating over time using the KDcurves.

CHAPTER 5. 3DSBM MODULE 4: PREDICTION

This chapter presents Module 4, a method to predict future deterioration and eventual end-of-life for distressed JPC pavements. This research posits that the reason models for concrete pavements are more difficult to develop than asphalt pavements is that the rating index is not truly "reset" at every maintenance treatment for concrete pavements like it is for asphalt pavements. When asphalt is milled and inlayed the segment is typically considered restored to 100% and the model is restarted. The slope of the deterioration line may change due to the condition of the underlying structure, but the surface is all at the same starting point. While there could still be differing failure mechanisms if the surface mix is somehow defective, that would be considered unusual and so the new surface would be expected to behave relatively similar along its length. Therefore, failures in the asphalt can provide indication of underlying structural support issues. Concrete pavements cannot be treated the same way with the expectation that maintenance restores the pavement to 100%. The slabs that are not removed can have microcracking from prior loading, where the replaced slabs have not been exposed to any loading but could have separate quality issues due to construction related issues, especially as related to JPC pavement repaired under traffic. It will be shown that by considering a slab as having reached the end of life when it is repaired, termed 'R' slab state, a more consistent deterioration trend over time can be developed for JPC cracking. First a location reference is described that is used to categorize the pavement to address R slab states, followed by the method of prediction.

5.1. Location Reference

The following describes the concept of Current Slab condition (CS) and Original Slab condition (OS) in describing a location reference for JPC pavement condition. As noted in the discussion in Chapter 2, changes in cracking in a JPC can be due to a variety of factors. For the purposes of this research, these are consolidated into 3 different possible distributions of cracking: 1) related to cracking from fatigue failure of the slabs, 2) related to environmental and foundation/construction issues, and 3) related to the nature and quality of any repaired slabs. These three distributions are described in more detail as follows:

1) Fatigue failure of the slabs. Fatigue failure is commonly considered transverse cracking, but due to inherent curl and warp and microcracking as described in Chapter 2, it can also involve longitudinal cracking or combined cracking. Since this failure is related to the materials and the loading, and the loading can be considered consistent for adjacent slabs (neglecting effect of traffic wander), it is mainly related to materials and is expected to have a normal distribution. So this distribution would consist of a random normal distribution of cracking or fatigue failure. In most cases it is also expected that this type of cracking would primarily be in the form of transverse cracking. For this research the slab state of T2 represents this type of failure, while CC and SS are also considered failed.
2) Failure due to environmental or foundation/construction issues. While construction issues would be expected to present as early failures, foundation or environmental issues can occur at later times. This type of failure would involve an unknown distribution. Where foundation issues would be expected to be random and clustered, environmental (i.e. curl and warp related) could be expected to be

consistent for a period of time (i.e. a days production). This type of failure would be expected to include longitudinal cracking but may include corner cracking or combined (SS) cracking. For this research the slab state of L2 most represents this type of failure, while CC and SS are also related.

3) Failures due to nature and quality of repaired slabs. This type of failure would also be an unknown distribution, that could have an underlying distribution due to the repairs being based on the fatigue failure mechanism of the original slabs or due to foundation/construction issues. But, continued cracking in the new replaced slabs can be a function of the repair material and quality of the maintenance activity. The replaced slabs themselves are indicative of the worst cracking locations, but also involve an unknown human component (i.e. slabs chosen for repair is subjective, if the repair project is over budget or has extra money the Project Engineer could not repair all the distressed slabs or repair slabs with less distress, in addition, slabs adjacent to repaired slabs may also be repaired for convenience.) As noted in Chapter 3, this research uses R as a slab state for a slab that has been repaired. The Slab State R will be discussed further here.

Due to these different failure mechanisms, pavements need to be looked at from different approaches. This research uses the Original Slab condition as that approach.

Original Slab (OS) condition considers all replaced slabs as Slab State R, in an effort to segregate the 3rd distribution noted previously, which is unknown. OS condition is analyzed using a concept of Remaining Service Life of Original Slabs (RSLOS). RSLOS does not include L2 slabs in an effort to also segregate the 2nd distribution which is also unknown. RSLOS is intended for use for prediction and is based on the typical mile length,

primarily due to the benefit of being able to compare to the traditional % slabs cracked per mile for PMED. RSLOS also includes CC and SS slab states since they are considered more severe than T2 and they would also have a high probability of going to R (i.e. being identified as candidates for replacement when performing slab repairs). OS identifies L1 and T1 slabs but does not use them in the RSLOS calculation. By focusing primarily on the fatigue deterioration, RSLOS is intended to provide a consistent indication of deterioration from cracking over time.

Current Slab (CS) condition includes all three components: fatigue cracking, unknown causes and cracking from repaired slabs. CS does not use Slab State R, but does involve all the remaining Slab States. CS condition is the actual condition and was used in developing the KDcurves in Chapter 4.

An example of OS and CS condition for a hypothetical pavement consisting of 10 slabs is shown in Figure 5-1. At the time of original construction, the slabs are all not cracked (state NC). The NC slab state is not shown in the figure for clarity, therefore, slabs with no slab state shown are NC.

At some time (X) after which this section of pavement has undergone full depth slab repairs to repair existing slabs (assumedly due to cracking) it will look like the second depiction of slabs (noted as CS). The number of slabs in year X for CS condition is the actual number of slabs at that time between the start and end point. Note, this value can go up and down, based on how repairs are made. The condition of the slabs at time X for CS is the actual condition of the slabs, whether original or repaired. The number of slabs and the slab states are shown to the right of the hypothetical pavements in the figure.

At the same time (X) the OS condition is based on the original number and location of the original slabs. OS condition will always have the same number of slabs as the original pavement. Slabs that are replaced will always be considered R, even if they do or do not crack again. R becomes an absorbing slab state.

As can be seen in Figure 5-1, OS and CS condition for the same pavement at the same time can have a different number of slabs and a different combination of slab states. The reasons for these differences and what they mean are discussed in the following sections. Note that OS and CS Condition for a pavement that has had no slab repairs is exactly the same.

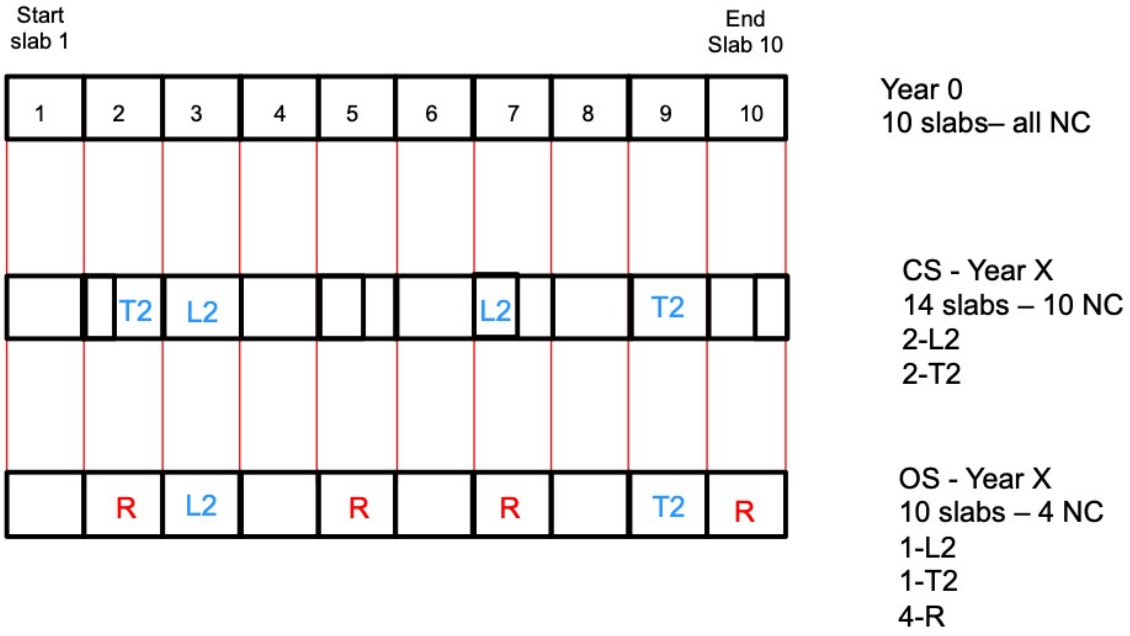

Figure 5-1 Current Slab and Original Slab condition example

5.2. Remaining Service Life of Original Slabs (RSLOS)

Remaining Service Life (RSL) is the amount of time from the present to when the pavement should be reconstructed or treated due to it being in an unacceptable condition [Elkins,

2013]. Remaining Service Interval (RSI), where the time frame is specifically related to treatment instead of reconstruction, is especially appropriate for asphalt pavements. Asphalt preservation typically involves seals or overlays that change the surface of the entire pavement. The underlying foundation and materials may still be different, but the surface condition is totally restored to a (theoretically) 100% condition. JPC pavement maintenance or preservation, especially as related to cracking distress, typically involves replacing individual slabs that have experienced cracking. Grinding may be performed over the entire JPC surface, but that does not change any cracking that was not repaired and it does not improve the cracking resistance of the unreplaced slabs (it may even reduce the cracking resistance due to a reduction in thickness). Therefore, maintenance in JPC pavements may change the current deterioration condition, but does not improve the entire condition of the pavement structurally. In addition, uncracked slabs are rarely removed prior to cracking unless they are affected by an adjacent cracked slab, so JPC maintenance is predominately reactionary. For these reasons, the nature of concrete end-of-life is more appropriate to be considered using RSL terminology instead of RSI. Washington State DOT recognizes this in their process. Figure 5-2 is from Washington State DOT's Pavement Asset Management Guide [Uhlmeyer, 2016]. The figure shows that the condition of a JPC pavement is shown to deteriorate to the point that reconstruction is necessary. They identify JPC pavements as structures that must be reconstructed at some point. The reported cracking related trigger values that they use for reconstruction are based on more than 15% of the slabs having multiple cracking (i.e. similar to SS) or more than 60% of the slabs with transverse or longitudinal cracking [Li, 2012]. Based on a personal discussion with Washington State DOT personnel, these values are based on

expert opinion and have not been validated, but it would be valuable to have a way to accurately predict the deterioration and identify appropriate trigger levels.

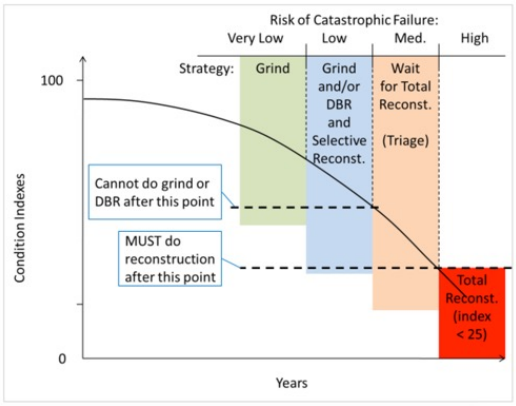

Figure 5-2 Washington State DOT concrete pavement deterioration model

For this research RSL is computed in relation to the original slabs. RSLOS (Remaining Service Life of the Original Slabs) is defined by the condition of the originally constructed slabs. Repaired or replaced slabs are failed slab states, noted as slab state R. The slab states of T2, CC, and SS are also considered failed states, such that the slab is considered at its end of life when it cracks to one of these states. The RSLOS value is the summation of the T2, CC, SS and R states divided by the total number of original slabs. Figure 5-3 shows the RSLOS versus Pavement Age relationship for the case study sections described in the Appendix. Consistent trends for each section can be identified in this manner. Note that the trends are consistent in the figure for each section, but variability in the different sections in each category is also evident (i.e. the two pavement sections noted as Cat1b have the same design, traffic, contractor, etc.)

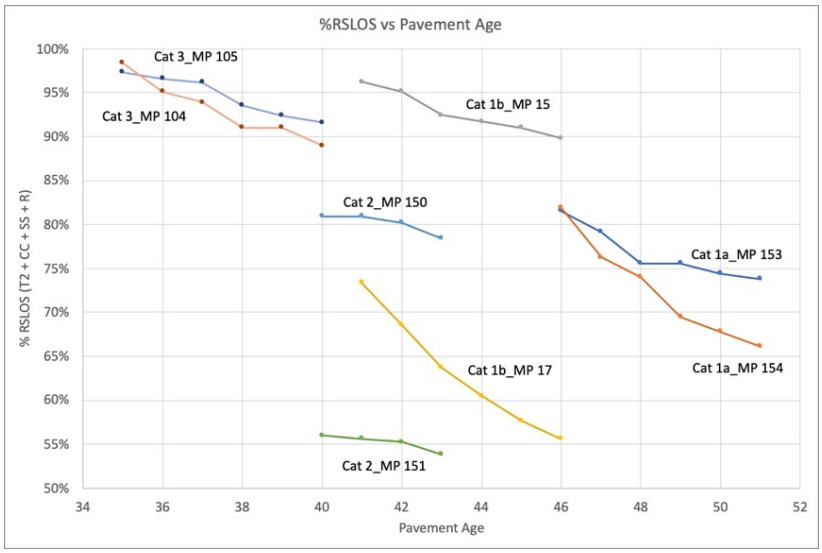

Figure 5-3 RSLOS vs Age, Case Study Sections

The RSLOS value is a conservative definition of failure, as T2 and even SS slab states may be addressed at least for a period of time, by crack sealing, instead of full depth replacement. It is envisioned that in the future faulting along the slab can be combined with the slab states to further differentiate slabs subject to movement and in most need of eminent repair, or nearest to failure.

5.2.1. Reliability Engineering

Reliability engineering is used in industrial and mechanical areas and has been taught in college level classes since at least the 1990s [Ebeling, 2010]. The Military has been using probability-based reliability methods even longer, a 1981 Military Standard defines Reliability as "The probability that an item can perform its intended function for a specified interval under stated conditions" [DOD, 1981]. Reliability Engineering also helps keep the planes we fly in the air and the cars that we drive moving on the roads. Aircraft engines and ball bearings used in vehicle brakes are maintained based on an immense amount of

data and probabilistic methods that model the life of the components. Life distributions of these components have been found to follow somewhat predictable patterns. Using reliability engineering tools, every ball bearing can be defined as having a probability of a certain lifetime. Reliability engineering models have even been used to compare failure rates of wind turbines in different countries in Europe [Tavner, 2007].

While not quite manufactured with the controlled conditions of ball bearings, or even wind turbines, each slab in a JPC pavement can similarly be identified as having a probability of a certain lifetime, based on observed life of similar slabs. The observations of the cracking behavior of a large number of slabs can be used to better define the probabilistic failure distribution of slabs. Weibull distributions are typically used in this type of failure analysis. Statistical tools used in reliability engineering provide the ability to account for pavements that are also observed or included in a study but still have not failed by the time of the last observation. When failure in an experimental study is not reached, the researcher is typically left with the choice of ignoring the non-failed section or waiting/postponing the research until a definite answer can be found, when the pavement actually does fail. This is not acceptable in practice, where a decision must be made now on the life of the asset for planning purposes.

Reliability tools are not new to pavements. Reliability is used as part of pavement design in AASHTO Pavement ME Design (PMED) as a function of the variability of distress observations [ARA, 2004] and it has been considered for rehabilitation analysis in concrete pavements [Liu, 2005]. Work by the National Technical University of Athens considered pavement sections from 15 countries in the European Union and developed reliability models based on a large database [Loizos, 2005] and most recently in Germany,

the German equivalent of the FHWA (BASt) is using reliability tools, such as hazard rate, for evaluation of concrete pavements [Villaret, 2018].

Reliability engineering uses mathematical models to define the probability that a component (like a ball bearing or a JPC slab) will survive over time. In practice these models are based on a large amount of data about the component. For this research the data is currently limited, but an immense amount of data will be available based on the number of State DOTs that are collecting 3D pavement data, as described earlier. This research lays out the framework of how that data can be used in the future using a finite sample of existing data.

Reliability and failure are intrinsically related by the simple relationship $F(t) = 1-R(t)$, where t is time. Both F(t) and R(t) are bounded by 0 and 1. If failures can be modeled by a parametric distribution the amount of failures at a time, t can be evaluated. Additional statistical information can also be derived from a parametric distribution, including the expected value E(t) or mean (termed Mean Time to Failure, MTTF) and slope at t (termed hazard rate or $\lambda(t)$), along with other common statistical measures such as mode and median and integrals. Using a parametric model also allows for the potential of predicting future values based on the form of the distribution.

Typical distribution types used in Reliability Engineering include exponential, Weibull, normal, lognormal and gamma distributions. The exponential provides a constant failure rate and is commonly considered the distribution used for the useful life of a component. Components are considered to have a varied rate of deterioration depending upon the age

of the component, as shown in Figure 5-4. This is known as the bathtub curve for component life.

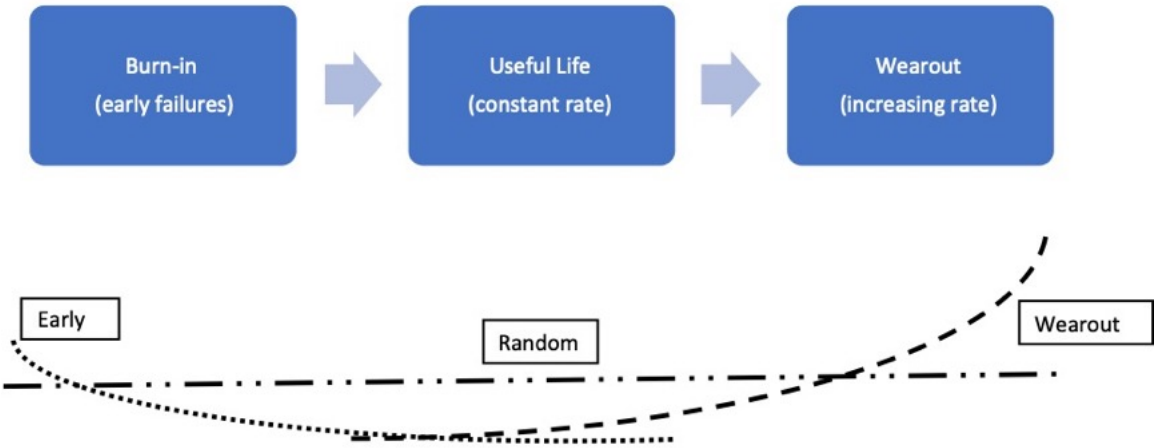

Figure 5-4 Bathtub Curve

The bathtub curve is composed of three components, Burn-in or early (i.e. construction related failures), Useful Life (constant rate) and Wear-out (i.e. fatigue related failures). In this research we are focusing on the wear-out portion of the bathtub curve, because the pavements that are being considered are at later stages of life, and the identification of this end-of-life is the goal. It is expected that the failure rate will increase during wearout so the exponential is not used for this research. The other distributions do vary over time. The normal and lognormal are common distributions in statistics but are used less frequently in reliability engineering. Since the normal distribution is defined for negative numbers (and time is not considered negative) it is not considered for this research. The log normal removes this problem, but since the integral is not a closed-form it presents other challenges. The gamma distribution faces the same challenges and is not widely used, especially since the Weibull does not suffer the same constraints. The Weibull distribution

is considered the most useful distribution in reliability engineering. It has integrals that can be evaluated numerically throughout the sample space of 0 to 1 and it is also very flexible, in that it can model increasing or decreasing failure rates, along with approximating an exponential and a normal distribution. It has a varied and long use in the civil engineering community for pavements also.

Prozzi and Madanat used a Weibull distribution to analyze the original AASHO Road Test data to come up with a more reliable predictor than the AASHO equations by considering probability and the effect of censoring in the pavement life [Prozzi, 2000]. A more recent paper used the Weibull hazard function to analyze different types of asphalt cracking in asphalt pavements (alligator, longitudinal and transverse) in the LTPP SPS 5 experiment [Dong, 2014]. The Weibull distribution has also been used in modeling concrete pavement cracking. California uses a pavement age model in their pavement management system to model 3rd stage cracking over time (3rd stage cracking is CalTrans terminology and is similar to SS in the 3DSBM). The model is based on a Weibull distribution and is defined by Lea as:

$$3^{rd}\text{ Stage Cracking } = 100 \text{ x } (1 - e^{-(\frac{t}{\alpha})^{\beta}}) \qquad \text{(Eq 5-1)}$$

Where t is the pavement age in years and α and β are model coefficients.

Lea identified different values for α and β based on traffic (related to ESALS) and climate levels (mild and severe) in California. The coefficients were identified as being developed based on expert opinion. The values of α noted varied from 90 to 200 and the value of β noted varied from 1.2 to 2.3 [Lea, 2014].

5.2.2. Definitions used in this Research

The Weibull distribution parameters specifically used in this research are defined as follows:

α, (sometimes noted as theta (θ) in other references) = the "characteristic life", also called the scale parameter. The value is in units of time (years) and represents the time where 63.2% of failures will occur. The parameter relates to both the mean and the variability of the data.

β = the shape parameter, also called slope parameter. The value changes the shape of the distribution. A value of 1 is equivalent to the exponential distribution. The value of β affects the rate of deterioration.

Failure distribution is $F(t) = 1 - e^{-(\frac{t}{\alpha})^{\beta}}$ (Eq 5-2)

Hazard function(rate) is $\lambda(t) = \frac{\beta}{\alpha}(\frac{t}{\alpha})^{\beta-1}$ (Eq 5-3)

MTTF, mean time to Failure or $E(t) = \alpha * \Gamma(1 + \frac{1}{\beta})$, where Γ is the gamma function (Eq 5-4)

Note that a 2 parameter Weibull is assumed. A three parameter Weibull includes a t_0 term that indicates that no failures will take place before a certain time, t_0. While physically that is preferred for JPC pavements (to have a maintenance free pavement for a period of time), since there is no way to identify t_0 with any confidence for the pavements analyzed here (since the time data is limited and it would introduce another unknown parameter), it was

not considered even though there is some indication that it may fit some of the data better as noted later.

5.2.3. Failed Slab States and Reliability Engineering

The slab states in 3DSBM provide a new way to look at reliability through the lens of reliability engineering. For this research failure is defined as the percent of slabs in a failed state compared to the total original number of slabs. Each slab is defined as Failed (considered in slab state T2, CC, SS or R) or not failed (all other slabs states). The % Failed at time t (age of the pavement) for different years data is fitted to a Weibull curve using a graphical least squares method [Ebling, 2010]. The slab states are added together (T2 + CC + SS +R) and divided by the original number of slabs to come up with the %Failed value. This method provides a continual trend over time for each pavement section.

Using the %Failed =∑(T2+CC+SS+R) and age of the pavement, the Weibull parameters, a and b, are computed for each OS pavement section (one mile) in the following manner:

From Equation 5-1: %Failed = 100 x (1- $e^{-(\frac{t}{a})^{\beta}}$)

1- $\frac{\%Failed}{100} = e^{-(\frac{t}{a})^{\beta}}$ and taking the natural log of each side

$\ln(1 - \frac{\%Failed}{100}) = \ln e^{-(\frac{t}{a})^{\beta}}$

taking log again,

$\ln \ln [1- \frac{\%Failed}{100}] = \beta \ln t - \beta \ln \alpha$

Using this relationship, we plot (x) =ln t and (y) =ln ln [1- $\frac{\%Failed}{100}$]. One of the one-mile pavement sections is shown as an example in Figure 5-5.

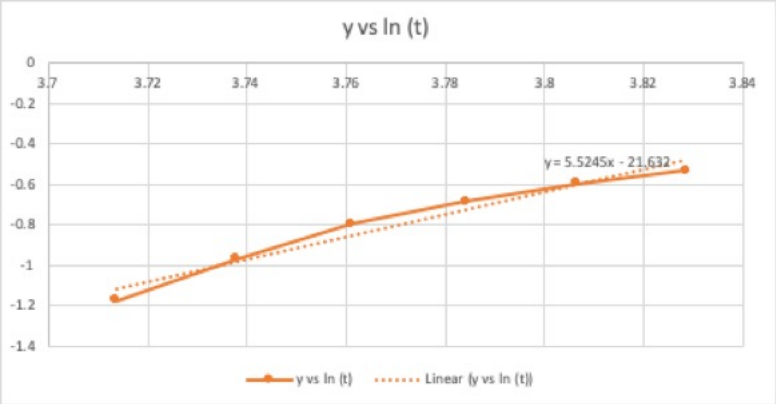

Figure 5-5 Least squares fit of Weibull distribution

Using the slope and intercept of the fitted linear equation,

Where β = slope of the line, and, $\alpha = e^{\frac{intercept}{\beta}}$

The Weibull parameters are found to be α = 50.3 and β = 5.5. The slight curve in the data suggests that t_0 is not zero, but as noted earlier, for various reasons, a three parameter Weibull was not considered in this research.

In a similar manner, Weibull parameters α and β can be defined for different pavement sections.

The Weibull parameters for another section shown below was found to be α = 51, β= 9.7.

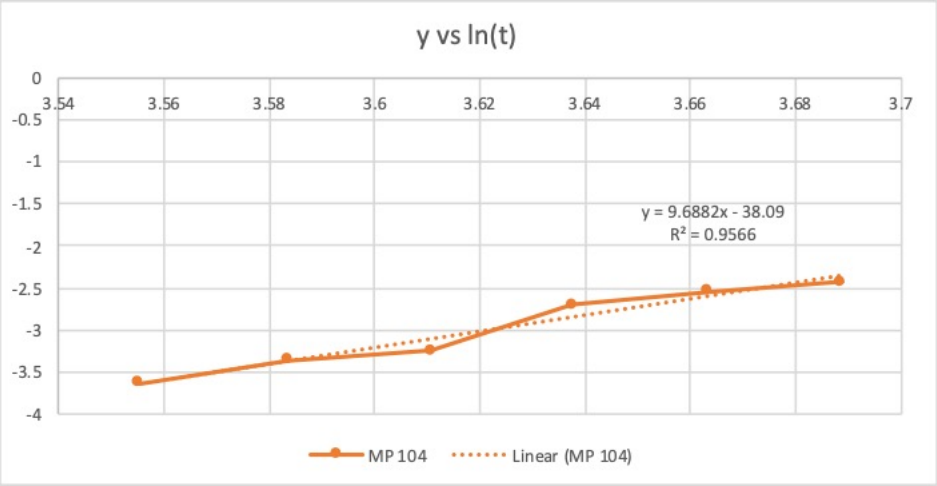

Figure 5-6 Another example of least squares fit

Weibull models were also checked for fit for each of the sections using Excel Solver and the GRGLNonlinear Solver Method and minimizing the squared deviation error. An example of the inputs and results for the same section in Figure 5-6 is shown in Figure 5-7. For the site which identified Weibull parameters of α=51 and β= 9.7 the Excel method provided α = 52 and β = 9.1 for a minimum SSE of 1.6. Inputting the values determined using the Weibull least squares method provided a SSE of 1.7, essentially the same. Since they were found to be similar and due to the improved SSE value the Weibull parameters identified using Excel were used for the data analysis.

A comparison to the California values noted earlier that were developed with expert opinion was made using the Excel method. Attempts at constraining the inputs to the values identified by CalTrans resulted in inferior models (SSE = 16 compared to 1.6). The models also showed a much lower standard deviation in cracking values when constrained. Since the CalTrans models were intended for all the pavements in their system which would be expected to have different ages, and also just for SS cracking, and the models for

this research involve pavement near the same age which is near the end of the pavement life, and include T2 and CC cracking along with replaced slabs, the models here would be expected to show deterioration at a higher rate than for a network level model. The α values are also more realistic than the California α values for this data. As noted earlier, the α value is also called the characteristic life and is indicative of a time for failure at a level of 63.2%. Some of the sections used in this research have % cracking (defined as T2+CC+SS+R) near 50% and they are 40 – 50 years old. It would not be expected that they would take another 50 to 70 years to go from the current value of 50% to 63.2% failures. It is also anticipated that the California pavements include much newer pavements that were designed to be Long Life Concrete Pavements and last 90 to 100 years.

%RSLOS Cracked Weibull Model

alpha	beta
51.9386129	9.0908248

1-e^(-((t/a)^b)))	%Cracking Model	Input %RSLOS Cracking	Age (t)	% Cracking (O-Model)	Squared Deviation
0.02727	2.727	2.6	35	-0.1267197	0.01605788
0.03508	3.508	3.4	36	-0.1084787	0.01176762
0.04478	4.478	3.8	37	-0.6783076	0.46010125
0.05671	5.671	6.5	38	0.82851365	0.68643488
0.07127	7.127	7.6	39	0.47293208	0.22366475
0.08887	8.887	8.4	40	-0.487317	0.23747787
	5.4	5.383333333		SE Minimized	1.63550425
	ModelAve	MeasAve			
	2.31	2.43			
	ModelSD	MeasSD		RMSE	0.52209582

a) Without constraints

%RSLOS Cracked Weibull Model

alpha	beta
130.4556135	2.3

1-e^(-((t/a)^b)))	%Cracking Model	Input %RSLOS Cracking	Age (t)	% Cracking (O-Model)	Squared Deviation
0.04735	4.735	2.6	35	-2.1348022	4.55738033
0.05044	5.044	3.4	36	-1.643615	2.70147029
0.05363	5.363	3.8	37	-1.5627268	2.44211511
0.05692	5.692	6.5	38	0.80788012	0.65267028
0.06032	6.032	7.6	39	1.56822988	2.45934496
0.06382	6.382	8.4	40	2.01835281	4.07374807
	5.5	5.383333333		SE Minimized	16.886729
	ModelAve	MeasAve			
	0.62	2.43			
	ModelSD	MeasSD		RMSE	1.6776337

b) With constraints

Figure 5-7 Excel Model, a) without constraints and b) with constraints

5.2.4. Prediction Using Reliability Engineering and RSLOS

For this research effort, RSL of Original Slabs (RSLOS) is defined as the reliability of the original placed JPC slabs. The original pavement after construction would be considered 0% original slabs cracked or 100% RSLOS. A pavement would reach 0% RSLOS when

all the slabs have either been replaced or are cracked such that they are classified as T2, CC or SS. It should be noted that a value of 50% RSLOS does not mean that 50% of the existing slabs have cracks. As noted earlier, previously repaired slabs could be cracked or not cracked, either way they are designated in a slab state of R and are considered failed. This removes the quality of the repairs from consideration, such that the condition of the original slabs can be solely monitored.

Considering that material failures are known to follow a normal distribution, and that the CDF for a normal distribution at 50% is continuing to increase in a linear fashion, fifty percent RSLOS cracked is used as an indicator of impending failure. If it follows a normal distribution and it is at the 50% point, that should be the highest concentration of deterioration.

As noted in Chapter 2.1.5., the use of percent cracked slabs as a sole performance indicator for JPC has known limitations. Percent cracking the year after a maintenance treatment will not be the same as before the treatment, but it could also not go back to zero if only the most deleterious slabs are repaired due to budget or resource issues. Even rate of cracking before and after a treatment may not be the same, especially if repairs did not solve the original issue, or the repairs were improperly constructed. Nevertheless, percent cracked slabs is a traditional definition used for JPC pavement deterioration as related to cracking. As noted previously, it is used in AASHTO Pavement ME Design (PMED) and used by FHWA for HPMS performance reporting. Currently the FHWA recognizes 0 to 5% cracking as Good, 5 to 15% as Fair and greater than 15% cracking as Poor, as part of their asset management assessment requirements.

Due to the proliferation of percent cracking in managing JPC pavements, this effort will compare %RSLOS to HPMS %cracking. But just as % cracking has limitations, %RSLOS also has limitations, this will be discussed in the next section as related to predicting deterioration.

5.2.5.1 Using %RSLOS to predict future deterioration

Due to the nature of how %RSLOS is defined it provides a consistent value over time. Modeling the future behavior based on the actual behavior is then possible using a functional form. As noted earlier, Equations 5-2, 5-3 and 5-4 provide different parameters based on a Weibull distribution. For each section that has been modeled with a Weibull equation with parameters α and β, a hazard rate and a MTTF can be determined at time t. Figure 5-8 shows the Weibull reliability over time curve using the α and b parameters defined using the technique described previously. Note that the form of the graph is consistent with traditional pavement deterioration curves like the one found in Section 2.1.2 (Figure 2-3). These curves anticipate that the pavement condition will stay rather flat for a period of time and then as they age the deterioration starts to increase at an increasing rate until it is almost a constant rate of deterioration over time. When the pavement reaches around the 50% condition level the deterioration continues to deteriorate in a linear fashion. Somewhere after the 50% condition level is the point where reconstruction is the suggested treatment. If a pavement follows this type of trend, the location of the actual pavement in the curve provides an indication of the future deterioration rate. If the pavement is on the top portion of the curve (i.e. <Age 25 in Figure 5-8) the rate should continue to be low. If the pavement is in the upper curved portion (Age 25 to 40) the deterioration rate may

increase, and if the pavement is in the linear portion of the curve (below 40 and as shown by the orange dots) the deterioration rate is at its maximum and will continue to deteriorate at the maximum rate. For this research the curve is defined specific to the individual pavement and is based on the cracking deterioration history.

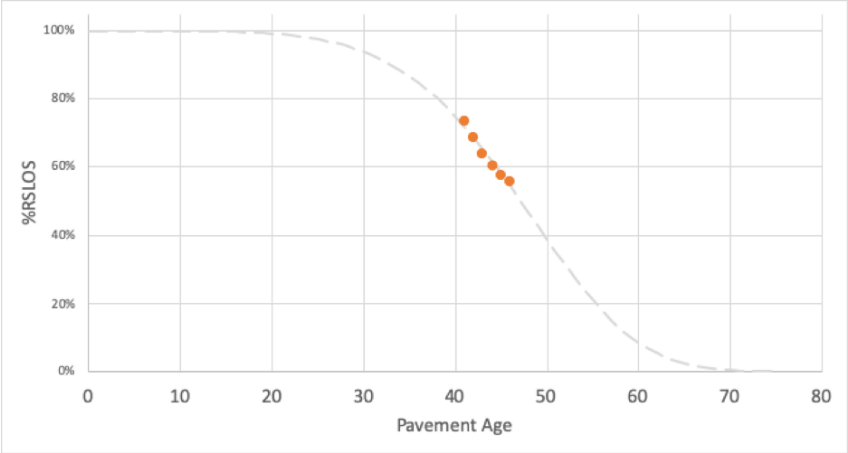

Figure 5-8 Example of Weibull curve and pavement data

The remaining life of the pavement to the expected value of failure is then MTTF minus the age of the pavement and is defined as RSL_yrs as shown in Equation 5-5. The hazard rate at the same time t is then computed using previous Equation 5-3.

$$RSL\_yrs = MTTF - t \qquad \text{(Eq 5-5)}$$

The result is a value of the remaining life in years which is plotted versus the hazard rate. In this way a combination of the condition, age and rate of deterioration is all considered. Plotting the Hazard rate vs RSL_yrs provide an indication of the rate of deterioration and the time left before the pavement will be over 50% cracked or replaced slabs.

Using the same example in Figure 5-8 with $\alpha = 50.3$ and $\beta = 5.5$ and $t = 46$:

MTTF = 46.3 therefore RSL_yrs = 46.3 – 46 = 0.3 and h(t)= 0.073.

Just as a concrete cylinder that is placed into a compression test machine and is not tested to failure, or a load test is performed on a foundation pile and the pile does not fail, without data to failure the actual failure criteria is not known with certainty, but can be estimated. In the case of JPC slabs there are actually two definitions of failure: 1) RSL definition where a slab has reached a slab state of T2, CC, SS or R and 2) failure of the pavement segment, where the rate of new cracking is not maintainable. Failure for definition 1 is defined using the definition of the slab states. Failure for definition 2 is more difficult to define, but a rationale for this follows using the pavement data considered in this research.

5.3. RSLOS Prediction of Pavement Life

The previous section presented the concept of %RSLOS and modeling cracking using a Weibull deterioration model. This section will evaluate the deterioration model using the Case study sections noted in the Appendix. As noted, a benefit of the Weibull model is that an instantaneous failure (hazard) rate and mean time to failure (MTTF) can be computed based on the model parameters α and β. The hazard rate is found by Eq 5-3 discussed previously:

$$\lambda(t) = \frac{\beta}{\alpha}\left(\frac{t}{\alpha}\right)^{\beta-1} \qquad \text{(Eq. 5-3)}$$

Table 5-1 shows the Weibull parameters and the r^2 value for the measured versus computed % cracking based on the Weibull model for the 8 Case Study sections. The majority of the

sites matched the data well using the Weibull model, with r^2 values on the order of 0.8 to 0.9.

Table 5-1 Hazard Rate, MTTF and RSLOS for Case Study Sections

Section	a	b	r^2	t	Hazard Rate at t	MTTF	RSLOS (years)
Cat 1a_MP153	70.6	3.5	0.87	51	0.022	63.5	12.5
Cat 1a_MP154	58.1	6.4	0.94	51	0.054	54.1	3.1
Cat 1b_MP15	61	7.7	0.89	46	0.019	57.3	11.3
Cat 1b_MP17	50.5	5.3	0.99	46	0.070	46.5	0.5
Cat 2_MP150	87.1	2.0	0.79	43	0.011	77.2	33.2
Cat 2_MP 151	72.4	0.93	0.85	43	0.013	74.9	31.9
Cat 3_MP104	51.9	9.1	0.94	40	0.021	49.2	9.2
Cat 3_MP105	49.9	9.6	0.92	40	0.029	47.4	7.4

Table 5-1 also shows the computed hazard rate for each Case Study section at time t using Equation 5-3. MP 17 has the highest hazard rate as expected due to its condition and cracking rate. MP 151 is interesting in that it has an equivalent β value of almost 1. A Weibull distribution with a β value of 1 is an exponential distribution, which has a constant hazard rate. This is equivalent to the constant rate portion of the bathtub curve presented previously (Figure 5-4). This could be related to the fact that the section is predominately longitudinally cracked. MP 150 and MP151 did not fit the Weibull model as well as the other sections, the pattern of cracking is also expected to be the cause. MP 150 and 151 have the lowest hazard rate, but the hazard rate is based on %RSLOS, which does not include L2. The remainder of the sections have a hazard rate around 0.02. Based on 200 slabs per mile and a 0.02 slabs/year hazard rate equates to an average of 4 slabs a year going to T2, CC, or SS. Based on the HPMS value of 15% cracking defined as poor condition, these sections would require maintenance every 7.5 years on average to keep the

condition above a poor level, if this rate was continued. The hazard rates based on the model were typically conservative and higher than the actual rate of cracking in the pavements.

Using the Weibull relationship, the MTTF and RSLOS in years (RSLOS_yrs) was computed for each section using the following formulas (repeated here for clarity):

$$\text{MTTF} = \alpha * \Gamma\left(1 + \frac{1}{\beta}\right), \text{ where } \Gamma \text{ is the gamma function} \quad \text{(Eq. 5-4)}$$

where α and b are defined previously, and

$$\text{RSLOS\_yrs} = \text{MTTF} - t \quad \text{(Eq. 5-5)}$$

RSLOS_yrs is the anticipated number of years until the section reaches the mean time to failure, and so is an indicator of remaining pavement life. The use of MTTF (50%) as the failure time is chosen here for simplicity, the characteristic life, α (63.2%), or another value of R(t) like 70% or 80% can and probably should be substituted for MTTF, if nothing more than for perception reasons. Colorado DOT moved away from using RSL calculations in their pavement management system because of the political fallout of too many of their roadways with a zero RSL, because their roadways deteriorated beyond their definition of failure. They now use a Drivability index that is more focused on IRI, but still includes cracking [NCHRP, 2013].

Figure 5-9 compares the RSLOS years (RSL_yrs) to the hazard rate. The size of the points are relative to the %RSLOS value, where larger points are larger %RSLOS values. In following with the bathtub curve deterioration for wear-out failures, as the hazard rate increases the remaining life of the pavement is reduced. But, as evidenced by the

variability of the size of the points, based on this model the %RSLOS at any one time does not clearly correlate to the rate or the remaining life of the pavement. Just as percent cracking by itself is not a good indicator of pavement condition, %RSLOS by itself is not useful as a stand-alone indicator.

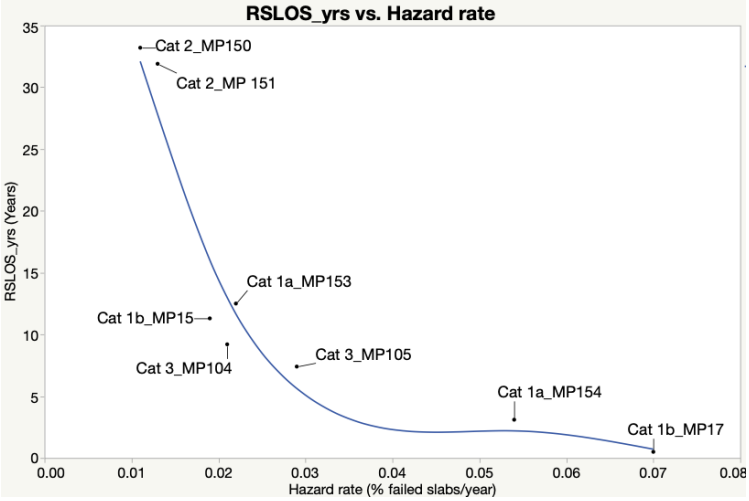

Figure 5-9 RSLOS_yrs vs Hazard Rate

An analysis of the ability of the Weibull models to predict the future cracking deterioration as denoted by the RSLOS value was performed. The resulting predictions of RSLOS almost all overestimated the future cracking and cracking rate, but since the bias appears to be consistent it could be recognized as a worst-case estimate. As more data was used to make the model at each site the MTTF value increased while the α value increased and the β value decreased. This was consistent for almost all the pavement sections. Based on a model with 4 data points versus 6, the α value increased by 4.8 on average, with a range of 2 to 8.3. The β value decreased by 2.7 on average, with a range of 1.5 to 3.9. An increase in the α value will increase the MTTF proportionally to the increase since MTTF is a direct multiplier of α (α*Gamma function). A decrease in the β value will decrease the MTTF.

But, a change from 2 to 10 varies the Gamma function only from a value of 0.89 to 0.95 so it does not have as much effect. As more data provides the probability that the pavement will live longer, it makes sense that the α value increase, as it is a measure of the 'characteristic life".

The different graphs that were predicted for MP 154 based on 4 years, 5 years and 6 years data is shown as an example in Figure 5-10. The actual measured %RSLOS are shown as orange points overlaid on the graphs. The MTTF increases from 51.9 to 54.1 years when additional data is used. This difference is really minimal in the realm of JPC where 5 years would be considered less than 10 percent of life, as compared to asphalt, where 5 years could indicate almost 50% of life. The hazard rate decreases from 0.09/year to 0.05/year. Once again this is relatively a small real difference, meaning the difference of needing maintenance in 2 or 3 years, but in this case both are not desirable. The pavement deterioration curves based on %RSLOS for all the Case Study sites are located in the Appendix.

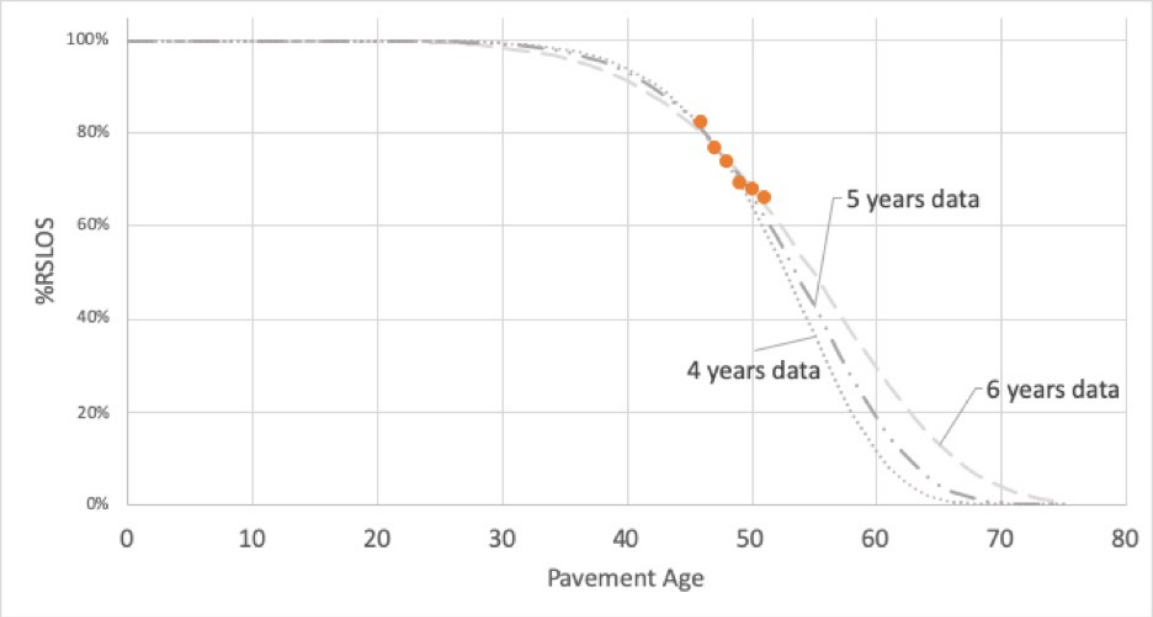

Figure 5-10 MP154 Comparison of Deterioration Prediction Trends by Years of Data

The actual RSLOS values and the predicted values using all the data (Model) and the predicted values using all but the last years data (Predicted) are shown in Table 5-2.

Table 5-2 Comparison of Predicted, Model and Actual RSLOS

Section	Predicted RSLOS	Model RSLOS	Actual RSLOS
Cat 1a_MP153	30.3	27.4	26.2
Cat 1a_MP154	40.7	35.2	33.9
Cat 1b_MP15	14.0	10.8	10.2
Cat 1b_MP17	50.2	45.6	44.4
Cat 2_MP150	20.1	21.6	21.6
Cat 2_MP 151	45.3	46.0	46.4
Cat 3_MP104	11.3	8.9	8.4
Cat 3_MP105	15.3	11.3	10.8

A strong relationship between the actual and predicted RSLOS values for the last year modeled, combining all the different models is shown in Figure 5-11a). The same graph using the values from the full model is shown in Figure 5-11b).

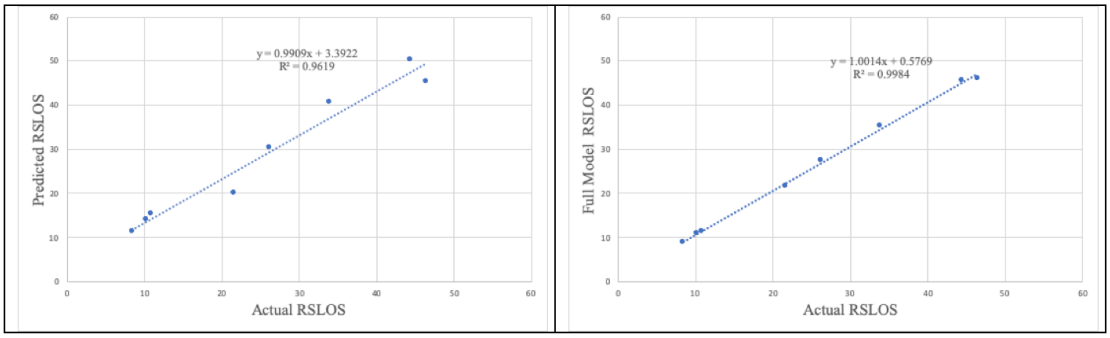

Figure 5-11 Predicted vs Actual RSLOS, a) Prediction and b) Full Data Model

5.3.1. Limitations of RSLOS due to Longitudinal Cracking

Two of the case study sections provide an opportunity to look at AASHTO PMED design prediction and %RSLOS. The figures below show the % cracking predicted by PMED by age in blue (the prediction was for 35 years). The orange dots are the %RSLOS values computed for the entire one mile sections. The mostly transversely cracked Site 13-3015 shows a relatively consistent trend with the PMED prediction, but the highly longitudinally cracked Site 13-3017 does not.

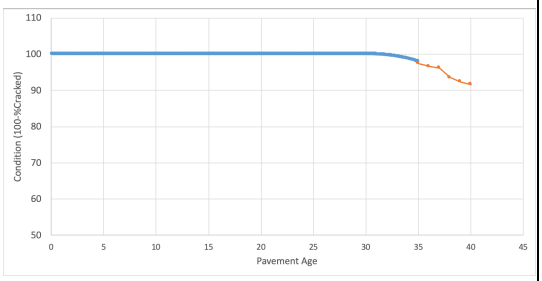

LTPP Site 13-3015

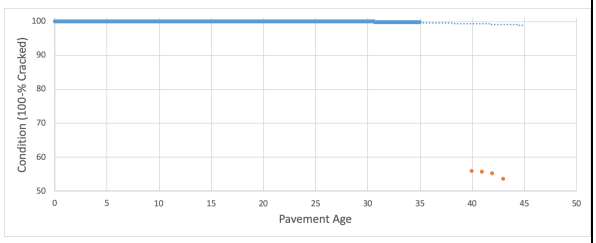

LTPP Site 13-3017

5.4. Prediction and Maintenance needs using RSLOS and KD

Maintenance needs for JPC pavement as related to cracking is primarily slab replacement as noted in Section 2. Predicting end-of life is also necessary so that the cracking rate does not cause the pavement to need additional maintenance in a short period of time. It is prudent to repair a pavement if the repairs provide an economical extension of life. If the repairs do not meet the economic criteria the maintenance effort will be considered a failure in hindsight. If the rate of cracking in the pavement is very high and continues after repairs, or if the rate of cracking increases after repairs, it can also create a perception by the public that the maintenance is not being properly performed. This research hypothesizes that by modeling the pavement cracking using Weibull distributions and identifying the potential location of the pavement slabs in their natural fatigue failure lifecycle, combined with data on sufficient JPC pavements modeled in the same way, end -of -life estimates can be improved. Combined with Life Cycle Cost Analysis, consistent, justifiable estimates can be made on maintenance actions to be taken on JPC pavements. A flowchart providing these type of decisions, based on the data involved in this research, is shown in Figure 5-12.

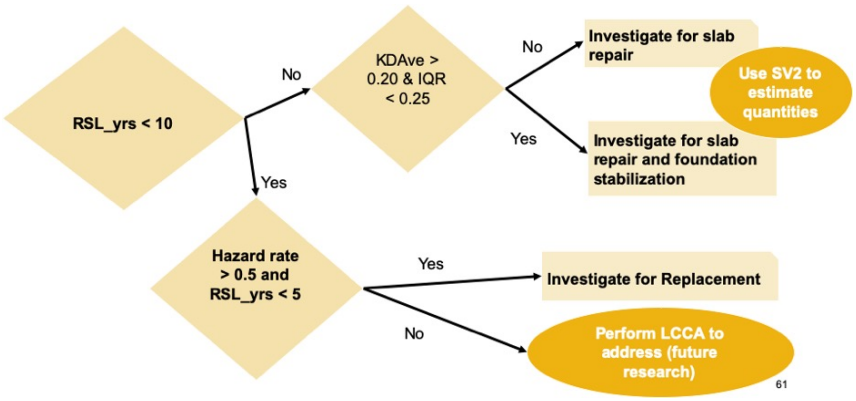

Figure 5-12 Maintenance Decision Tree

CHAPTER 6. 3D PAVEMENT DATA AND PMED LOCAL CALIBRATION

A number of States in the US are using or considering AASHTO Pavement ME Design (PMED) software as part of their pavement design decision-making considerations. Originally called the Mechanistic Empirical Pavement Design Guide (MEPDG) process in 2004, PMED has evolved into an AASHTO supported software that is part of the AASHTOWare suite of transportation tools. PMED uses a mechanistic approach to predict distress in pavements due to loading and environmental factors, and the software provides a recommended design for the conditions modeled. Calibration of the mechanistic models to real–world conditions is necessary due to the complexity of the conditions affecting the distresses. The PMED has been calibrated nationally using Long Term Pavement Performance (LTPP) data as noted earlier and reported in the NCHRP 1-37A, NCHRP 1-40D and NCHRP 20-07/Task 228 and Task 327 reports. To improve the accuracy of their designs and account for local conditions, local calibration has also been performed by over half the States. LTPP data is used in the PMED national calibrations and is also a key part of local calibrations. Calibration involves comparing the measured distresses to the distresses predicted from the PMED software and adjusting calibration factors to improve the correlations. This requires a statistically significant number of pavement sections and enough distress data to make a clear correlation. A number of States, including Georgia, have reported issues with having sufficient sections or sufficient distress to perform the most efficient local calibration [Mallela et. al, 2015, and, Von Quintus et. al, 2015].

6.1. Jointed Plain Concrete (JPC) LTPP Sections

The Long Term Pavement Performance database (infopave.fhwa.dot.gov) contains the most comprehensive information on pavement performance in the world. LTPP sections with concrete surfaces are found in General Pavement Studies (GPS) 3, 4, 5, 7R and 9 and Specific Pavement Studies (SPS) 2, 4, 6, 7 and 8. The difference between GPS and SPS is that GPS sections were typically selected out of existing pavement sections and the SPS sections were designed experimental studies with control and experiment sections [Elkins et al. 2017]. GPS sections 4 and 5 are jointed reinforced concrete pavement and continuously reinforced concrete pavements, respectively. GPS sections 7 and 9 are related to overlays. This research concentrates on the original GPS experiments related to jointed plain concrete pavements (GPS-3) as noted earlier.

LTPP data like that collected for the GPS-3 experiment has assisted in refining pavement design. As noted previously, the existence of the LTPP database provided the ability to nationally calibrate the original 2004 Mechanistic –Empirical Pavement Design (MEPDG) software to real world conditions. Subsequent national calibrations of AASHTO Pavement ME Design (PMED) have also used LTPP data. Users of the current software also utilize LTPP data from their State or region to perform local calibration. For jointed plain concrete (JPC) pavements PMED predicts transverse cracking and faulting as indicators of performance, therefore transverse cracking and faulting distresses are needed to perform local calibration of the software. Faulting and deflection data in the LTPP concrete pavements have been reviewed in several reports which looked at distresses in the LTPP sections [Khazanovich et al. 1998, and, Yiang &Tayabji 2000], but, potentially due to

minimal distress, limited studies have been performed on cracking in the GPS 3 concrete pavements.

Of course, concerns over sufficient cracking data for JPC pavements is not new and has been an issue since the original precursor of PMED, MEPDG (mechanistic empirical pavement guide) software, was first shared with State DOTs in 2004 as part of the NCHRP 1-37A project. Figure 6-1 is from a TRB paper that described national calibration performed at that time [Darter et. al 2005] and shows the measured percent slabs cracked in relation to the estimated fatigue damage from the JPC cracking model. The graph identifies 520 observations but the shape of the model is clearly driven by a fraction of that total amount, as most of the observed percent slabs cracked are 0.

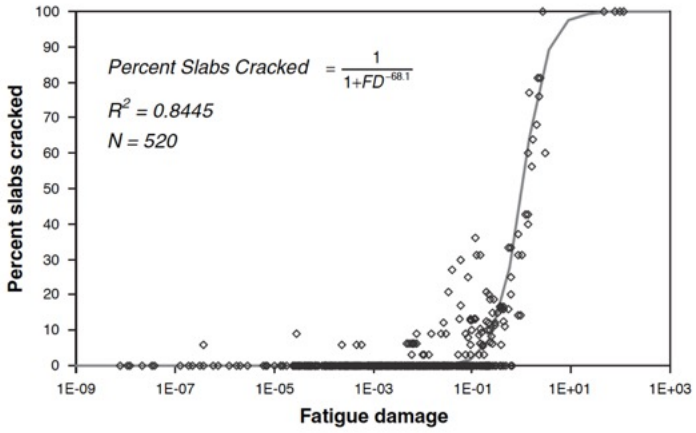

Figure 6-1 JPCP Cracking model (from Darter et al. 2005)

Even the JPC example in the AASHTO "Guide for Local Calibration of the Mechanistic-Empirical Pavement Design Guide" has insufficient cracking data to adequately perform a local calibration [AASHTO 2010].

The lack of JPC cracking data was identified even prior to the data being used in local calibration of the pavement design software. A TRB paper from 1998 noted that the GPS-3 sections were on average 12 years old in 1995, and that only 26% of the sections had transverse cracking at that time as shown in Figure 6-2 [Moody 1998].

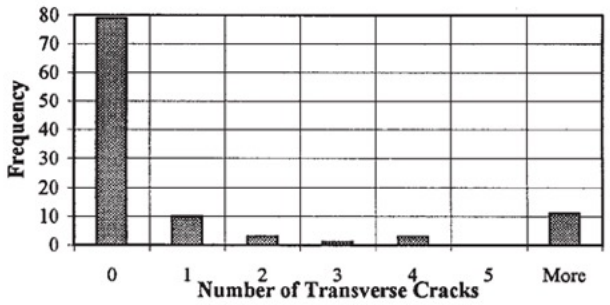

Figure 6-2 Cracking in LTPP GPS-3 sections (from Moody 1998)

Many of the GPS-3 LTPP sections still have zero transverse cracking. Twenty years later the pavements have aged 20 years, but, based on a review of the 2017 MON_DIS tables (which include distress information in the LTPP database) out of 129 total GPS 3 sections, 67 (52%) have no transverse cracked slabs. So, in over 20 years that 26% has still only risen to 48%. At that rate we could still wait another 40 years before we have all the data needed to identify cracking greater than 0!

A number of State DOTs have performed local calibration of the PMED to their data and conditions. Many of the concerns with the local calibrations were due to the lack of distress data to perform a meaningful regression for calibration. While previous observations of zero cracking cannot be changed, it is possible that we may be able to gather additional information out of existing sections that continue to provide observations of zero cracking. Figure 6-3 shows the construction date (from the INV_AGE table) of the existing 77 active

GPS 3 sections along the horizontal axis, and the number of transverse cracked slabs in the section as of the last survey date reported in 2017 in InfoPave on the y-axis. Each point is 1 LTPP location. The sections with zero cracking are shown as filled red diamonds to emphasize their range. Clearly, they are not the newest sections, but cover almost the whole range of construction dates as all the existing sections. Additional information about the potential for cracking in these sections could be valuable to the current needs of pavement design and rehabilitation.

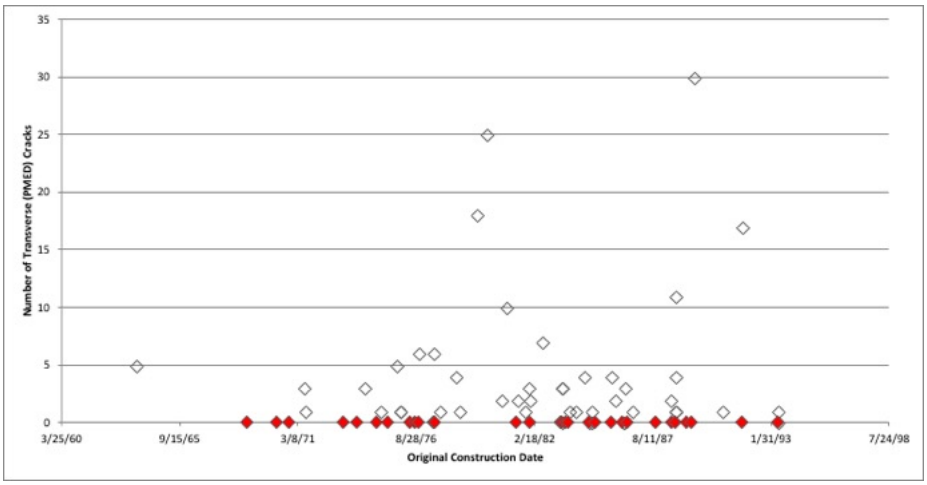

Figure 6-3 Construction Date vs Number of Transverse cracked slabs - Active GPS 3 Sections

LTTP data is an immense temporal resource of pavement condition at a location under measured conditions, but it does not tell us about the probabilistic distribution of conditions over the entire pavement section that shares similar traits (i.e. the distribution of distresses in a pavement section constructed at the same time). Continuous collection of pavement conditions, such as what can be gathered utilizing 3D lasers on vehicles driven at highway speeds, can provide a complete picture of the distribution of condition and distresses along an entire pavement section.

6.2. Combining LTPP and continuous 3D pavement data

Uniting LTPP data and 3D pavement data could improve the reliability of decisions that are made now using LTPP data alone. LTPP GPS-3 sections were constructed prior to being identified as LTPP sections, but there was some bias that was necessary for the actual site selection, due to safety and testing concerns. These biases would tend to place the LTPP sections in locations where they would be expected to perform better than the average in the section (i.e. flatter sections for good sight distance for future traffic control needs, areas with no known construction or materials deficiencies). Of course, the LTPP sections have high quality material and historical performance data and therefore lower standard deviation for inputs, and, irreplaceable historic time series data. Nonetheless, a pavement section as a whole should retain a relatively normal distribution of inputs with the standard deviation reasonably assumed to be the construction range of quality for the materials for the time of construction.

Empirical calibration of the cracking model in PMED uses the percent of slabs with transverse cracks from the LTPP section. The original MEPDG cracking model documentation recognized that this "may not well represent a longer project length" [Yu and Darter 2003]. The benefit in using a larger segment (i.e. 250-280 slabs per 1.6 km (mile) vs 25-30 slabs for LTPP) is the possibility of providing non-zero and non-discrete data for the section. Even if there is cracking within the LTPP section, since the LTPP site is only 0.1 mile the cracking % are restricted to values related to the number of slabs in the 0.1 mile section (For example, 1 crack in a 25 slab section is 4%, 2 is 8%, 3 is 12% etc.;

therefore no observations other than 4%, 8% or 12% measured cracking are possible). Combining this LTPP section data with the % transverse cracking in a longer section may improve the prediction value of the regression equations used in local calibration, especially as related to zero cracking values. Due to the amount of LTPP sections still not exhibiting transverse cracking, almost half of the sections/data that can be used in current models are based on data that is right censored. Right censored in this case means that we know the amount of fatigue damage they can resist without failure, but we cannot predict what their actual failure limit is, as it has not yet been met. What can we do to prevent waiting another 20 – 40 years or more to make inferences about the majority of LTPP concrete pavement sections?

As shown in the following section, a method is proposed to use 3D pavement data to support LTPP data for PMED local calibration purposes now. This chapter also provides a case study examining this concept using the two LTPP JPC sections in Georgia described in the Appendix. As noted in the Appendix, the location of the actual 25 slabs in the LTPP sections in Case Study categories 2 and 3 were identified and the condition and change in condition of the LTPP slabs were compared to the full section. These LTPP sections were also recently used to locally calibrate the PMED software for Georgia DOT. The results of that calibration for transverse concrete cracking in JPC are compared to the predictions that would be made based on the distribution of distresses using the distresses identified using 3D pavement data. The results show that combining these two data sources can improve the usability of LTPP data for pavement design and local calibration purposes.

6.3. Method to identify probabilistic cracking using Monte Carlo Simulation

The following steps are proposed to identify probabilistic transverse cracking values for use in PMED local calibration using 3D pavement data:

1) Identify extent of original construction around the LTPP location. This information is not in the LTPP database, but some State DOTs have archived construction plans or have separately documented the history of their pavement sections. In the absence of any construction information, a section of pavement approximately one mile before and one mile after the LTPP section should be considered, unless pavement conditions change dramatically, in which case the section should be shortened to that point.
2) Identify the 3D pavement data from this section of pavement and identify the specific LTPP slabs/location within the full section.
    a. Remove bridges or other known anomalies (i.e. construction related cracking due to late sawing will be parallel and very close to the transverse joint and found at an early age)
    b. Eliminate sections with any major traffic changes (i.e. major interchanges such that truck traffic is different on one side of the interchange)
3) Classify slabs in the 3D pavement section as to PMED cracking criteria. The PMED cracking criteria is based on the LTPP Distress Identification Manual [Miller and Bellinger 2014] and includes any type of transverse cracking greater than 0.3 m (1 ft), of any severity level (low, medium or high). It is measured as a percentage based on number of transverse cracks/number of slabs in the LTPP section. In this research this is considered T1, T2 and SS slab states.

4) Calculate a new probabilistic value of % cracking for the LTPP section based on a Monte Carlo simulation sampling of sections that have the same number of slabs or same length as the LTPP section in the complete section
    a. The MC simulation is performed by defining each slab in the section as either 0 for not PMED cracked or 1 for PMED cracked
    b. Sample the data randomly in 1500 m (500 foot) sections (LTPP length) and compute the average value for each section (average of the sum of the 0 and 1 values).
    c. Sample at least three thousand times and average the results to compute the MC simulation average/ 500 ft.
5) Substitute the Monte Carlo probabilistic values in the calibration calculation for the LTPP site for the previous zero or discrete values.

6.4. GDOT JPC PMED Local Calibration using LTPP sites

Following is an example of how 3D pavement data can be used by exploring some of the data used in the recent local calibration for GDOT. The final measured versus predicted cracking for JPC from this calibration effort is shown in Figure 6-4 [Von Quintus et al. 2015]. Clearly most of the measured data are clustered around values of 0, 4, and 8%.

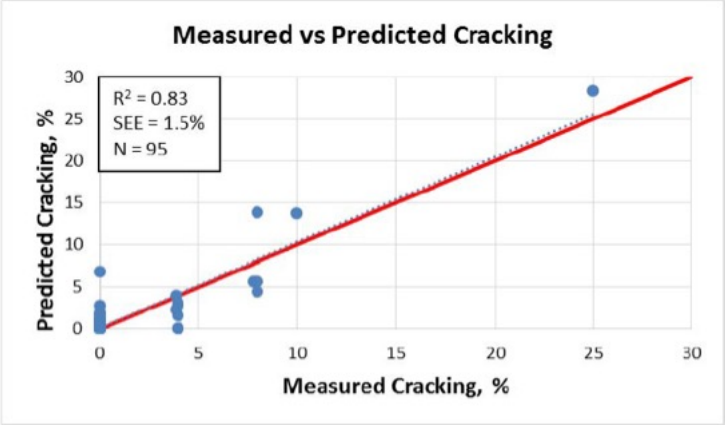

Figure 6-4 Georgia Local Calibration Graph for JPC Transverse cracking (from Von Quintus et al. 2015).

GDOT used 8 LTPP sites in their calibration (and 12 non-LTPP sites), including LTPP sections 13-3015 and 13-3017. As noted earlier, the LTPP 13-3015 section showed no transverse cracking (beyond map cracking) until the 2014 LTPP evaluation and the LTPP 13-3017 section still shows no transverse cracks as of the last distress map located on the LTPP site, 2016.

A surrounding ~2 mile section was used in this analysis. The individual slabs in the LTPP section were identified in each section. The location of the slabs identified as PMED cracked are shown in Figure 6-5. The x-axis is the MP location and the y-axis shows the PMED cracked slabs in 2013, 2014 and 2015 (note that the slabs are at an exaggerated scale to show them clearer, so they may overlap). A total of 15 slabs were identified as transversely (PMED criteria) cracked in the section surrounding LTPP section 13-3015 in 2013. The LTPP locations are noted in the Figures as beveled rectangles surrounding all three years data, each was 24 slabs in length. The two stars in the LTPP section in Figure 6-5a (2014 and 2015) show the one LTPP identified transverse cracked slab in section 13-

3015, which was previously described as not being identified in the 3D pavement data. A total of 19 slabs were identified as transversely cracked in 2013 in the section that encompassed LTPP section 13-3017 as shown in Figure 6-5b. Note, these figures do not show all the cracked slabs in these sections, if a slab was only longitudinally cracked it is not shown, as longitudinal cracking is not currently modeled in PMED.

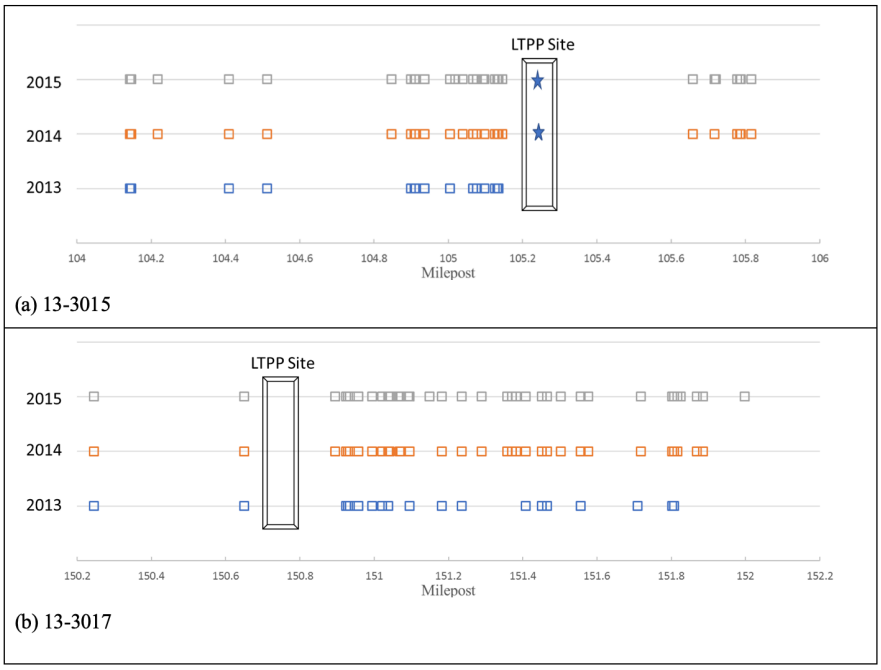

Figure 6-5 a) and b) PMED cracked slabs surrounding sections (a)3015 and (b)3017 based on 3D Pavement data

Tables 6-1 and 6-2 show the distribution of transverse cracked slabs in LTPP Sections 13-3015 and 13-3017 (#PMED cracked in LTPP Section) for each of the three years, 2013, 2014 and 2015. The Table also includes the number of PMED cracked slabs in the section surrounding the LTPP site (#PMED cracked in 3D section). The number of PMED cracked slabs in the section are also shown as compared to the number of slabs in the section (Ave #PMED cracked/#slabs), an average per 1500 m (500 ft) (Running Ave/500ft) and a Monte

Carlo simulation using a 1500 m (500 ft) section and 3000 simulations (MC simulation ave /500 ft). The MC simulation was performed as noted previously in Step 4 of the proposed method. Three thousand samples were collected, and they were averaged to compute the MC simulation average/ 500 ft. Inspired by the central limit theorem, the MC simulation reserves the characteristics of the sample areas while inherent pavement variability is taken into account.

Table 6-1 LTPP Section 13-3015, PMED transverse cracking values

13-3015 1.7 miles	#PMED cracked in LTPP section	#PMED cracked in 3D section	Ave # PMED cracked/ #slabs	Running Ave/500ft	MC simulation Ave/500 ft
2013	0	15	0.0294	0.8672	0.7865
2014	1	25	0.0490	1.3029	1.3154
2015	1	28	0.0549	1.4834	1.4724

Table 6-2 LTPP Section 13-3017, PMED transverse cracking values

13-3017 1.8 miles	#PMED cracked in LTPP section	#PMED cracked in 3D section	Ave # PMED cracked / #slabs,	Running Ave/500ft	MC simulation Ave/500 ft
2013	0	19	0.0277	1.1011	0.9595
2014	0	32	0.0468	1.8709	1.6179
2015	0	37	0.0541	2.1353	1.8691

The %Cracked Slabs Measured vs Fatigue Damage computed curve for the LTPP sections (similar to Figure 7-1) is shown in Figure 6-6. The grey dots are the curve as predicted by the nationally calibrated PMED fatigue prediction equation (Equation 1) that was identified at the time of the GDOT calibration. FD is fatigue damage calculated by the PMED software.

Percent Cracked slabs = $\frac{1}{1+C_4(FD^{C_5})}$, where C_4=0.6 and C_5= -2.05 (7-1)

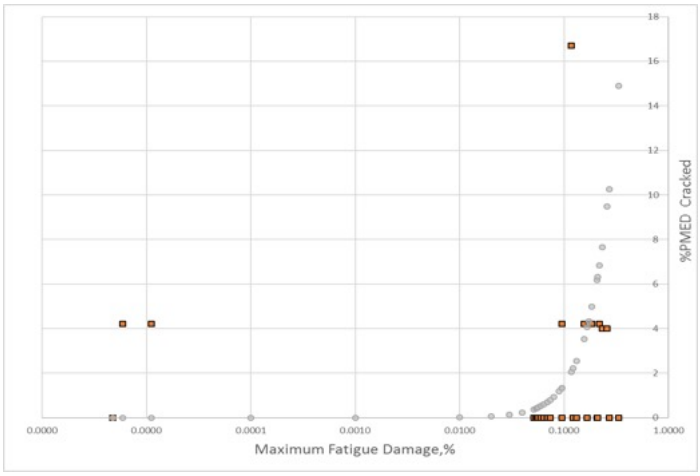

Figure 6-6 Measured Fatigue Cracking (%PMED Cracked) versus Fatigue Damage based on LTPP sections

The orange squares are the measured cracking % from the LTPP data based on the Fatigue Damage from the PMED software. You can see that the measured values are either 0, 4. 4.2 or 16.7 which corresponds to 1/25, 1/24, and 4/24 which were the only measured cracking in the 8 LTPP sections (these LTPP sections consisted of either 24 or 25 total slabs).

Figure 6-7a) shows the bottom right portion of Figure 6-6 blown-up to see the curved portion of the model in more detail. Figure 6-7b) is the same location but replacing the 6 LTPP data points from sections 3015 and 3017 with the data from the Monte Carlo simulations. Four values that were 0% PMED cracking in Figure 6-7a) can now be seen to have values different than 0 in Figure 6-7b). Similarly, two sections that were at 4.2% have values below 4%. Based on the new data the power curve appears that it possibly should shift some to the right. Additional data for the remaining sections clustered around

the 4% cracking value could lead to even better projection. Unfortunately, 4 of those 5 points are from two sections (13-3016 and 13-3018) that were taken out of study in 2004 and 2000, before 3D data was available. Interestingly, the sections appear to have been taken out of service due to extensive longitudinal cracking, not transverse cracking.

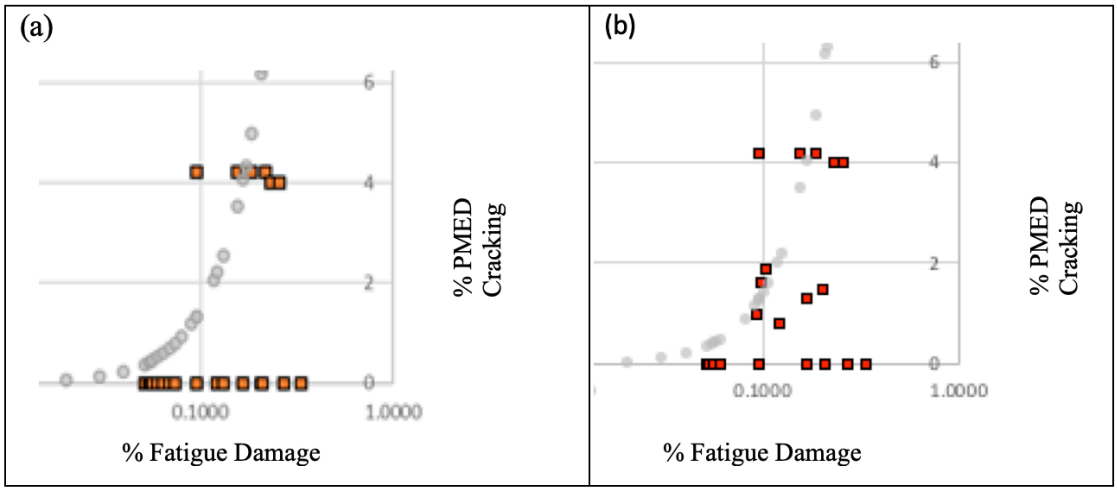

Figure 6-7 (a) Enlarged section of bottom right portion of Figure 6-6 and (b) Same section but showing the Monte Carlo values for predicted cracking from Table 6-1 and 6-2

6.5. Summary

The foresight that provided for the LTPP pavement data that we have today has been an immeasurable benefit to pavement design practitioners for many years. New technology, such as that which can provide high quality continuous 3D pavement data, can now be combined with the LTPP data to provide even greater benefits. As shown, the discrete, detailed data from LTPP can be combined with continuous data on the variability of the distresses to provide more intricate models of pavement performance. The use of this method could improve the results of local calibration of the PMED software. This method is limited to GPS sections, as SPS experiments do not have the benefit of surrounding slabs

constructed the same way Of course, care must be taken to not include anomalies that are not related to the pavement design, such as construction related cracking. As 3D pavement data becomes more standardized, anomalies in the distress data will be more easily identified.

CHAPTER 7. CONCLUSIONS AND RECOMMENDATIONS

7.1. Contributions

The contributions of this research are the following:

- First time to define the slab-level distress types and condition 'states' based on slab level crack pattern and their possible distress progression/deterioration from one state to the other at a topological level. The 3DBSM provides for the first time an objective means to comprehensively characterize cracking in a JPC pavement, and changes in cracking over time.
- Created a new method to quantify the patterns of cracking in a JPC pavement using 3DSBM and a kernel density regression (KD) based smoothing technique. KD provides the opportunity to address that the condition of a slab can have an impact on the adjacent slabs and is shown to be a tool to identify clustering in cracking, along with identifying differences in deterioration rates using KDAve and IQR. KDcurves also have future benefit in correlating with other continuous roadway measurements, like smoothness (IRI) or structural conditions (traffic speed deflectometers).
- Developed a new model (%RSLOS) to track deterioration in concrete pavements temporally by incorporating the impact of replaced slabs on the condition of the pavement as related to the pavement age. This provides a direct comparison of condition of a pavement (RSLOS_yrs), regardless of recent maintenance history. It also provides a potential method to predict end-of-life for JPC, to properly identify optimum maintenance treatments.

- Developed a method to supplement LTPP data for calibrating pavement design models to actual conditions using 3DSBM and Monte Carlo sampling techniques.

7.2. Findings

The 3DSBM provides an opportunity to identify:

- Spatial and Temporal Differences in cracking orientation and cracking rate in JPC pavements.
- Distinct pavement families that can differentiate the types of cracking that develop in JPC pavements temporally. This recognizes the impact and effect of cracking orientation as a driver in future deterioration of slabs. This may also be an indirect indication of the built-in stresses of a pavement and be correlated with curl and warp measurements in future research.
- Potential end-of-life for JPC pavements using RSLOS and reliability theory along with 3D pavement data.

It also provides an opportunity to:

- Understand more about variability in JPC pavements
- Improve our understanding of longitudinal cracking in JPC pavements
- Improve PMED local Calibration

7.3. Implementation Considerations

To bring this research to fruition, the slab states need to be automatically allocated using machine learning or another mechanized tool so an entire network can be easily classified.

The definition and classification of the slab states are designed such that they can be automated, and others are currently working on this aspect as noted in the following section. The slabs and slab states should be established in a geographic information system (GIS) environment to facilitate the location referencing needed to identify repaired slabs over time. Sections of pavements should be queryable such that the %RSLOS value can be tied to the graphical representation (KDCurve) of the pavement at any time as shown in Figure 7-1.

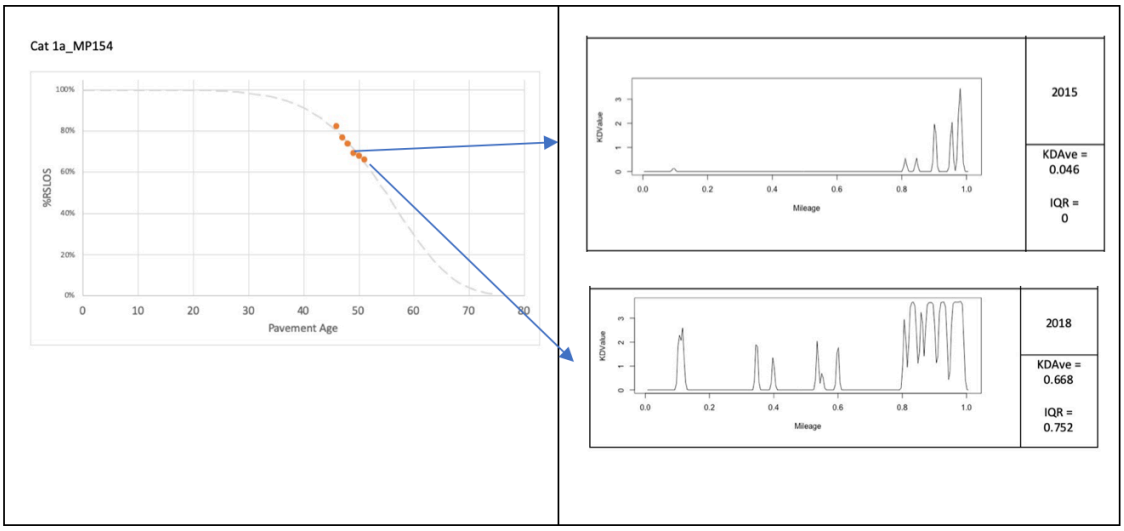

Figure 7-1 Conceptual Pavement Asset Management system view

The pavement asset management (P.A.M.) system should include triggers for IQR >0 and should identify pavement sections subject to clustering by comparing IQR and KDAve automatically. As part of asset management, the changes in slab states should trigger a check in the maintenance portion of the system to provide a quality assurance check of the separately imported maintenance data. As more data is developed additional models and advancements can be developed. The benefits, value and time frame of the improvements

that can be realized by implementing this research is shown in Table 7-1. The benefits cover several different categories related to concrete pavements. The area(s) that are affected are noted in the table under the following category abbreviations: Fundamental Pavement Behavior (FPB), Design (D), Maintenance and Rehabilitation (M&R) and Pavement Asset Management (PAM).

Table 7-1 Future Benefits and Value of Implementation

Benefits	Category	Value	Time Frame
Systematic, standardized description of slab states to define real world cracking spatially and temporally in JPC pavements at multi-scales which can provide the feedback necessary to provide for sustainable and resilient JPC pavement design and optimized asset management	FPB, D, M&R, PAM	Major improvement, no current standard exists	Immediate availability
Characterize pavements as to classical transverse cracking or combination of cracking to assist in maintenance considerations	FPB, M&R	Marginal improvement, simple measurements could identify now	Immediate availability
Use 3DSBM to improve calibration of AASHTO Pavement ME Design	D	Incremental improvement	Immediately available
Identify slabs to be repaired using slab states	M&R	Minimal improvement now, but could be an incremental improvement if	Immediately available, some time needed to include faulting into the decision

Benefits	Category	Value	Time Frame
		faulting is also considered	
Define clustering statistically and use the results as a trigger for pavement maintenance decisions	FPB, M&R, PAM	Incremental improvement in pattern recognition	Minimal time needed to further analyze additional data to define trigger points
Use patterns from KDcurves to perform QA on maintenance data	PAM	Incremental improvement in QA	Can be incorporated into P.A.M. system
Use statistical value from patterns (IQR) to perform triage for maintenance	M&R, PAM	Marginal improvement	Can be incorporated into P.A.M. system
Monitor pavements using the RSLOS concept to allocate budget priorities	PAM	Minor improvement, uncertainty in end-of-life still a consideration	Can be incorporated into P.A.M. system
Analyze longitudinal cracking using the slab states to develop models for deterioration related to longitudinal cracking	FPB, D, PAM	Major improvement, currently no data like this is readily available	Minimal time needed to gather data after automation is compete, research to develop models will take longer
Predict “catastrophic failure” (a pavement section that experiences more failures than economically maintainable) in a pavement in enough time to budget for the major reconstruction necessary	FPB, M&R, PAM	Major improvement, this capability does not currently exist	Time will be needed to gather additional data and perform research to validate the model and identify the appropriate end

Benefits	Category	Value	Time Frame
			of life value (i.e. MTTF) to use

7.4. Recommendations for Future Work

- This research was focused on different categories of pavements historically used in Georgia. This research was also limited to one lane of data. Additional 3D data for spatio-temporal analysis of different pavement designs and locations, and for adjacent lanes of pavement could provide for additional statistical opportunities to analyze patterns. Multi-lane data would be especially beneficial for identification of foundation related issues.

- The definitions and defined classification of the Slab States provides a potential for machine learning to be used to automatically categorize Slab States. Dr. Tsai's multi-disciplined research team is currently investigating this research.

- Although not presented in detail in this research, a new faulting method using 3D pavement data has shown promise and incorporating faulting at a slab level, and faulting related to cracks, could provide enhanced identification of the most distressed slabs. Faulted cracks indicate slabs that are more susceptible to movement under traffic, which would indicate a more severe condition than just cracked slabs. Dr. Tsai's multi-disciplined research team is currently working on incorporating faulting into the SV2 application.

- Although this research did not investigate the relationships, the KDcurves are intended to be combined and correlated with other continuous measurements, such as IRI

or structural data, like what can be obtained from a Rolling Weight Deflectometer/ Traffic Speed Deflectometer.

- Tie RSLOS conditions to economic factors using Life Cycle Cost Analysis to identify optimal timing for maintenance activities on concrete pavements. Dr. Tsai's multi-disciplined research team is investigating these considerations.

- The different location reference representations of the current condition of slabs and the original condition of slabs can be compared to provide a rate and remaining service life just for repaired slabs. This information would be valuable in a study of the quality of different types of repair materials, repair methods or replacement strategies as part of a research project on improving JPC pavement maintenance.

- Certain portions of this research can be extended to materials related distress in JPC. 3D Pavement data can be used to measure ASR (alkali-silica reaction), D-cracking, spalling or map cracking. These types of distress can be hard to detect at low severity, but, can be identified as present or not present in a slab at higher severity. Spalling of joints and cracks can also be identified. But, due to the nature of these types of distress, it is not expected that prediction models could be developed.

- While the slab states and method identified herein is not readily applicable to Jointed Reinforced Concrete Pavement (JRCP) or reinforced concrete bridge decks (due to the different forms of cracking distress based on the presence of reinforcing steel), 3D data could still be used to evaluate either of these systems. Methods that are closer to those being used to evaluate cracking in asphalt, especially asphalt alligator cracking, may be appropriate for JRCP and bridge decks.

- Concrete overlays (previously termed whitetopping) would be an especially relevant type of pavement that would be appropriate to analyze using the 3DSBM.

7.5. Conclusion

The HPMS criteria of % transverse cracking, and the historical considerations of % cracking can now be realized in a distinctively more complex and detailed way with 3D pavement data. The current condition of pavements can be visualized and categorized using kernel density regression smoothing techniques and 3DSBM slab states. Average distress values (KDAve) and measures of clustering (IQR) of distress can be used to define and quantify pavement condition. Looking at the (OS) original slabs location reference condition and using the %RSLOS value to model the distress using Weibull equations, a consistent trend of cracking deterioration by age is possible. Weibull relations can also be used to identify end-of-life consideration for concrete pavements.

With a consistent method (3DSBM) to classify and evaluate cracking in concrete pavement, and the amount of 3D pavement data that is coming available, unlimited additional statistically significant trends can be identified for cracking in concrete pavements. This will lead to improved design, maintenance and rehabilitation decisions related to JPC pavements.

APPENDIX A. PAVEMENT SECTION SITES

A.1 Case Studies

This Chapter presents case studies of four different type of pavements found in Georgia, assessing the 3DSBM condition, KDcurves and RSLOS condition and statistics for each. The KDcurves and RSLOS/Weibull graphs follow in Section A.2 and A.3.

The earliest 3D pavement data was from 2013 and the latest data used in this research was from 2018, potentially 6 years of slab states for each section. The pavement sections reviewed for this project were chosen to include some of the most distressed locations, and as such many already had experienced slab rehabilitation at the time of first inspection using 3D pavement data. To further complicate this, many of the pavement sections included random joint spacing, making identification of slab replacements challenging in some instances. Most concrete construction projects use leave -outs (sections of paving that are left out to allow construction ingress and egress during construction) which are filled in after that section of pavement is completed. These leave-outs do not necessarily follow the same pattern as the mainline paving, and each area had to be reviewed closely to ascertain if it was a repair or a leave out. After the initial year, identification of subsequent repaired slabs was possible by following a registering process, but identification of already repaired slabs was done manually and it is recognized that there could be some error in this identification. It is also recognized that the timing of the original slab replacements is unknown, beyond the consideration that the slab was replaced sometime before the initial dataset, 2013.

For the purposes of this effort, each beginning and end slab was identified for each mile and the resulting distance from the summation of all the slab lengths was noted as the length for that section in that year. The accumulated distance per year was normalized to the starting (2013) year for each subsequent year and the number of slabs per year determined.

The sections include each of four different types of pavement constructed by Georgia DOT in the late 1960's to the late 1970s. Georgia DOT pavement design changes over this time period include going from a soil base to a stabilized base, changes in joint spacing and orientation, and addition of load transfer (dowels).

The sites are categorized into 3 different major categories and one minor subcategory, based on the categories identified in previous research by Tsai etal.(Tsai, 2012) and delineating different time periods of designs for Georgia DOT. Two of the major categories are undoweled, with one category (Category 3) doweled.

- Category 1 includes undoweled pavement, 9-10 inches thick, placed directly on soil or soil-cement. This category includes two different types of joint configuration, broken into subcategories; (a) 30 ft joints and (b) Varied joint spacing (17 ft., 16 ft., 22 ft., 23 ft.) with skewed joints. This pavement category was constructed in the mid to late 1960's. Category 1a and 1b Case Study sites are located on different sections of I-16.

- Category 2 is also undoweled pavement, 9-10 inches thick but on a GAB or cement stabilized GAB base. This category includes joints at a skew with alternate spacing (16, 17, 23, 22). Category 2 Case study site is located on I-20 and includes the LTPP site 133017. This pavement category was constructed in the mid- 1970's.

- Category 3 is doweled pavement, 10 inches thick with an HMA interlayer over soil cement. Category 3 Case Study site is located on I-16 and includes LTPP site 133015. This pavement category was constructed in the late- 1970's.

This project utilized progressive years data from pavements from each of the 3 categories. The following section focuses on 2 sections (miles) from each category and subcategory.

Case Study Section Overview

Pavement of each category is reviewed in depth in this section to provide information on the location, design, history and condition of the pavement sections. The sections will be referenced by the category number or milepost as noted below:

1a) MP153 and MP154, I-16, EB (undoweled, 30 ft joints on soil base)

1b) MP17 and MP15, I-16, WB (undoweled, skewed random joints on soil cement base)

2) MP150 and MP151, I-20, EB (undoweled, skewed random joints on aggregate cement-stabilized base)-LTPP 13-3017

3) MP104 and MP105, I-16, EB (doweled, 20ft jts, on HMA interlayer over soil cement)- LTPP 13-3015

Sites 2 and 3 are also LTPP sites as noted and both sections are still active. The last LTPP inspection included on the Infopave website is from 2016.

Each Case Study consists of sections of pavements constructed at the same time, under the same construction contract, with the same pavement design and similar if not identical

traffic. The Case Study Sections will first describe the full section in general terms. Each Case study starts with a table like Table . The age of the pavement and the pavement design is from Georgia DOT historical records (including project plans), or in the case of the LTPP sites, from the LTPP Infopave website. "D/U" indicates if the section is doweled or undoweled, as noted earlier, only the Case Study 3 site is identified as doweled. "Bridge?" Indicates if the section includes a bridge. Bridge decks and approach slabs were considered NC or were removed for analysis. "ADT/%trucks" is the 2018 reported average daily traffic and percent trucks from the closest Georgia DOT traffic volume site (https://gdottrafficdata.drakewell.com/publicmultinodemap.asp) from the GDOT TADA website. The 2018 truck volume based on the ADT and truck percent varied from 5700 to 7000 trucks/day for the 4 sites. The traffic was not used in this research, it is only provided for information.

Table A-1 Case Study Pavement Information Headings

Age in 2013	Slab Thickness	Joint Spacing	D/U?	Base/ Subbase	Shoulder	Bridge?	ADT/ % trucks

Category 1a Case Study

Site 1a is located on I-16, EB MP153 & MP154 in Chatham County. The site is just west of the intersection of I-16 and I-95. The Savannah Port is located just east of I-95, and trucks traveling to and from Atlanta traverse this section of I-16. Information on the pavement is included in Table A-. This is the oldest pavement section of the 4 Case Studies.

Table A-2 Category 1a Pavement Information

Age in 2013	Slab Thickness	Joint Spacing	D/U?	Base/ Subbase	Shoulder	Bridge?	ADT/ % trucks
46	10 inch	30 ft	U	Soil/Soil	Asphalt	Y	48,800 14%

As expected due to the age and traffic, Site 1a showed cracking distress throughout the two miles at the first year of data collection (2013). Cracking was predominately in the form of transverse cracking, or slab state T2. Based on the 30 ft slab length it is expected that transverse cracking would dominate, as 15 foot joint spacing is now used in Georgia due to the tendency of 30 foot joint spacing to crack transversely near the center of the slab. Using 30 ft expected joint lengths and evidence of prior slab replacements it was identified that 16 slabs were already replaced by 2013 in the 2 mile section (both MP153 and MP154). One additional slab was repaired by 2014. By the 2015 data collection this section of pavement had been extensively repaired. An additional 67 total slabs were replaced by 2015. This aged section (pavement was ~48 years old in 2015) with extensive repairs provided an opportunity to observe and document the result of major full depth slab replacement in an aged pavement.

KDCurves Site 1a

The KDcurves for 2013 and 2014 for MP153 are shown in the Appendix section A.2 All slabs were repaired and there was no cracking in 2015, so the KDAve and IQR for 2015 is 0. The KD curves provide a visual overview of the spatial distribution of the cracking distress and how it changed in one year. These two sections changed from 21 to 24(MP153) and 24 to 34 (MP154) T2 slabs from 2013 to 2014. Similarly, MP153 had a lower KDAve value in 2013 and 2014 and a lower increase in KDAve from 2013 to 2014 as compared to MP154. MP154 was also repaired in 2015, but the 2015 3D inspection did identify cracking, and the slabs that were identified as cracked in 2015 were not cracked in 2014. The two sections also behaved differently after the repairs were made. MP 153 went from 25 T2 to 0 back up to only 8 T2 in 2018. MP 154 went from 34 T2 back to 34 T2 slabs in 2018. As evident in the KDcurves the majority of the cracking for MP154 is between 0.8 and 1, the same area with the highest amount of distress prior to repairs. Potentially additional effort could have been put into addressing any foundation issues in the area, if the KDcurves had been available prior to the repairs.

OS Condition Site 1a

The Original slab conditions for MP 153 and MP 154 (Appendix A.2, Table A-10) provide a look at the pavement segment without the noise of repaired slabs. It can be seen that the new T2 slabs grew from 2013 to 2014 from 20 to 24 (4/year). After repairs the section went two years without any new cracking and then the rate of new T2 continued at a slower rate than previously. The before and after repair rate (based on a limited pre-repair time frame) is 4/year versus less than 1/year. Contrast this with MP 154, which showed an

increase of T2 slabs from 24 to 33 (9/year), and after repairs the T2 slabs grew to 16 in a span of 3 years (~5/year), a 9/year versus 5/year rate. Both apparently reduced in the new cracking rate after repairs. This contradicts anecdotal concerns that the rate of repairs needed will increase after repairs are performed due to disturbing the base.

Both sections had different rates of cracking before repairs and both sections reduced in the rate of new T2 slabs after repairs. But, it is evident that the economics of doing another slab replacement or a full lane reconstruction for just these two adjacent sections would be vastly different if the observed rate of cracking continues, even though they are the same age, same design, etc. It will be shown that these two sections are actually rather close in performance in comparison to Case Study Sites 1b and 2.

The Weibull graphs identified for these sections are also shown in Appendix. The increased deterioration rate for MP 154 is evident in the graphs. The kink in each of the data points appears to be due to the replaced slabs, as noted previously, slab replacements are an unknown distribution and although the OS condition is designed to minimize the effect, it appears it can still be observed, as can the rate decrease after repairs.

Category 1b Case Study MP15 and MP17

Site 1b is located on I-16, WB MP17-14 in Twiggs County, east of Macon, Georgia. The original project included a little over 11 miles of pavement approximately from MP 11.9 to 23.3. Site 1b includes two bridges, one located between MP 17-16 and the other between MP 16-15. Mile 17-16 and 16-15 were both highly deteriorated and already had a number of replaced slabs in 2013, so were somewhat similar. Therefore, this Case study concentrates on MP 17-16 and MP 15-14.

Table A-3 Case Study 1b Pavement Information

Age in 2013	Slab Thickness	Joint Spacing	D/U?	Base/ Subbase	Shoulder	Bridge?	ADT/ % trucks
41	9 inches	Random Skew 17', 16', 22', 23'	U	Soil Cement /Soil	Asphalt	Y – MP 17 and MP 16	25,900 22%

Site 1b also provides an example of pavement sections that have the same design, constructed at the same time, but show vastly different behavior, even more different than Case 1a. MP 17-16 had almost 10% of slabs already replaced in 2013 (24 replaced slabs out of 248 original slabs). MP 15-14 had only 1 slab replaced prior to 2013. New cracking was identified at a rate of ~9 slabs cracking a year for MP 17, while MP 15 averaged 3-4/year.

<u>KDcurves Site 1b</u>

The difference between these two sites is evident looking at the KD curves. MP 15 has a few distinct areas where distress has occurred and MP 17 has much more widespread distress.

One of the reasons to look separately at the original slabs (OS Condition) and current slabs (CS condition) is due to the concern that cracking rates after repairs may be more related to the construction quality of the repairs instead of the overall pavement health. Figure A- shows the CS condition of the individual slabs in MP 17 aligned along the length of the road (the slab number is shown in the x axis). The squares that are above the 0.0 line are cracked in some manner, the higher up they are the more severe the cracking (i.e a T2 slab is at 2.0 and a SS is at 3.0). The slabs in red and yellow were identified as previously repaired slabs. This figure shows that some of the slabs replaced prior to 2013 that were not cracked in 2013 did crack again before 2018(slabs in red). Of the 39 slabs that were involved in some type of repair prior to 2013, only 13 were not cracked again in 2018. It also shows the extent of cracking in MP 17; there are three areas in 2018 where more than 10 contiguous slabs are cracked (slabs~43-64, ~132-149 and ~193-203). In contrast to MP 17, MP 15 only had one slab apparently repaired before 2013. This same repaired slab was repaired again in 2015 along with an adjacent slab, indicating also that the repair was not of high quality, or the area has foundation issues.

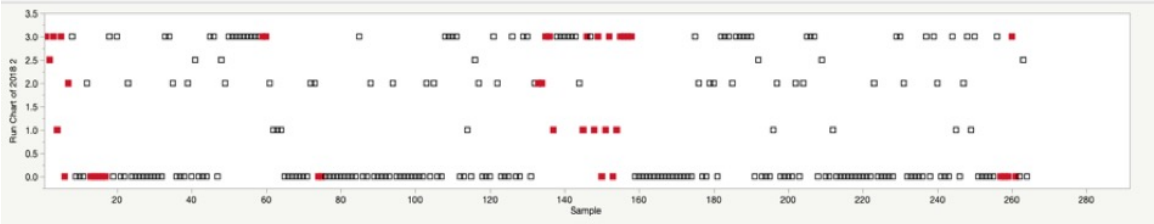

Figure A-1 MP17 CS condition with replaced slabs in red

OS Condition Site 1b

The OS distributions of cracking for MP 15 and MP 17 are provided in the Appendix, Table A-10. The distributions show that the SS increased by 34 (17 to 51) for MP 17, but only by 8 (9 to 17) for MP 15. The predominate slab state for both sections is SS. This points out the different ways failure in a pavement can be described. Figure A-a) and b) show MP 17 and MP 15 survival curves using different definitions of failure. While the values are greatly different (~95% survival rate for MP 15, while MP 17 is below 80%) the variability based on the definition of failure is also vastly different and appears to increase with age and/or distress (2% different for MP 15 in 2013 and 5% in 2018, 12% different for MP 17 in 2013 and 14% in 2018).

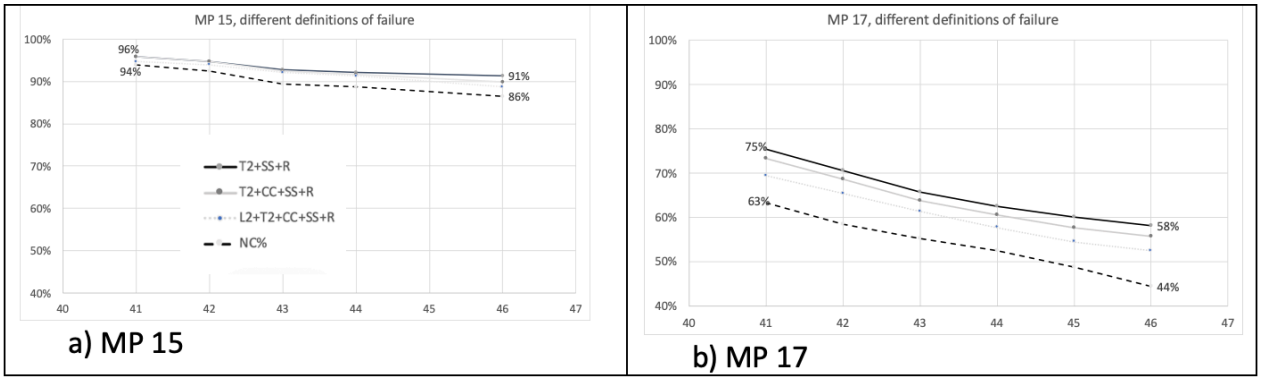

Figure A-2 Different Definitions of Failure, MP15 and MP17

For MP 17, over half the slabs that were longitudinally or transverse cracked in 2013 (30) cracked further to SS by 2018. Figure A- shows the original distribution of the condition of the slabs for MP 17 in 2013 that were later identified as SS in 2018. Of the 51 SS in 2018, 25% were already SS in 2013 at first inspection, but the other 75% of the slabs in 2013 varied in how they developed into a SS as shown in the Figure: 3 CC, 8 L1, 7 L2, 12 T2 and 8 not cracked. Of the 8 not cracked in 2013, half of them turned T2 before going

to SS, but the other 4 each went from a T1, L1, L2 or not cracked directly to SS. Looking at slab level details can provide insight into patterns, or maybe just as important, lack of patterns, of cracking progression in pavements.

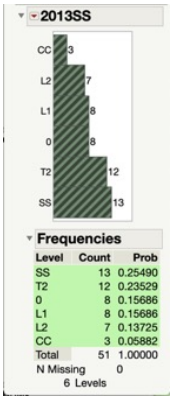

Figure A-3 MP 15, 2013 condition of slabs that became SS in 2018

MP 17 provides an opportunity to view how transverse cracked slabs develop spatially, similar to what was identified in the LTPP sections in Chapter 2. Figure A- shows how the transverse cracked slabs have spread by 2018.

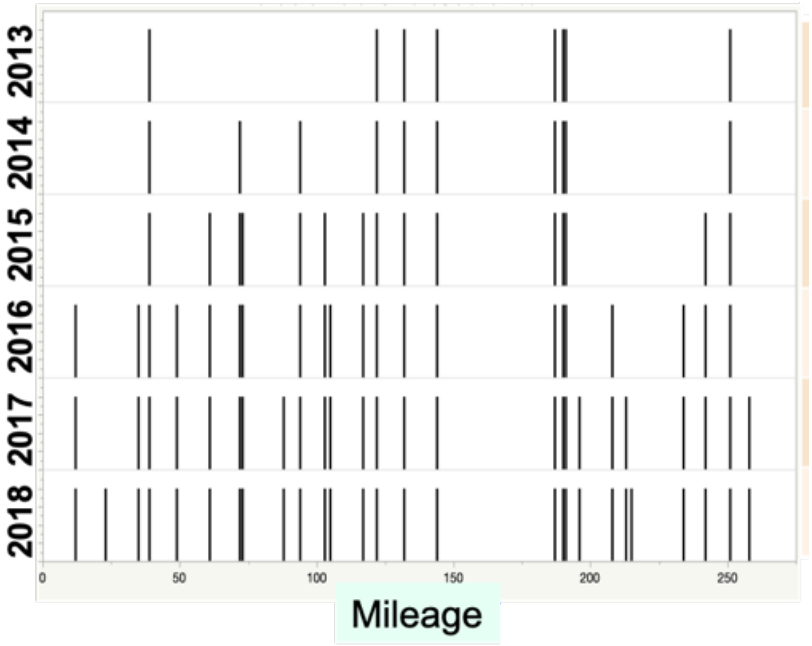

Figure A-4 MP 17, growth in T2 slab states over time

The Weibull graphs identified for these sections are shown in Appendix A2. The estimated deterioration curves are very different for the two sections. If these sections were modeled as a pavement family based on their thickness, design and age, they would share the same deterioration model.

Category 2 Case Study, MP150 and MP151

Site 2 is located on I-20, EB MP 150-152 in Taliaferro County. This site is located between Atlanta and Augusta, GA. This is also a location of one of the LTPP sites - LTPP Site 133017 is located at MP 150.7. The original project included a little over 15 miles of pavement approximately from MP 137.7 to 153. Site 2 does not include any bridges. Information on the pavement is included in Table A-. This site has experienced predominately longitudinal cracking, both in the 3D pavement data and in the LTTP section. It should be noted that the LTPP inspections online noted pumping in the section, which indicates water induced failure. This competing failure mode will be evident in the analysis of this pavement section.

Table A-4 Case Study 2 Pavement Information

Age in 2013	Slab Thickness	Joint Spacing	D/U?	Base/ Subbase	Shoulder	Bridge?	ADT/ % trucks
40	10 inches	Random Skew 17', 16', 22', 23'	U	Cement Stabilized GAB/Soil	Asphalt	N	29,200 24%

KDcurves Site 2

The KDAve and IQR value for MP151 is double that for MP150, while the maximum KD value for MP150 is higher than MP 151. This indicates the cracking in MP 150 is more clustered and the cracking in MP 151 is more distributed. It will be identified in the next section that another large different in these two sections is the quantity of repaired slabs, and the cracking in the repaired slabs, as opposed to the original slabs.

OS Condition Site 2

Table A- provides a comparison of the percentage of the different slab states in MP150 and MP151 for 2013 and 2016. Neither site had a bridge so the original slab numbers are almost the same (273 and 274). There is a large difference between the amount of repaired slabs in MP150 vs MP151 at the time of first inspection. As noted later, the repairs appear to be related to issues at the joints, and not typical fatigue failure.

Table A-5 MP150 and MP151 OS Slab State Percentages, 2013 and 2016

	2013		2016	
	MP150	MP151	MP150	MP151
L1	7.7	7.7	**17.6**	8.8
T1	0.4	0.7	0	0.7
L2	2.9	5.5	7.3	**24.1**
T2	1.5	0.7	1.5	0.7
CC	1.1	0.4	1.5	0
SS	1.1	0	1.5	2.6
R	15	43	17	43

Both sites show a high jump in L2 slab states between 2015 and 2016. MP151 shows almost a 5 time increase in L2 slabs, while MP150 shows less than a 3 time increase, but the increase in L1 slabs for MP150 is greater. This increase in longitudinal cracking is also evidenced in the LTPP section as noted in the next Section.

Site 2 and LTTP Section 13-3017

This and Site 3 Case Study provide an opportunity to compare the detailed 3D data for several years with the LTPP section data for almost the whole life of the pavement. This LTPP section (13-3017) was constructed in 1973 and first inspected in 1989. No cracking was identified in 1989. The first evidence of cracking showed up in the 1997 inspection. While the LTPP site does not have any transverse cracks, the LTPP section has extensive

longitudinal cracking (15 of the 25 slabs have some type of longitudinal cracking in 2016). The longitudinal cracking did not show up in the LTTP section until 24 years after construction, therefore it was not due to late joint sawing. This section also has a standard 12 ft lane width, so it was also not due to a widened slab. The LTTP records note that the LTPP pavement was ground in 2000 and one slab was repaired in 2001. A repaired slab is evident in the LTPP inspection picture from 2002 as shown in Figure A-.

Figure A-5 Replaced slab in LTPP Section 13-3017

Short longitudinal cracks on both sides of the joint were the only distress identified at the joint prior to the repair. Pumping was noted in a number of the LTPP inspections, so water intrusion was a definite factor. The 2016 faulting is really low (0.3mm), indicating doweled pavement, but Georgia DOT records and the LTPP records identify it as undoweled.

Based on the cement stabilized base and the pumping it is conjectured that the slab has debonded from the stabilized base and that coupled with water intrusion is driving the longitudinal cracking. A comparison of the LTPP slab state percentages and the MP 150 CS condition full mile slab state percentages are shown in Table A-.

Table A-6 Comparison of CS and LTPP Slab States 13-3017

	2014 CS/mile	2014 LTPP	2016 CS/mile	2016 LTPP
NC	79.6%	48%(12/25)	66.8%	44% (11/25)
L1	11.7%	48% (12/25)	18.6%	36% (9/25)
L2	4.2%	4% (1/25)	10.4%	16% (4/25)
T1	0.3%	0	0%	0
T2	1.6%	0	1.6%	4% (1/25)
CC	1.3%	0	1.3%	0
SS	1.3%	0	1.3%	0

As noted previously, one slab was repaired in the LTPP section at a joint between the 1999 and 2002 inspections. This affected two slabs since it was at a joint. 42 repaired slabs were identified in the complete mile in 2013, such a high number is most likely due to repairing joints and leaving remnants on each side of the joint repair, just like in the LTPP section. Another 5 slabs were repaired in 2015.

A hypothesis test that the data from the 3DSBM for the mile and the LTPP data came from the same population can be made using non-parametric analysis. A non-parametric version of the paired t-test, the Mann-Whitney U Test (also equivalent to the Wilcoxon Sum Rank Test) is used to compare the populations. The test statistic is computed by:

$$W_n = \sum_{i=1}^{n} iS_i(X, Y)$$

Using a 95% confidence level, the p value of 0.271 for 2014 indicates that we cannot reject the null hypothesis that they are from the same population. The p value for 2016 is much stronger, with a p-value of 0.834. Combining the data provided a p value of 0.726. Although the hypothesis test implies that the LTPP site and the full mile are from the same population it appears that the LTPP site can identify L1 type cracking better, but, due to

the small sample size, the percent T2 cracking that is present in the section is under or overestimated in the LTPP section. This and its effect on AASHTO PMED calibration was discussed in Chapter 6.

Repair Condition

An analysis of the difference between the slab states identified in OS and CS condition can provide an example of the condition of the repaired slabs. The MP151 pavement section shows a great difference between CS (Table A-9) and OS (Table A-10) slab states, indicating that a large proportion of the slabs that are cracking were previously repaired. For MP151, in 2013 the CS condition identified 62 L2 slabs, while the OS condition identified only 15. This means that 47 slabs repaired prior to 2013 had cracked again. This information alone would lead to a concern for continuing to repair this section of pavement.

Category 3 Case Study, MP104 and MP105

Site 3 is located on I-16, EB MP 104-106 in Candler County, between Macon and Savannah, Georgia. This site also includes the other LTPP location, Site 133015 is located at MP 105.2. The pavement was originally completed approximately in 1978. The original project included a little over 12 miles of pavement approximately from MP 103.4 to 115.7. Site 3 is the only site with dowels and an asphalt base. It is also the only site that had no repairs in 2013, at the time of first inspection, although there were a number of repairs identified after 2015. It has predominately transverse cracking, in contrast to Site 2 that had predominately longitudinal cracking.

Table A-7 Case Study 3 Pavement Information

Age in 2013	Slab Thickness	Joint Spacing	D/U?	Base/ Subbase	Shoulder	Bridge?	ADT/ % trucks
35	10 inches	20 ft	D	1" HMA over 6" soil cement/Soil	Asphalt	Y- at end of MP 106	24,100 26%

KDcurves Site 3

This section is the youngest and least distressed section. It should be noted that due to that the scale used for the KDcurves for this site is different than the other sections. The IQR values for both sections are 0 for 2013. Repairs were made in both sections between the 2015 and 2016 inspection.

OS Condition Site 3

As noted, this ~2 mile section had no apparent repaired Slabs in 2013, therefore the actual condition (Table A-9) and OS condition (Table A-10) are the same for 2013, 2014 and 2015.

Between the 2015 and 2016 data collection time 31 slabs were replaced, and one additional slab was replaced before 2017. Of the 31 slabs replaced by 2016, 60% were not cracked in 2013, and 25% were not cracked in 2014. 20 of the 21 T2s were repaired in 2016, along with 2 of the 3 T1, all of the SS and CC (2 each) and 2 of the 3 L1, leaving 4 slabs that were identified as not cracked but replaced in 2016. Although 1 of these was directly adjacent to a cracked slab, the other three were not, indicating that they cracked badly enough in one year to warrant replacement. Two of these slabs, although they did not crack in the following year, the slabs directly adjacent to them did. The rate of T2 cracking before the repairs averaged 5/year, while the rate after was 3/year. Considering T2 +SS cracking the rate before was 6/year while the rate after was 5/year, not as much of as decrease. As in the 1a Case Study the rate of cracking decreased in the years after repairs. As noted earlier, anecdotally there is concern that cracking rates increase after repairs, additional information like this from 3D pavement data can address some of the concerns of the unknowns of concrete pavement rehabilitation. The rate decrease is also evident in the RSLOS curves shown previously in Figure 5-9 RSLOS_yrs vs Hazard Rate.

Site 3 and LTTP Section 13-3015

From the LTPP maintenance information on the website the pavement was ground in 2009. Prior to this the LTPP section did not exhibit any cracking distress. At the last inspection LTPP section 13-3015 only has one cracked slab, a transverse crack that emanates from

the centerline but does not go all the way across the slab, it is identified as 2.6 m long (8.5 ft). It first showed up in 2014 and did not change in 2016. The interesting thing about this crack is that it did not show up in the 2014, 2015, 2016, 2017 or 2018 3D pavement data as a cracked slab. I personally stopped at the LTPP site on a trip to Savannah in 2019 to see it with my own eyes. From an observation point on the shoulder, the slab was visibly cracked, although it was a hairline crack, which can barely be seen in Figure A-.

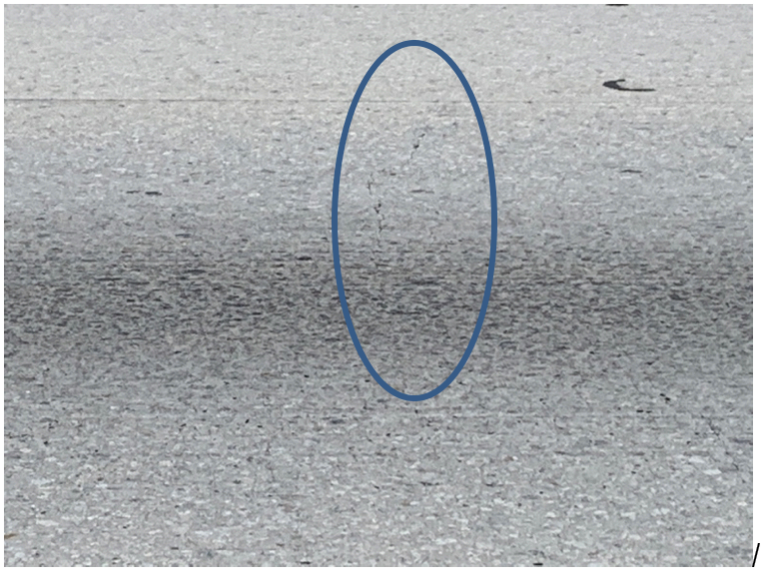

Figure A-6 T2 cracked slab in LTPP 13-3015

Unlike the 133017 LTPP section, the cracking in MP 105-106 and the LTPP section are mainly transverse and are relatively similar as shown in Table A-, except that T1 are not present in the LTPP site. Similar to the 133017 LTTP section, due to the small sample size, the percent T2 cracking that is present in the section does not appear to change at the same rate as the full section, this and its effect on AASHTO PMED calibration was discussed in Chapter 6.

Table A-8 Comparison of CS and LTPP Slab States 13-3015

	2013 CS/mile	2014 CS/mile	2015* CS/mile	2014 and 2016 LTPP
NC	97.2%	94%	92.8%	96% (24/25)
T1	1.2%	1.2%	1.2%	0
T2	1.6%	4.8%	6.0%	4% (1/25)
L1	0	0	0	0
L2	0	0	0	0
CC	0	0	0	0
SS	0	0	0	0

*Slab repairs were performed after 2015 in the mile section.

Figure A- shows a representation of the entire 2 mile section (MP104-MP106) with the yellow and black lines representing individual slabs. The slabs that were repaired after 2015 are shown in yellow and the new cracking is shown in black. New cracking is evident near the areas that were repaired along with cracking outside those areas. This cracking is all T2 cracking. This indicates that the new cracking is additional fatigue related cracking that would be expected to "fill-in" to other areas that have not cracked yet. The LTPP site is located between the 1.2 and 1.3 mileage points shown in the x-axis. As can be seen, between 1.2 and 1.6 is the only area in the 2 mile section that is not showing any cracking. The Figure also identifies clustering near the 1 mile area. This points out a concern with just looking at cracking per mile, and the importance of looking at pavements in multi-scale; the clustering evident around mile 1 would be masked if the process just looked at the individual mile information.

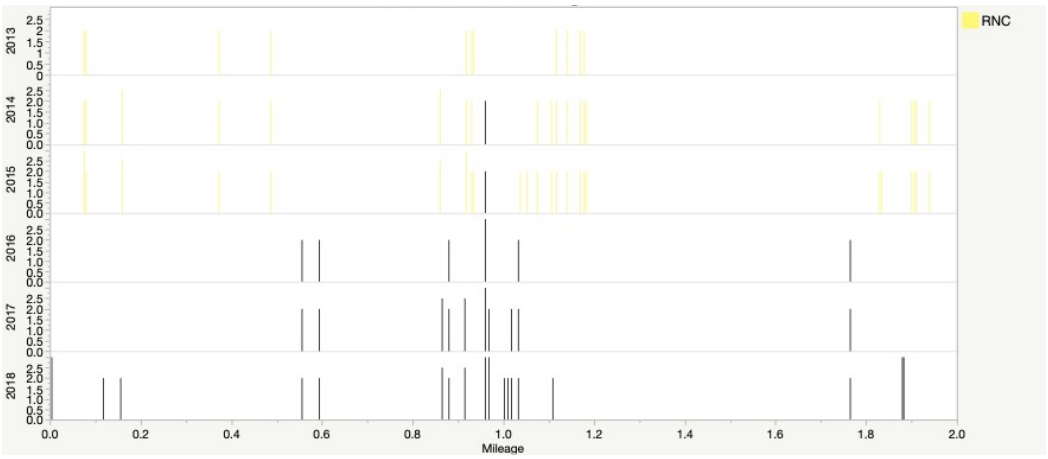

Figure A-7 MP104 and MP105 slab states by mileage (T1 and L1 not shown)

A.2 Slab States by Case Study Section

Table A-9 Condition and %HPMS

	CS	NC	L1	T1	L2	T2	CC	SS	Total#	%T2+SS (%HPMS)
MP153	2013	148	1	6	1	21	0	1	178	12.40%
	2014	142	1	5	2	25	1	2	178	15.20%
	2015	195	0	0	0	0	0	0	195	0.00%
	2016	193	0	0	0	4	0	0	197	2.00%
	2017	189	0	1	0	6	0	0	196	3.10%
	2018	187	1	2	0	8	0	0	198	4.00%
MP154	2013	148	2	9	0	24	1	1	185	13.50%
	2014	144	2	1	1	34	2	1	185	18.90%
	2015	198	1	2	0	4	0	0	205	2%
	2016	194	0	0	0	17	0	0	211	8.10%
	2017	179	0	0	0	32	0	0	211	15.20%
	2018	175	0	2	0	34	0	0	211	16.10%
MP 15	2013	249	3	1	4	0	0	9	266	3.40%
	2014	245	4	1	3	0	0	13	266	4.90%
	2015	239	5	2	2	4	1	13	266	6.40%
	2016	237	7	0	2	4	1	15	266	7.10%
	2018	231	3	3	4	4	4	17	266	7.90%
MP17	2013	176	15	3	15	29	6	21	265	18.90%
	2014	163	14	6	12	31	6	33	265	24.20%
	2015	155	13	3	12	26	5	52	266	29.40%
	2016	150	11	3	13	30	5	54	266	31.70%
	2017	138	6	8	14	33	7	60	266	35.10%
	2018	127	10	11	14	30	7	67	266	36.60%
MP150	2013	252	29	1	14	5	4	3	308	2.6%
	2014	245	36	1	13	5	4	4	308	2.9%
	2016	205	57	0	32	5	4	4	307	2.9%
MP151	2013	212	83	6	62	2	1	7	373	2.4%
	2014	204	82	3	69	4	0	11	373	4.0%
	2016	188	41	2	121	3	0	16	371	5.1%
MP104	2013	254	0	1	0	7	0	0	262	2.7%
	2014	251	1	1	0	7	2	0	262	2.7%
	2015	250	2	0	0	6	2	2	262	3.1%
	2016	264	5	2	0	3	0	1	275	1.5%
	2017	264	2	1	0	5	2	1	275	2.2%
	2018	260	1	3	0	6	2	3	275	3.3%
MP105	2013	242	0	3	0	4	0	0	249	1.6%
	2014	234	0	3	0	12	0	0	249	4.8%
	2015	231	0	3	0	15	0	0	249	6.0%
	2016	264	0	0	0	2	0	0	267	0.7%
	2017	261	0	3	0	3	0	0	267	1.1%
	2018	256	0	4	0	6	0	2	267	3.0%

Table A-10 Original Slab (OS) condition and %RSLOS

	OS	NC	L1	T1	L2	T2	CC	SS	R	%T2+CC+SS+R	RSLOS
MP153	2013	132	0	5	0	20	0	1	10	18.5%	81.5%
	2014	127	1	4	0	24	1	1	10	21.4%	78.6%
	2015	127	0	0	0	0	0	0	41	24.4%	75.6%
	2016	127	0	0	0	0	0	0	41	24.4%	75.6%
	2017	124	0	1	0	2	0	0	41	25.6%	74.4%
	2018	122	1	1	0	3	0	0	41	26.2%	73.8%
MP154	2013	137	0	9	0	24	1	0	6	17.5%	82.5%
	2014	133	1	2	0	33	1	0	7	23.2%	76.8%
	2015	130	0	1	0	3	0	0	43	26.0%	74.0%
	2016	123	0	0	0	10	0	0	44	30.5%	69.5%
	2017	120	0	0	0	13	0	0	44	32.2%	67.8%
	2018	115	0	2	0	16	0	0	44	33.9%	66.1%
MP 15	2013	249	2	1	3	0	0	9	1	3.8%	96.2%
	2014	245	4	1	2	0	0	12	1	4.9%	95.1%
	2015	237	5	2	1	4	1	13	2	7.5%	92.5%
	2016	235	7	0	1	4	1	15	2	8.3%	91.7%
	2018	229	3	3	3	4	4	17	2	10.2%	89.8%
MP17	2013	**157**	**14**	**1**	**10**	**20**	**5**	**17**	**24**	26.6%	73.4%
	2014	**145**	**12**	**5**	**8**	**21**	**5**	**28**	**24**	31.5%	68.5%
	2015	**137**	**12**	**3**	**6**	**18**	**5**	**42**	**25**	36.3%	63.7%
	2016	**130**	**10**	**3**	**7**	**25**	**5**	**43**	**25**	39.5%	60.5%
	2017	**121**	**6**	**8**	**8**	**26**	**6**	**48**	**25**	42.3%	57.7%
	2018	**110**	**9**	**11**	**8**	**27**	**6**	**51**	**26**	44.4%	55.6%
MP150	2013	191	21	1	8	4	3	3	42	19.0%	81.0%
	2014	184	28	1	8	4	3	3	42	19.0%	81.0%
	2015	183	27	1	8	4	2	1	47	19.8%	80.2%
	2016	146	48	0	20	4	4	4	47	21.6%	78.4%
MP151	2013	116	21	2	15	2	1	0	118	44.0%	56.0%
	2014	114	23	1	15	3	0	1	118	44.4%	55.6%
	2015	114	23	0	15	2	0	3	118	44.7%	55.3%
	2016	56	24	2	66	2	0	7	118	46.2%	53.8%
MP104	2013	254	0	1	0	7	0	0	0	2.7%	97.3%
	2014	251	1	1	0	7	2	0	0	3.4%	96.6%
	2015	250	2	0	0	6	2	2	0	3.8%	96.2%
	2016	241	2	2	0	3	0	1	13	6.5%	93.5%
	2017	239	1	2	0	4	2	1	13	7.6%	92.4%
	2018	236	1	3	0	5	2	2	13	8.4%	91.6%
MP105	2013	242	0	3	0	4	0	0	0	1.6%	98.4%
	2014	234	0	3	0	12	0	0	0	4.8%	95.2%
	2015	231	0	3	0	15	0	0	0	6.0%	94.0%
	2016	230	0	0	0	2	0	0	19	8.4%	91.6%
	2017	224	0	3	0	3	0	0	19	8.8%	91.2%
	2018	219	0	3	0	6	0	2	19	10.8%	89.2%

A.3 KDCurves, KDAve, and IQR by Case Study Section

Cat 1a_MP 153

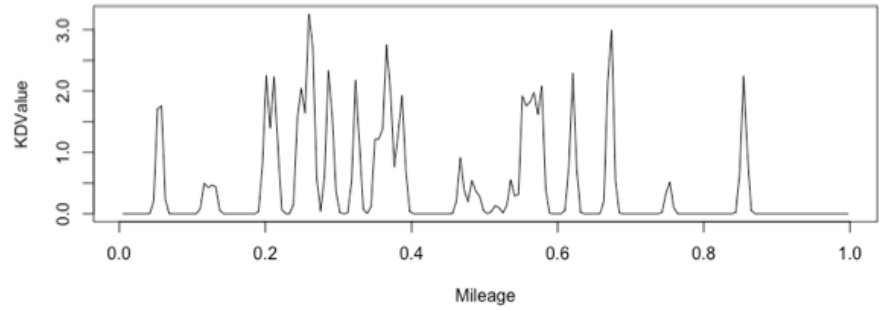	2013 KDAve = 0.419 IQR = 0.504
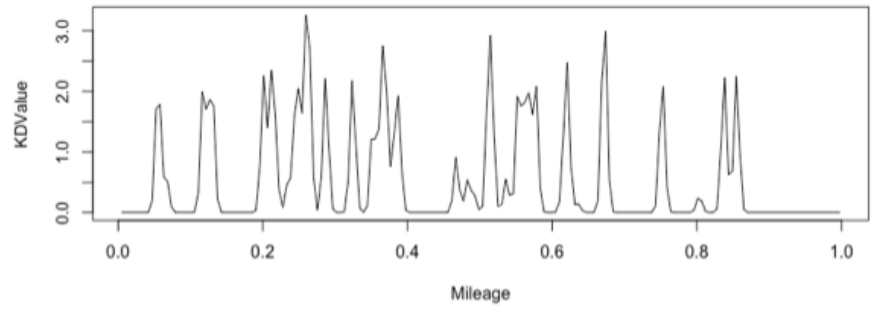	2014 KDAve = 0.538 IQR = 0.769
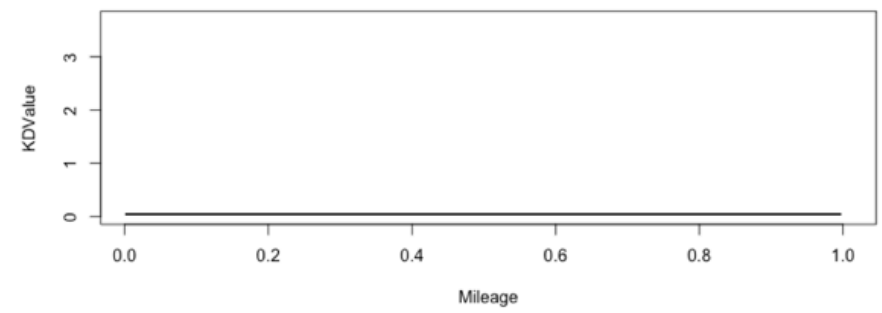	2015 KDAve = 0 IQR = 0
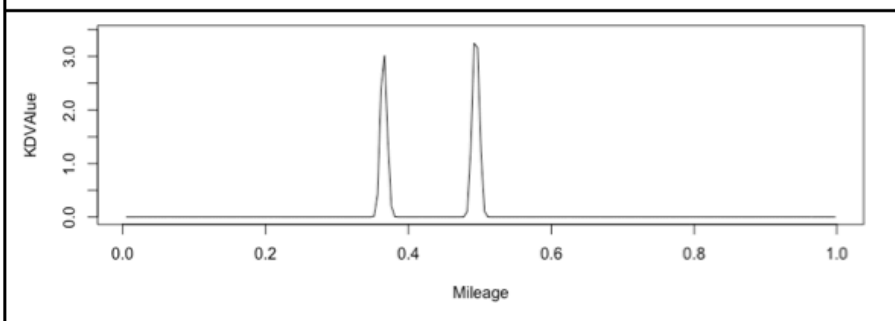	2016 KDAve = 0.080 IQR = 0

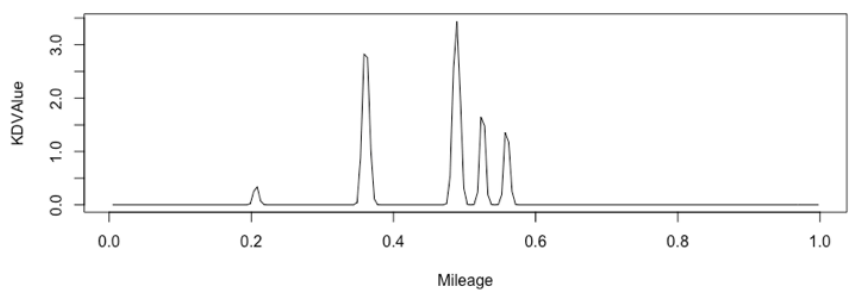	2017
	KDAve = 0.115 IQR = 0
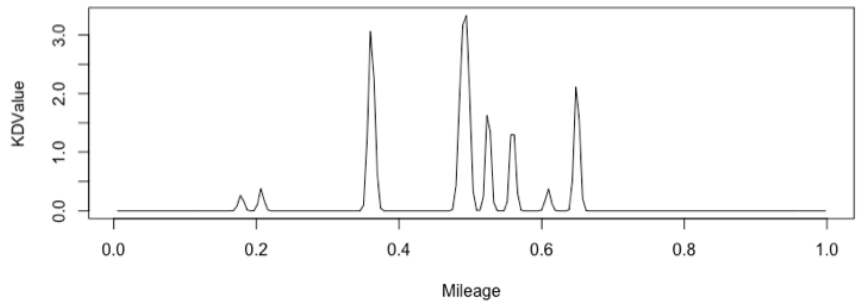	2018
	KDAve = 0.150 IQR = 0.0002

Cat 1a_MP 154

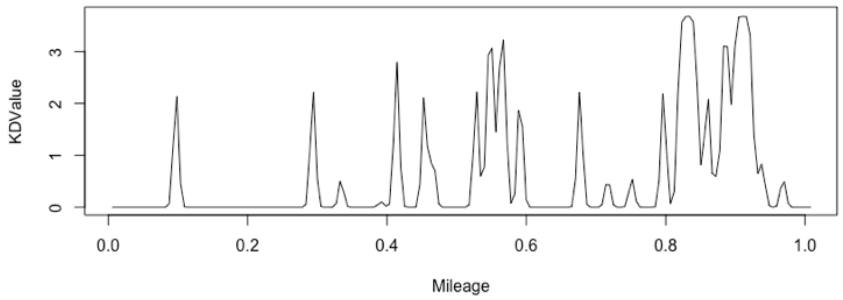	2013 KDAve = 0.583 IQR = 0..652
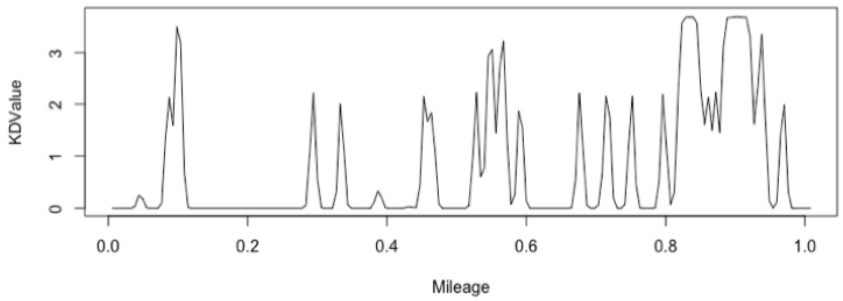	2014 KDAve = 0.764 IQR = 1.448
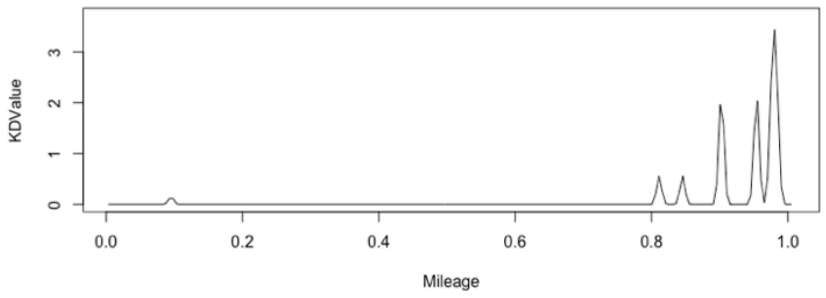	2015 KDAve = 0.046 IQR = 0
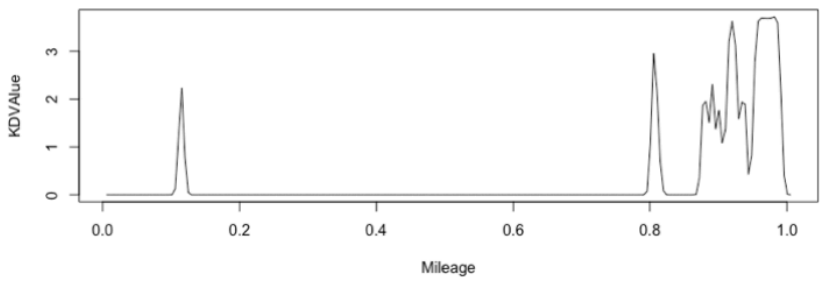	2016 KDAve = 0.344 IQR = 0

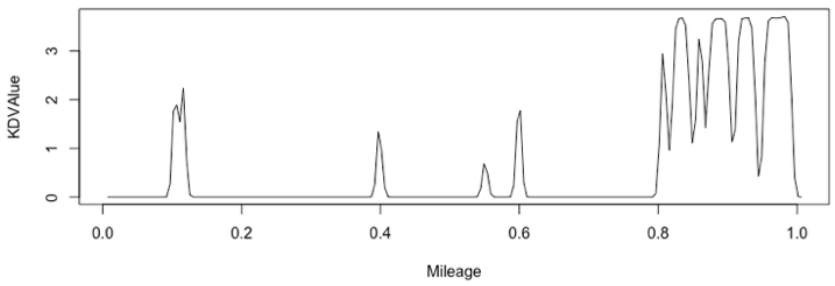	2017 KDAve = 0.619 IQR = 0.035
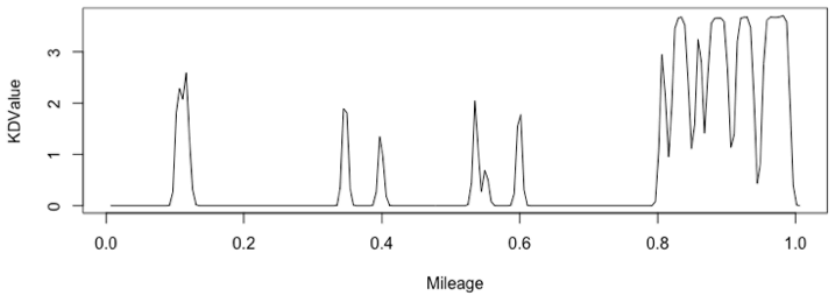	2018 KDAve = 0.668 IQR = 0.752

Cat 1b_MP 15

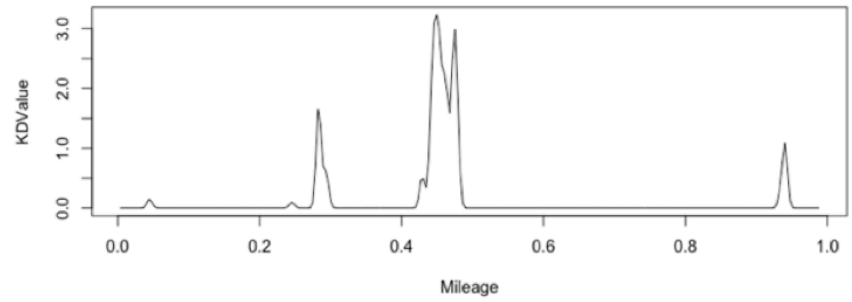	2013 KDAve = 0.148 IQR = 0
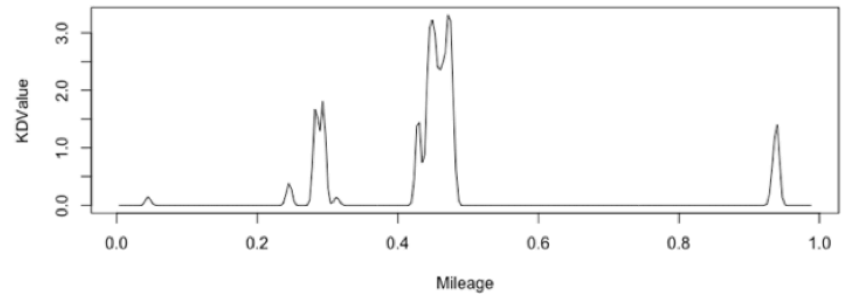	2014 KDAve = 0.188 IQR = 0
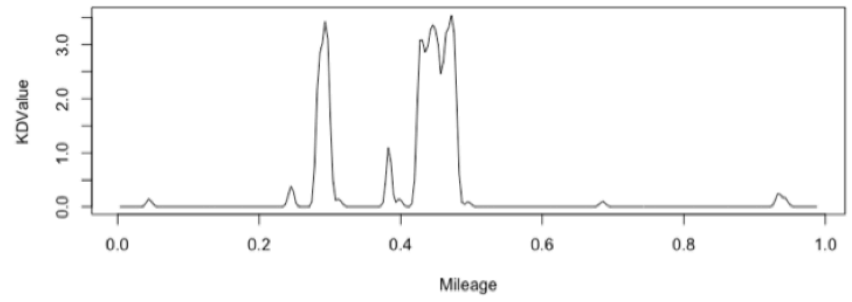	2015 KDAve = 0.247 IQR = 0.003
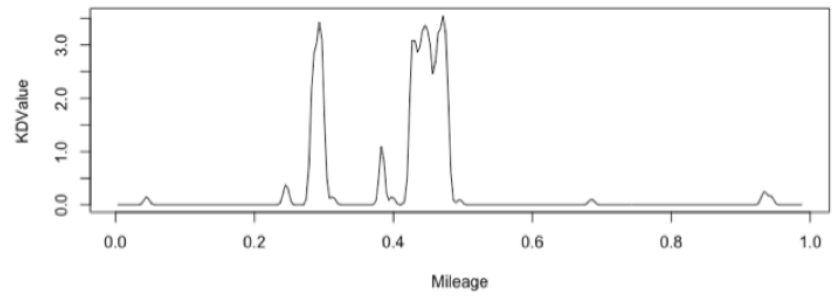	2016 KDAve = 0.272 IQR = 0.016

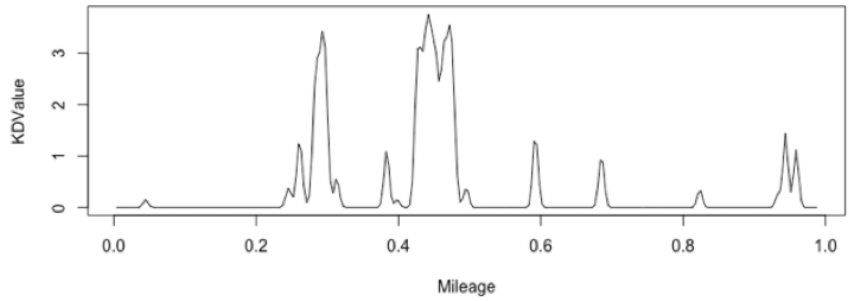	2018
	KDAve = 0.346 IQR = 0.140

Cat 1b_MP 17

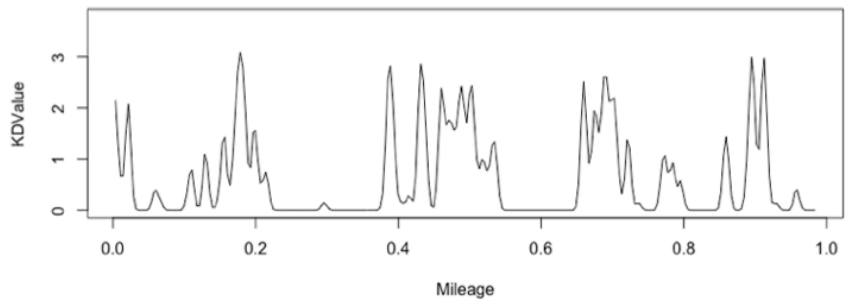	2013
	KDAve = 0.618 IQR = 0.99
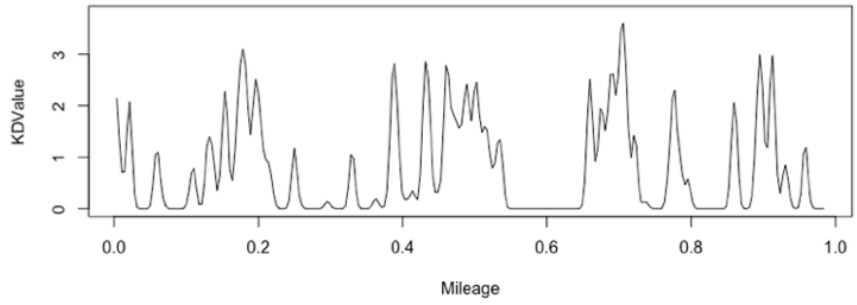	2014
	KDAve = 0.773 IQR = 1.35
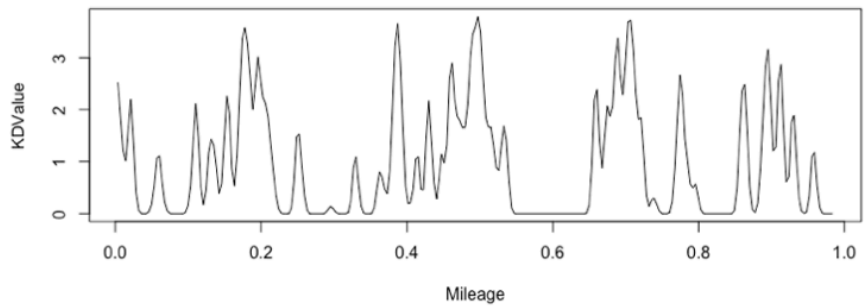	2015
	KDAve = 0.945 IQR = 1.64
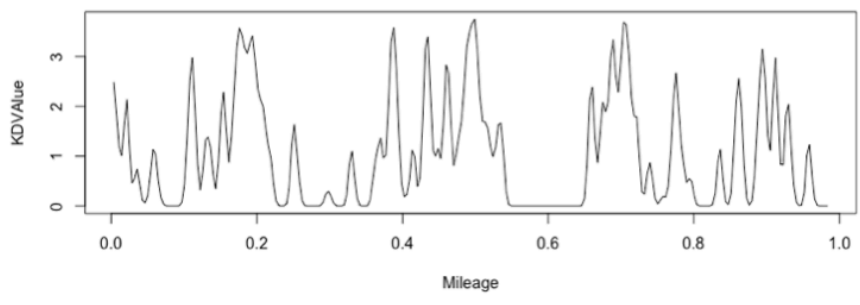	2016
	KDAve = 1.03 IQR = 1.66

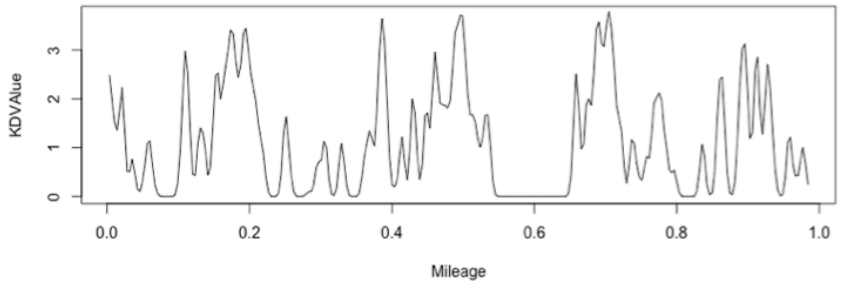	2017 KDAve = 1.11 IQR = 1.77
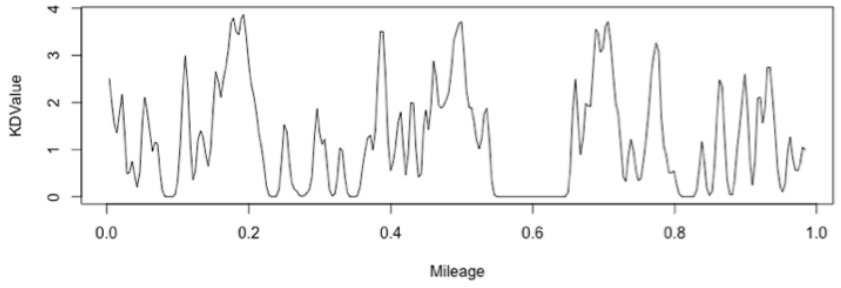	2018 KDAve = 1.20 IQR = 1.74

Cat 2_MP 150

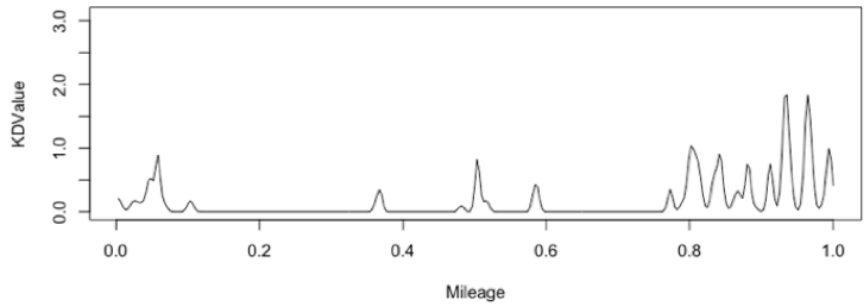	2013 KDAve = 0.153 IQR = 0.159
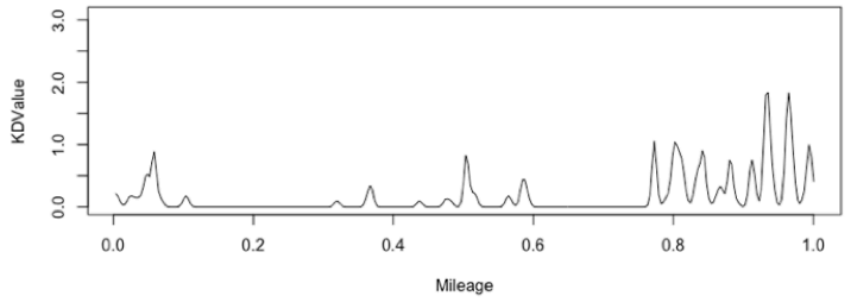	2014 KDAve = 0.166 IQR = 0.175
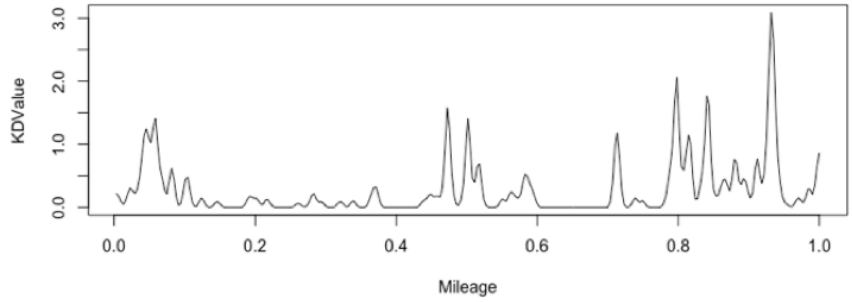	2016 KDAve = 0.278 IQR = 0.350

Cat 2_MP 151

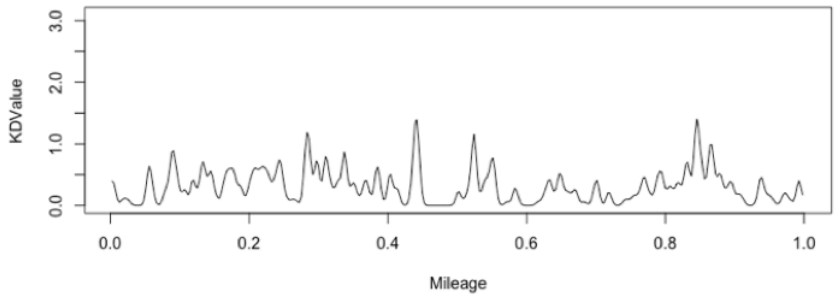	2013 KDAve = 0.315 IQR = 0.362
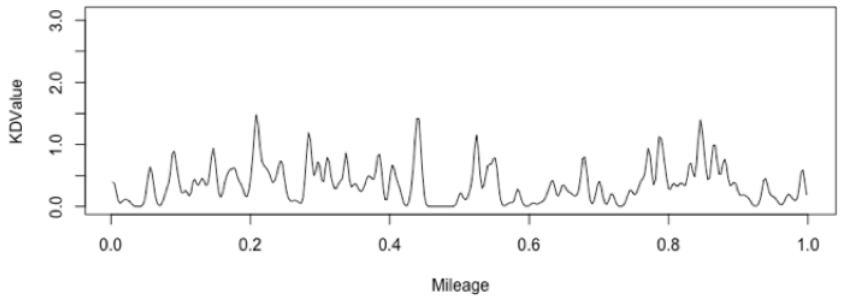	2014 KDAve = 0.367 IQR = 0.415
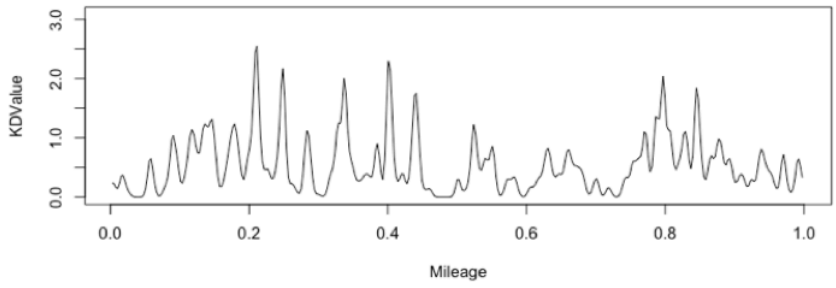	2015 KDAve = 0.546 IQR = 0.530

Cat 3_MP 104

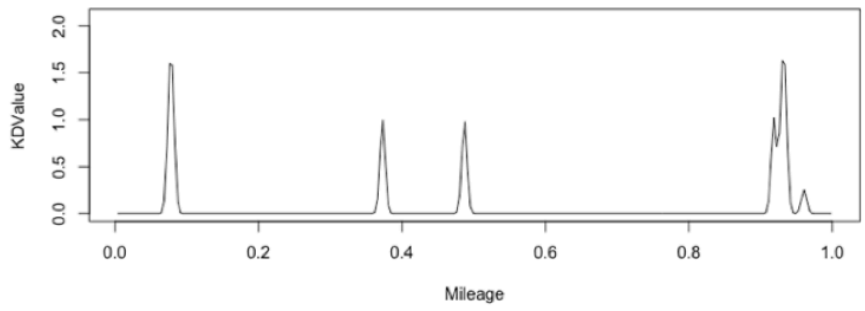	2013 KDAve = 0.068 IQR = 0
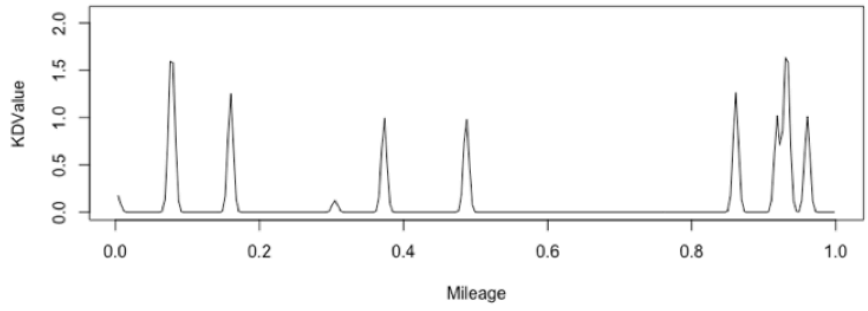	2014 KDAve = 0.093 IQR = 0.0005
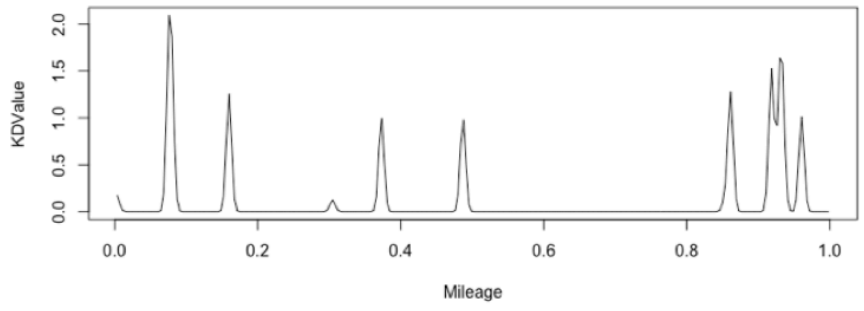	2015 KDAve = 0.111 IQR = 0.001
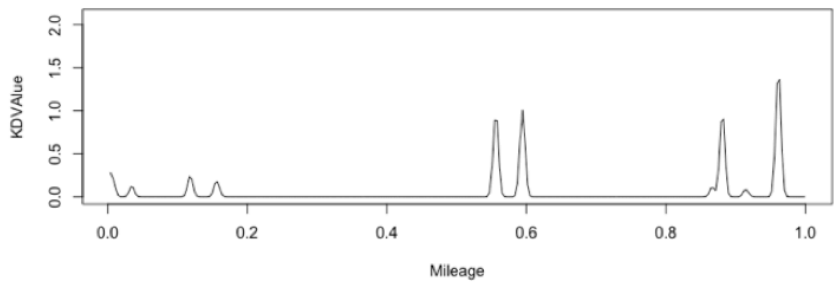	2016 KDAve = 0.052 IQR = 0.0004

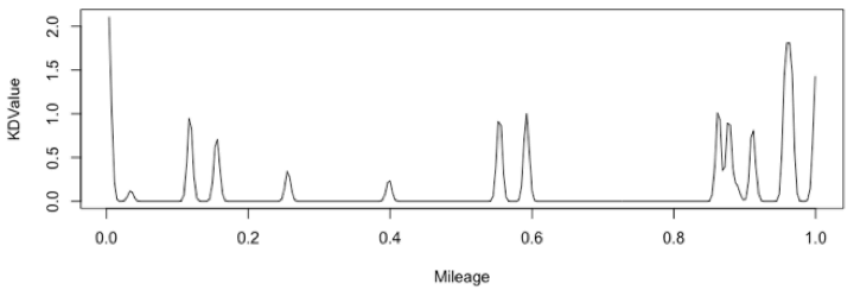	2018 KDAve = 0.120 IQR = 0.018

Cat 3_MP 105

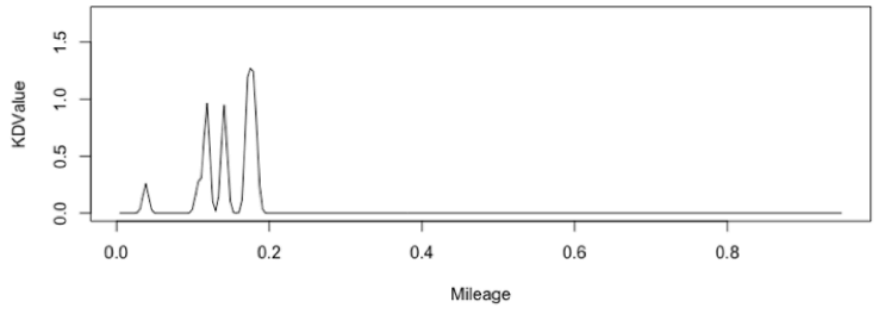	2013 KDAve = 0.046 IQR = 0
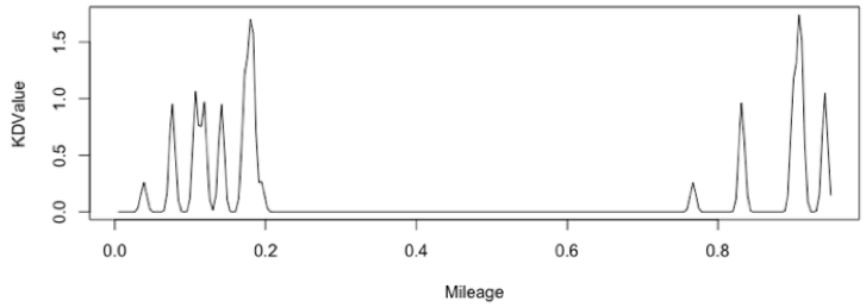	2014 KDAve = 0.125 IQR = 0.008
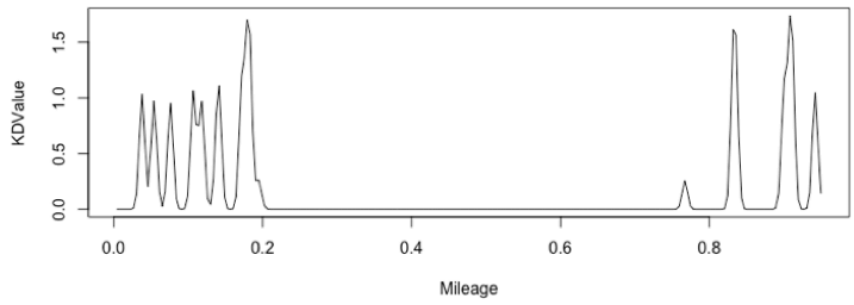	2015 KDAve = 0.155 IQR = 0.027
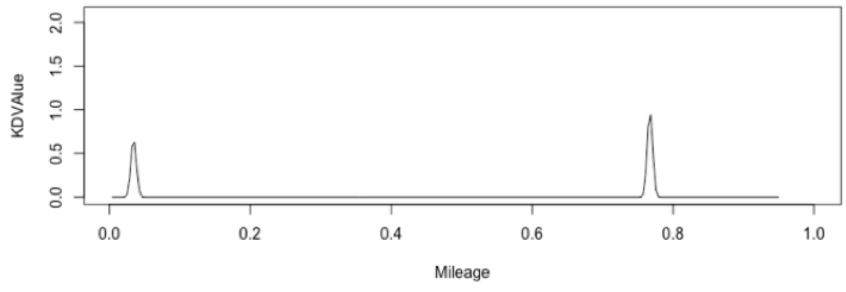	2016 KDAve = 0.017 IQR = 0

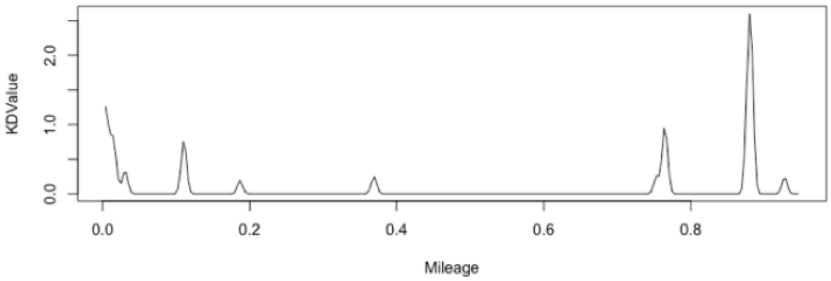

2018

KDAve = 0.076

IQR = 0

Cat 1b_MP19-14

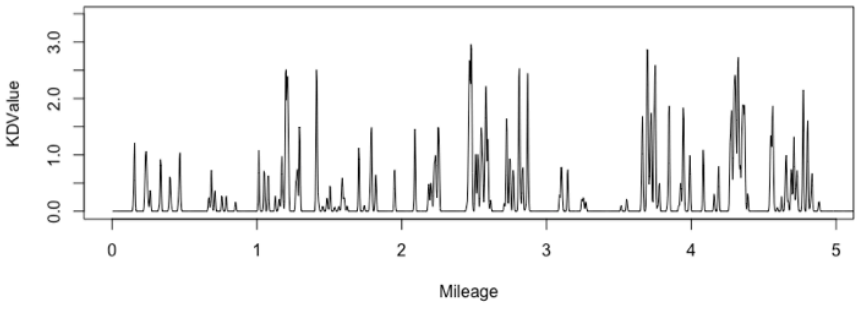

2013

KDAve = 0.236

IQR = 0.199

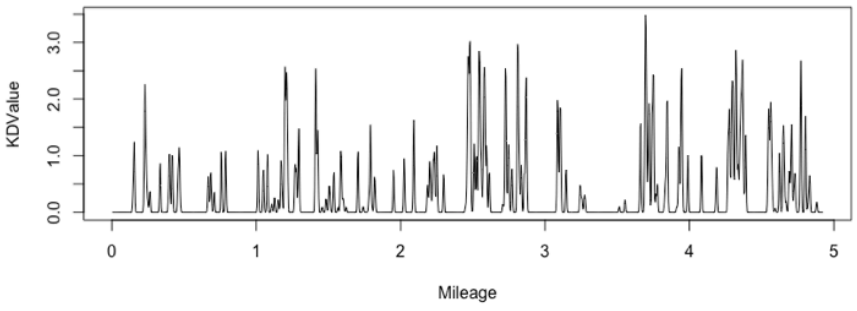

2014

KDAve = 0.298

IQR = 0.320

A.4 Weibull Curves by Case Study Section

Cat 1a_MP 153

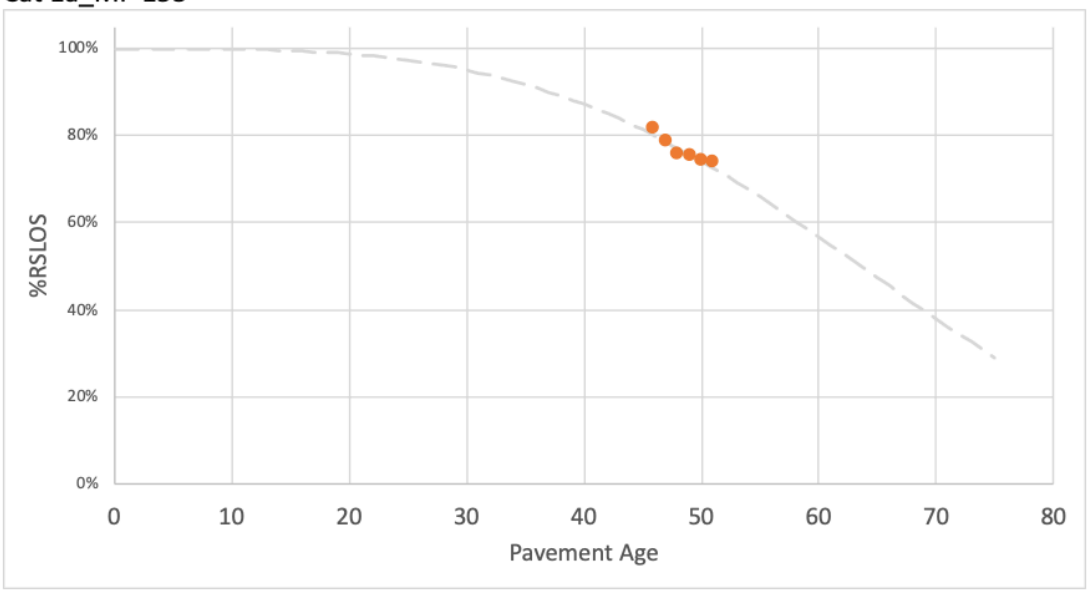

Cat 1a_MP154

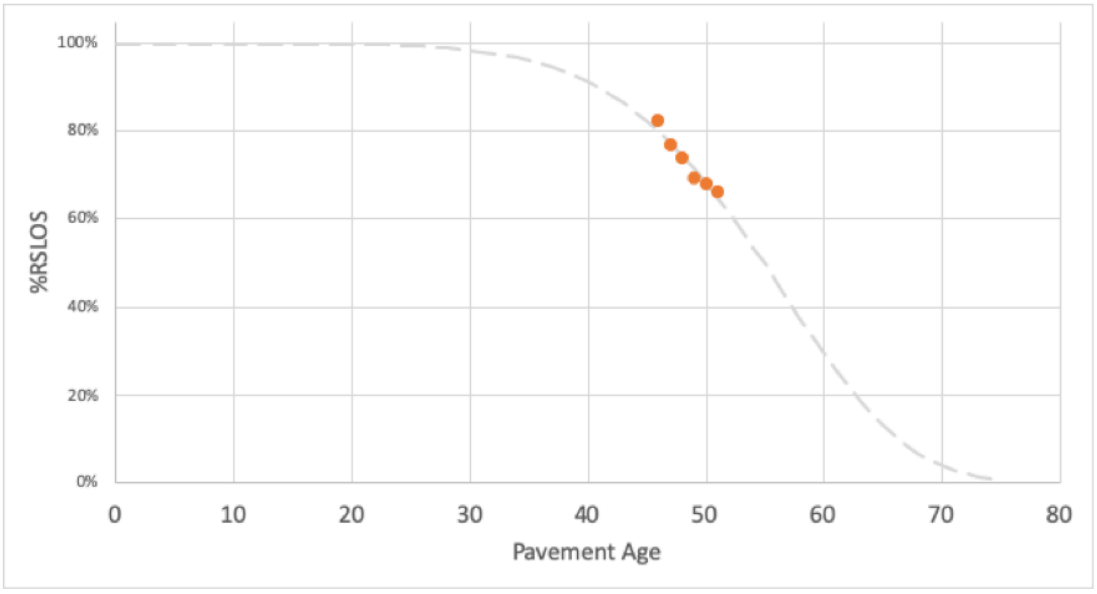

Cat 1b_MP 15

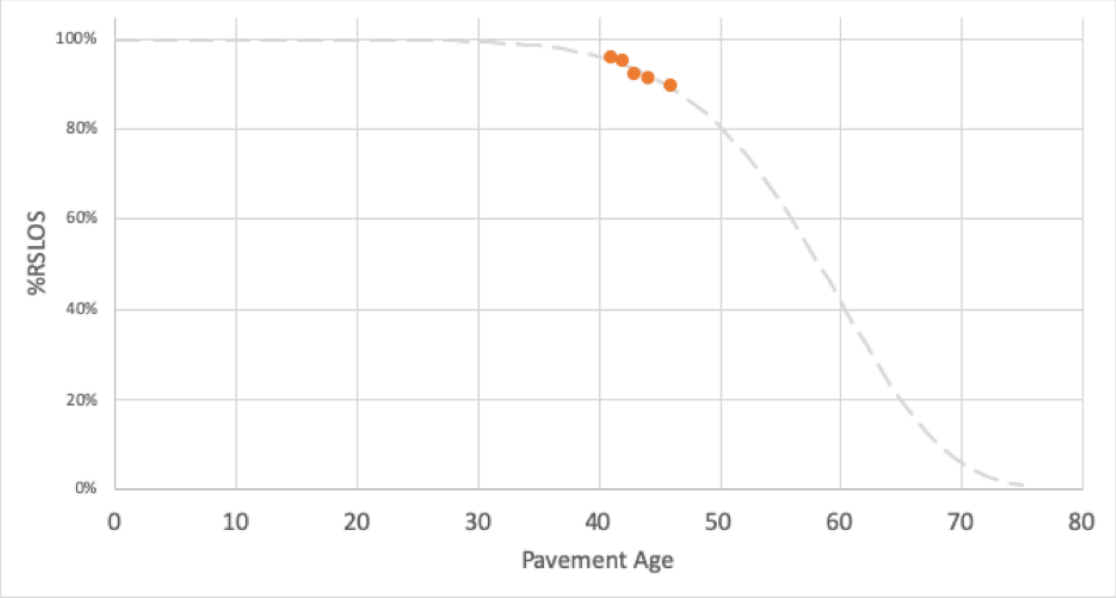

Cat 1b_MP 17

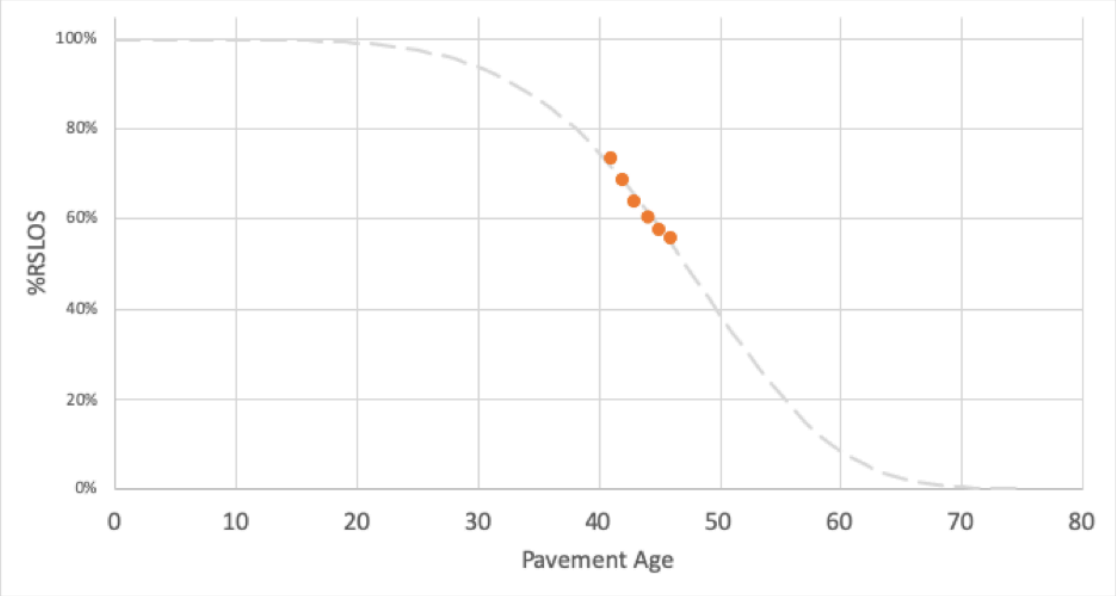

Cat 2_MP150

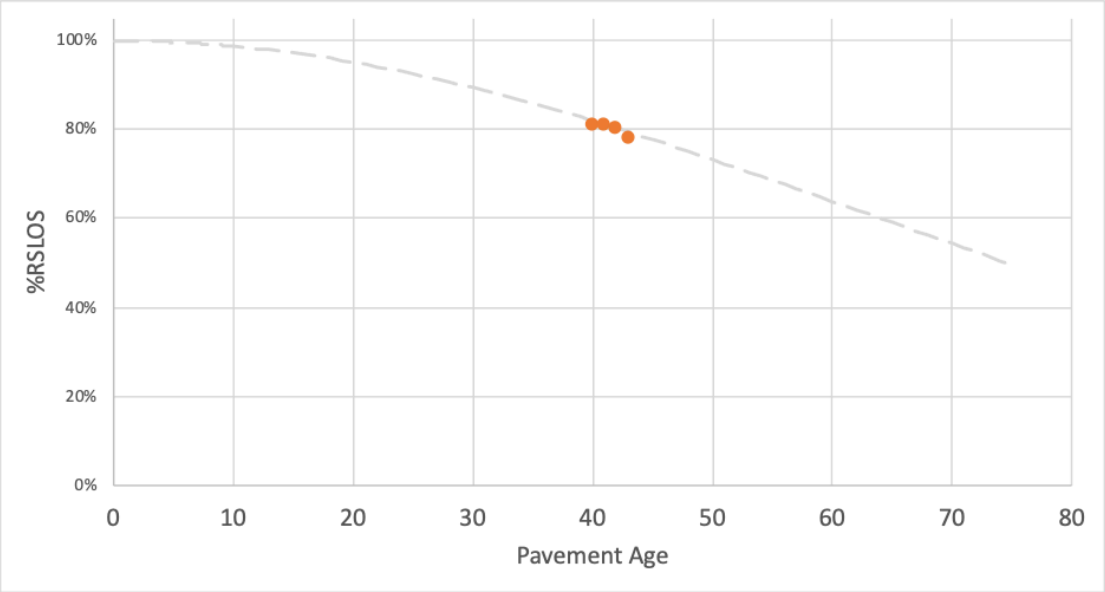

Cat 2_MP 151

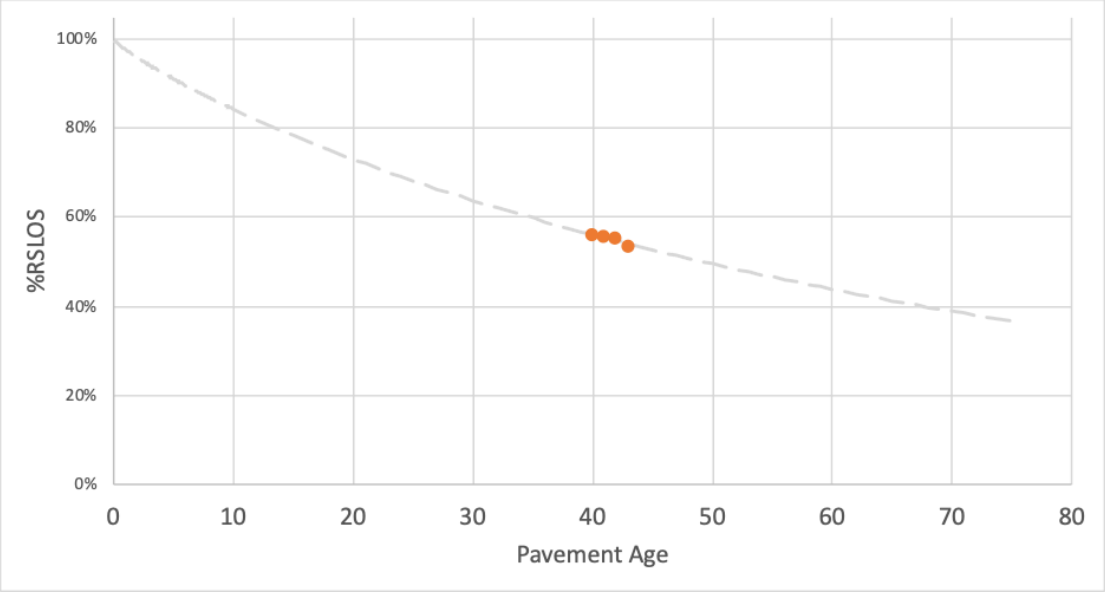

Cat 3_MP104

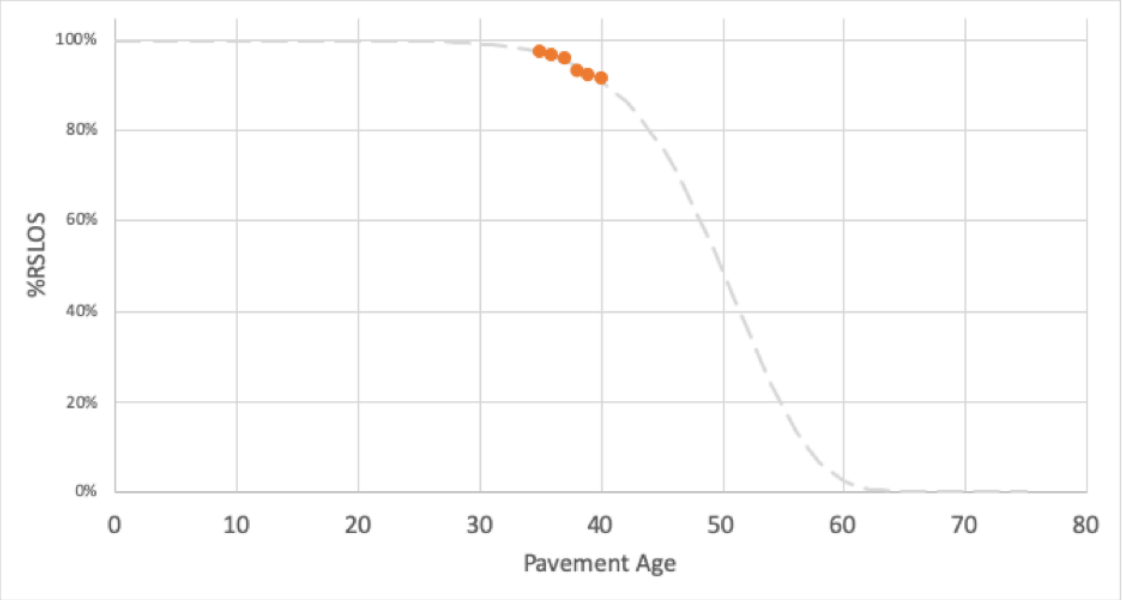

Cat3_MP105

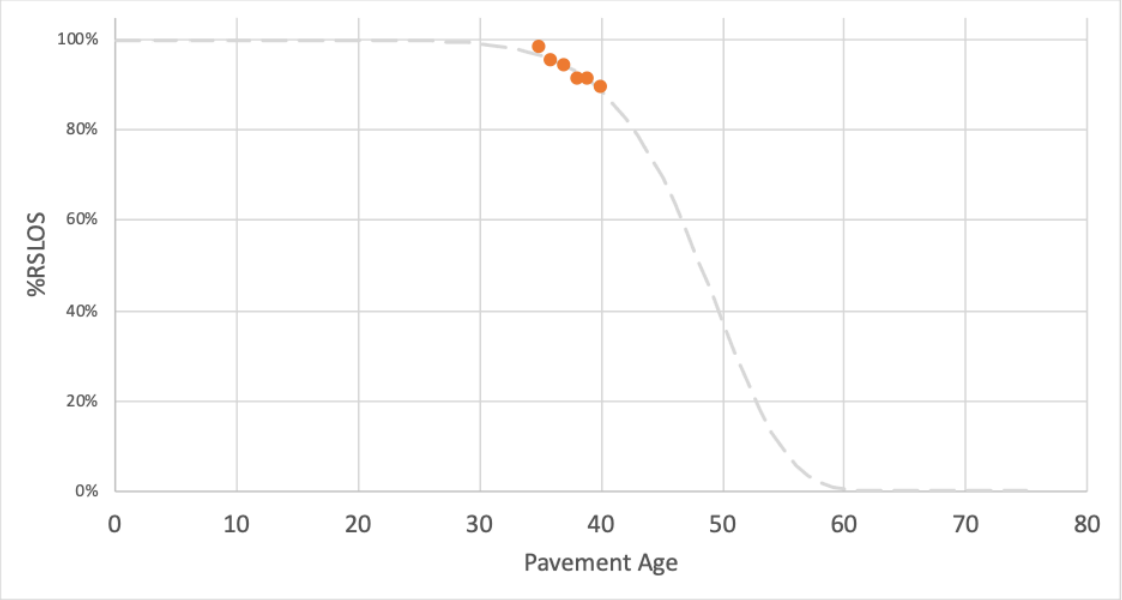

A.5 GPS3 WNF Study Sites Summary

Table A-11 identifies the LTPP Site Number, the second column is an objective indication of the predominate cracking at the last inspection date. A summary of the slab states identified is provided in the next two columns separated by transverse and longitudinal cracking. The last two columns are self-explanatory, note some sections are out of service and so the last inspection is not recent. The sections that are shaded are the ones that had no observable cracks at last inspection.

Table A-11 Wet no Freeze LTPP Sites Reviewed

LTPP Site #	L/T	Transverse Cracking	Longitudinal Cracking	Thickness, joint spacing, doweled (DOWEL) or undoweled (UD)	# of Slabs/ Year Constructed/ Last inspection
01_3028	T	3 slabs transversely cracked joint to joint (T2). Slab 4 (26 yrs), 12(40 yrs),18((33 yrs). No other cracking	None	10" JPC, 20ft jts UD	24/ 1971/ 2015
05_3011		None	None	10" JPC, 15 ft jts, DOWEL	33/1983/2013
12_3811	T/SS	11 slabs cracked transversely at year 15. By year 29 only slab 2, 17 and 24 were not cracked (7 SS, 14 T2, 3 NC)	Only after the slab cracked transversely	9.4" JPC, ave 20ft jts UD	24/1976/ 2005
12_4000	L	No transverse cracks	One longitudinal crack at a joint after 23 years	8.3" JPC, skewed jts UD	24/1974/ 2015
13_3007		None	None	9" JPC, 20 ft. jts, DOWEL	24/1981/2014
13_3011		None	None	10" JPC, random, skewed jts, UD	25/1975/2016
13_3015	T	One transverse crack after 36 years (T1)	None	9.8" JPC DOWEL	24/1978/ 2016
13_3016	L/T	3 T1 slabs	8 L2 slabs, 2 cracked within 1 inspection period, others took as long as 5 years	11" JPC, 20 ft jts DOWEL	24/ 1977 / 2004
13_3017	L	No transverse cracks	Longitudinal cracking at both joints on 8 slabs. 15 L1 and 1 L2 slabs. L2 took 13 years to extend	9.9" JPC, skewed jts UD	25/ 1973/ 2014

13_3018	L	1 small transverse crack on a L2 slab	13 L2, 12 L1 Cracking starts at joints and meets in the center later	9.9" JPC, skewed jts UD	25/ 1973 /1999
13_3019	L/T	1 small T1 patched, 1 T1, 1 T2	12 L1	8.9" JPC 20 ft jts DOWEL	24/ 1981 / 2014
13_3020	T/L	1 T2 at 14 years, patched at 22	4 L1	10" JPC 20 ft jts DOWEL	24/ 1985/ 2016
21_3016	T/L	1 T2 at 23 years, 2 T2 at 31 years. 12 slabs patched between yr. 29 and yr. 31	1 L2 at 24 years	11.8" JPC skewed jts DOWEL	32/ 1985/ 2016
28_3018		None	None	9" JPC, 20 ft jts, DOWEL	25/1984/ 2010
28_3019	T/L	1 T2 at 30 years, 1 transverse crack to make a SS at 8 years	Longitudinal cracking looks like a construction issue, 8 consecutive slabs L2 at first inspection after 7 years	9.4" JPC D, 20 ft jts DOWEL	25/ 1984/ 2014
37_3008	L/T	1 T2 at year 12, Entire section overlaid with asphalt after 18 years	19 L2 after 17 years, 6 slabs with double cracking, longitudinal cracking later identified as map cracking	7.9" JPC, DOWEL	22/ 1984/ 2002
37_3044	L/T	1 T2 at 29 yr.	1 L2 and 3 L1	9" JPC UD	20/1966/ 1995
37_3807	T	4 T1, 1 T2 at yr 27	Longitudinal cracking later noted as map cracking	9.4" JPC DOWEL	23/ 1980/ 2015
40_3018	L	No transverse cracks	1 L1 at 26 years, 3 more L1 at 28 yrs	8.9" JPC UD	32/ 1976/ 2004
40_4157		None	None	9" JPC, 15 ft jts, UD	33/1986/ 2015
40_4160		None	None	9" JPC, 16 ft jts, UD	31/1979/ 2007
40_4162	L	No transverse cracks	1 L2 at 14 years, out of study at 14 years	9" JPC UD	33/ 1985/ 1999
45_3012	T/L	1 T2 at 33 yrs, 2 T1 at 31	2 L1	10" DOWEL	23/ 1981/ 2014
48_3003	L	No transverse cracks	1 L1 at 32 years	9.3" JPC DOWEL	33/ 1975 /2007
48_3589		None	Spalling noted, no cracks identified at last inspection at 40 yrs	9.9" JPC UD	33/ 1960 / 2000

REFERENCES

Agurla, M., and S. Lin. (2015) Long Term Pavement Performance Automated Faulting Measurement. US DOT, FHWA-HRT-14-092. McLean, Virginia.

Ai, C., and Y.-C. J. Tsai. (2015) Critical Assessment of an Enhanced Traffic Sign Detection Method Using Mobile LiDAR and INS Technologies. Journal of Transportation Engineering, Vol. 141, No. 5, 2015, p. 04014096.

Ai, C., and Y. J. Tsai. (2016) An automated sign retroreflectivity condition evaluation methodology using mobile LIDAR and computer vision. Transportation Research Part C: Emerging Technologies, Vol. 63, pp. 96-113.

American Association of State Highway and Transportation Officials (AASHTO). (2010). "Guide for the Local Calibration of the Mechanistic-Empirical Pavement Design Guide." Washington, DC.

AASHTO (2012). "Pavement Management Guide, Second Edition." AASHTO Joint Technical Committee on Pavements, Washington, D.C.

AASHTO (2017a). "R36-17, Evaluating Faulting of Concrete Pavements." Standard Specifications for Transportation Material and Methods of Sampling and Testing, AASHTO, Washington, D.C.

AASHTO (2017b). "R43-13(2017), Quantifying Roughness of Pavements." Standard Specifications for Transportation Material and Methods of Sampling and Testing, AASHTO, Washington, D.C.

ARA, Inc., ERES Division. (2003) Guide for Mechanistic-Empirical Design. Appendix JJ: Transverse Joint Faulting Model. Transportation Research Board. Washington, D.C.

ARA, Inc., ERES Division. (2004) Guide for Mechanistic-Empirical Design. Part 3. Design Analysis. Chapter 4 Design of New and Reconstructed Rigid Pavements. Transportation Research Board. Washington, D.C.

Baladi, G.Y., Dawson, T., Musunuru, G., Prohaska, M. and K. Thomas. (2017) Pavement Performance Measures and Forecasting and the Effects of Maintenance and Rehabilitation Strategy on Treatment Effectiveness, Michigan State. Report FHWA-HRT-17-095. McLean, Virginia.

Bazant, Z.P. (1999) Fracture Mechanics of Concrete: Concepts, Models and Determination of Material Properties (Reapproved 1999), in ACI Committee 446 Report ACI 446.1R-91. Farmington Hills, MI.

Birgisson, B., et al., (2012) Nanotechnology in Concrete Materials: A Synopsis, in E Circular E-C170. Transportation Research Board (TRB): Washington, D.C.

CalTrans. (2015) Concrete Pavement Guide. Division of Maintenance. Sacramento, CA.

Ceylan, H., Yang, S., Gopalakrishnan, K., Kim, S., Taylor P. and A. Alhasan. (2016) Impact of Curling and Warping on Concrete Pavement. IHRB Project TR-668. Ames, IA.

Chang G., Karamihas, S.M., Rasmussen, R.O., Merritt, D. and M. Swanlund. (2008) Quantifying the Impact of Jointed Concrete Pavement Curling and Warping on Pavement Uneveness. Symposium on Pavement Characteristics (SURF). Slovenia.

Darter, M., Khazanovich, L., Yu, T. and Mallela, J. (2005). "Reliability Analysis of Cracking and Faulting Prediction in the New Mechanistic-Empirical Pavement Design Procedure." Transportation Research Record: Journal of the Transportation Research Board, No. 1936, Transportation Research Board of the National Academies, Washington, D.C.

Department of Defense. (1981) Military Standard: Definition of Terms for Reliability and Maintainability. Washington, D.C.

Dong, Qiao and B. Huang. (2014) Evaluation of Influence Factors on Crack Initiation of LTPP Resurfaced-Asphalt Pavements Using Parametric Survival Analysis. Journal of Performance of Constructed Facilities. DOI: 10.1061/(ASCE)CF.1943-5509.0000409.

Ebeling, Charles E. (2010) An Introduction to Reliability and Maintainability Engineering, McGraw-Hill. Number of pages: 489.

Elkins, G., Thompson, T., Groeger, J., Visintine, B. and G. Rada. (2013) Reformulated Pavement Remaining Service Life Framework. Publication FHWA-HRT-13-038. FHWA, U.S. Department of Transportation.

Elkins, G.E., Thompson, T., Ostrom, B., Simpson, A. and B. Visintine. (2017). "Long Term Pavement Performance Information Management System User Guide". FHWA-RD-03-088 (Update).

FHWA Office of Highway Policy Information. (2016) Highway Performance Monitoring System Field Manual. OMB Control No. 2125-0028. Washington, D.C.

Florida DOT. (2015). 2015 Rigid Pavement Condition Survey Handbook. State Materials Office. Gainesville, FL.

Gaedicke, C. and J. Roesler (2009a). Fracture-Based Method to Determine the Flexural Load Capacity of Concrete Slabs. For the Federal Aviation Administration. University of Illinois at Urbana-Champaign. Urbana, IL.

Gaedicke, C., J. Roesler, and S. Shah (2009b). Fatigue crack growth prediction in concrete slabs. International Journal of Fatigue. 31(8-9): p. 1309-1317.

Geary, G., Tsai, Y. and Y. Wu. (2018). An Area-Based Faulting Measurement Method Using Three-Dimensional Pavement Data. Journal of Transportation Research Record, 2672(40), National Academy of Sciences. PP. 41-49.

Georgia DOT. (2016). Jointed Plain Concrete Pavement Evaluation System (JPCPACES) Instruction Manual. Prepared by Georgia Tech. Atlanta, GA.

Hashimoto, S., Yoshiki, S., Saeki, R., Mimura, Y., Ando, R. and Shutaro Nanba. (2016) Development and application of traffic accident density estimation models using kernel density estimation. Journal of Traffic and Transportation Engineering; 3 (3), pgs 262-270.

Hiller, J. and J. Roesler. (2002). Transverse Joint Analysis for Mechanistic -Empirical Design. Journal of Transportation Research Record, 1809(1), National Academy of Sciences, pp. 42-51.

Illinois DOT. (2010). Chapter 53-Pavement Rehabilitation. Bureau of Design and Environment Manual. Springfield, IL.

Ioannides, A. (1997). Fracture Mechanics in Pavement Engineering, The Specimen-Size Effect. Transportation Research Record: Journal of the Transportation Research Board, Vol. 1568, Transportation Research Board of the National Academies, Washington, D.C., pp. 10-16.

Iowa State University. (2019) Iowa Pavement Management Program Web Portal. Assessed at: https://ctre.iastate.edu/ipmp/ipmp-web-portal/

Isenberg, J. (1968). Properties of Concrete Change When Microcracking Occurs. in Causes, Mechanism, and Control of Cracking in Concrete. Philadelphia, PA: American Concrete Institute, Detroit, Michigan.

Jackson, N. (2009). "Development of Revised Pavement Condition Indices for Portland Cement Concrete Pavement for the WSDOT Pavement Management System." WA State Transportation Center, Olympia, Washington.

Janisch, D. (2015). "An Overview of Mn/DOT's Pavement Condition Rating Procedures and Indices." Minnesota DOT, Maplewood, MN.

Jiang, (Jane) Y. (2016). TechBrief: LTPP-Pavement Performance Measures and Forecasting and the Effects of Maintenance and Rehabilitation Strategy on Treatment Effectiveness. Pub No. FHWA-HRT-16-046. Federal Highway Administration, U.S. Department of Transportation. Washington, D.C

Jiang, C. and Y. Tsai. (2015) "Enhanced Crack Segmentation Algorithm Using 3D Pavement Data", ASCE Journal of Computing in Civil Engineering, 2015, 30(3): 04015050.

Jiang, C., Tsai, Y., Z. Wang. (2016) "Crack Deterioration Analysis Using 3D Pavement Surface Data: A Pilot Study on Georgia State Route 26." Journal of Transportation Research Record, National Academy of Sciences, 2016 (2589): 154-161.

Jiang, Y.J. and S.D. Tayabji. (2000). "Evaluation of Concrete Pavement Conditions and Design Features Using LTPP FWD Deflections Data" ASTM STP 1375, ASTM, West Conshohocken, PA.

Karihaloo B.L. and P. Nallathambi. (1991) Test Methods for Determining Mode I Fracture Toughness of Concrete. In: Shah S.P. (eds) Toughening Mechanisms in Quasi-Brittle Materials. NATO ASI Series (Series E: Applied Sciences), vol 195. Springer.

Khazanovich, L., Darter, M., Bartlett, R. and T. McPeak. (1998) Common Characteristics of Good and Poorly Performing PCC Pavements. FHWA-RD-97-131. U.S. DOT, Federal Highway Administration, McLean, VA.

Kvam, P., Vidakovic, B. and S-J Kim. (2007) Nonparametric Statistics in Science and Engineering. John Wiley & Sons.

Lea, J., J. Harvey, and E. Tseng. (2014) Aggregating and Modeling Automated Pavement Condition Survey data of Jointed Concrete and Sensor data for use in Pavement Management, in TRB Annual Meeting 2014, Transportation Research Board, Washington, D.C. 2014.

Lee, M., & A.J. Khattak. (2019). Case Study of Crash Severity Spatial Pattern Identification in Hot Spot Analysis. Transportation Research Record, 2673(9), Washington D.C., pgs 684–695.

Loizos, Andreas and Matthew Karlaftis. (2005) Prediction of Pavement Crack Initiation from In-Service Pavements, A Duration Model Approach. Transportation Research Record: Journal of the Transportation Research Board, No. 1940, pp. 38–42.

Li, J., Luhr, D.R., Uhlmeyer, J.S. and J. Mahoney. (2012) Preservation Strategies for Concrete Pavement Network of Washington State Department of Transportation. Transportation Research Record: Journal of the Transportation Research Board,

No. 2306, Transportation Research Board of the National Academies, Washington, D.C., pp. 11–20.

Li, Z. and W. Liang, Advanced Concrete Technology. (2011) Hoboken, US: ProQuest ebrary.

Liu, J., Zollinger, D. G., Tayabji, S. D. and K. D. Smith. (2005) Application of Reliability Concept in Concrete Pavement Rehabilitation Decision Making. Transportation Research Record: Journal of the Transportation Research Board, No. 1905, pp. 25–35.

LTPP InfoPave (2018). U.S. Department of Transportation. Federal Highway Administration. Accessed at htpps://infopave.fhwa.dot.gov

LTPP Program. (2010). "Long-Term Pavement Performance Program, Accomplishments and Benefits: 1989-2009." FHWA-HRT-10-071. Turner-Fairbank Highway Research Center. McLean, VA.

Mallela, J., Titus-Glover, L., Sadasivam, S., Bhattacharya, B., Darter, M. and H. Von Quintus. (2015). "Implementation of the AASHTO Mechanistic Empirical Pavement Design Guide for Colorado." CDOT Report CDOT-2013-4, Denver, CO.

Markou, I., Rodrigues, F., & F.C. Pereira. (2017). Use of Taxi-Trip Data in Analysis of Demand Patterns for Detection and Explanation of Anomalies. Transportation Research Record, 2643(1), 129–138.

Miller, J. S., and W.Y. Bellinger. (2014). "Distress Identification Manual for the Long-Term Pavement Performance Program." LTPP DIM, U. S. DOT, Federal Highway Administration, McLean, VA.

Moody, E.D. (1998). "Transverse Cracking Distress in the LTPP Jointed Concrete Pavement Sections". Transportation Research Record: Journal of the Transportation Research Board, No. 1629, Transportation Research Board of the National Academies, Washington, D.C.

NCHRP, (2013) Measuring Performance Among State DOTs: Sharing Good Practices-Pavement Structural Health, NCHRP 20-24(37) Report. Washington, D.C. http://onlinepubs.trb.org/onlinepubs/nchrp/docs/NCHRP20-24(37)J_FR.pdf

North Carolina DOT (2011). "NCDOT Digital Imagery Distress Evaluation Handbook." NCDOT, Raleigh, NC.

Oregon DOT (2010). "Oregon DOT Pavement Distress Survey Manual." Oregon DOT, Oregon.

Ozer, H., M. Ziyadi, and Y. Feng. (2018) Revised Condition Rating Survey Models to Reflect All Distresses: Volume 1. Report FHWA-ICT-18-002. Urbana-Champaign, IL.

Pierce, L. and K.D. Smith. (2015). "AASHTO MEPDG Regional Peer Exchange Meetings." Publication No. FHWA-HIF-15-021. Federal Highway Administration, Washington, DC.

Prozzi, Jorge and Samer Madanat. (2000) Using Duration Models to Analyze Experimental Pavement Failure Data. Transportation Research Record: Journal of the Transportation Research Board, No. 1699, pp. 87-94.

Rao, Shreenath, and D. Raghunathan. (2018). Construction and Rehabilitation of Concrete Pavements Under Traffic. NCHRP Synthesis 530. Washington, D.C.

Roesler, J. and E.J. Barenberg. (1999) Fatigue and Static Testing of Concrete Slabs. Transportation Research Record 1684, Washington. D.C.

Selezneva, O., J. Jiang, and S. D. Tayabji. (2000). Preliminary Evaluation and Analysis of LTPP Faulting Data - Final Report. FHWA-RD-00-076. McLean, Virginia.

Signore, J., Hiller, J., Kannekanti, V., Basheer, I. & J. Harvey. (2012). Prediction of Longitudinal Fatigue Cracking in Rigid Pavements Using RadiCAL. International Conference on Concrete Pavements. Quebec City, Quebec, Canada.

Smith, K., Harrington, D., Preshant L. P. and K. Smith. (2014). "Concrete Pavement Preservation Guide, Second Edition." National Concrete Pavement Technology Center, Ames, Iowa.

Stone, J. (1991). "Design, Operation, and Maintenance Manual for Georgia Digital Faultmeter." Publication SP 9010, GDOT, Forest Park, Georgia.

Taylor, P., Integrated Materials and Construction Practices for Concrete Pavement: A State-of-the-Practice Manual. 2006, Ames, Iowa: Iowa State University.

Tavner, P.J., Xiang, J. and F. Spinato. (2007) "Reliability Analysis for Wind Turbines." Wind Energy.10:1-18.

Tsai, Y. and A. Chatterjee. (2017) "Pothole Detection and Classification Using 3D Technology and Watershed Method", ASCE Journal of Computing in Civil Engineering, 32(2), 04017078

Tsai, Y.C., and G. Geary. (2017) Study of Real-World Slab Level JPCP Deterioration Behavior Using 3D Technology. Presented at International Conference on Maintenance and Rehabilitation of Constructed Infrastructure Facilities (MAIREINFRA 2017). Seoul, South Korea.

Tsai, Y. and F. Li. (2012). "Detecting Asphalt Pavement Cracks under Different Lighting and Low Intensity Contrast Conditions Using Emerging 3D Laser Technology." ASCE Journal of Transportation Engineering, 138(5), 649–656.

Tsai, Y., Li, F. and Y. Wu. (2013) "A New Rutting Measurement Method Using Emerging 3D Line-Laser Imaging System", Int. Journal of Pavement Research and Technology, Vol. 6(5):667-672.

Tsai, Y. C. and Z. Wang. (2013). "A Remote Sensing and GIS-Enabled Asset Management System (RS-GAMS)" Final Report for USDOT project: DTOS59-10-H-0003.

Tsai, Y. C. and Z. Wang. (2014). "A Remote Sensing and GIS-Enabled Asset Management System (RS-GAMS) Phase 2." Final Report for USDOT project: RITARS-11-H-GAT.

Tsai, Y. and Z. Wang. (2015) "Development of an Asphalt Pavement Raveling Detection Algorithm Using Emerging 3D Laser Technology and Macrotexture Analysis", National Academy of Science NCHRP IDEA-163 Final Report.

Tsai, Y., Wang, Z. and F. Li. (2015) "Assessment of Rut Depth Measurement Accuracy of Point-based Rut Bar Systems using Emerging 3D Line Laser Imaging Technology", Journal of Marine Science and Technology, Vol. 23, No. 3, pp. 322-330 (2015), DOI: 10.6119/JMST-014-0327-1.

Tsai, Y. C., Wu, Y.C., and C. Ai (2011). Feasibility Study of Measuring Concrete Joint Faulting Using 3D Continuous Pavement Profile Data. Presented at TRB 2011, Washington, D.C.

Tsai, Y. C., Y. Wu, and J. Doan. (2015). A Critical Assessment of Jointed Plain Concrete Pavement (JPCP) using Sensing Technology - A Case Study on I-285.In 9th International Conference on Managing Pavement Assets, Washington, D.C.

Tsai, Y.C., Wu, Y. and G. Geary. (2019). Study of Temporal Pavement Cracking in 3D to Determine Optimal Time and Cost-Effective Treatment Methods. FHWA-GA-19-1601. Forest Park. GA. (in review)

Tsai, J.Y., Wu, Y and C.R. Wang. (2012) Georgia Concrete Pavement Performance and Longevity. GDOT RP 10-10. Forest Park, GA.

Tsai, Y., Wu, Y., Ai, C. and E. Pitts. (2012) "Feasibility Study of Measuring Concrete Joint Faulting Using 3D Continuous Pavement Profile Data," ASCE Journal of Transportation Engineering, 138(11), 1291-1296.

Uhlmeyer, J.S., D.R. Luhr, and T. Rydholm. (2016) Pavement Asset Management, Washington State DOT, Pavement Branch. Seattle, Washington.

Van Dam, T., Smith, K., Snyder, M., Ram, P. and N. Dufalla. (2019) Strategies for Concrete Pavement Preservation. FHWA Report HIF-18-025. Washington, D.C.

Villaret, S. and M. Wieland. (2018) Assessment of Structural Performance for Systematic Maintenance Planning. 13th International Symposium on Concrete Roads. Berlin, Germany.

Von Quintus, H. L., Darter, M. I., Bhattacharya, B., Sadasivam, S. (2015). "Calibration of the MEPDG Transfer Functions in Georgia." Task 4 Interim Report, GADOT-TO-02-Task4. Georgia DOT, Forest Park, Georgia.

Wang, Chieh. (2017). A Spatiotemporal Methodology for Pavement Rut Characterization and Deterioration Analysis Using Long-Term 3D Pavement Data. Georgia Tech PhD Dissertation. Atlanta, GA.

Wang, K. C. P., L. Li, and J. Q. Li. (2014) Automated Joint Faulting Measurement Using 3D Pavement Texture Data at 1 mm Resolution. ASCE T&DI Congress, Orlando, FL.

Wolters, A. and K. Zimmerman. (2010). Research of Current Practices in Pavement Performance Modeling. Report No. FHWA-PA-2010-007-080307. Harrisburg, PA.

Xu, C and D. Cebon. (2017). " LTPP Tech Brief: Analysis of Cracking in Jointed Plain Concrete Pavements." FHWA-HRT-16-073. Turner-Fairbank Highway Research Center. McLean, VA.

Yu, T. and M. Darter. (2003). "Guide for Mechanistic-Empirical Design of New and Rehabilitated Pavement Structures Final Report, Appendix KK: Transverse Cracking of JPCP". NCHRP 1-37A. Transportation Research Board. Washington, D.C.